DIPLOMARBEIT

Energy-coupled isopropanol biosynthesis by engineered *E. coli* W from acetate

ausgeführt zum Zwecke der Erlangung des akademischen Grades eines Diplom-Ingenieurs unter der Leitung von

Univ. Ass. Dipl.-Ing.(FH) Dr. nat. techn. Stefan PFLÜGL

und Associate Prof. Dipl.-Ing. Dr. nat. techn. Oliver SPADIUT

betreut durch

Dipl.-Ing. Regina KUTSCHA

am Institut für Verfahrenstechnik, Umwelttechnik und Technische Biowissenschaften

Technischen Universität Wien
von

Uliana SMIRNOVA, BSc

Wien, am	Unterschrift des Betreuers	eigenhändige Unterschrift

Eidesstattliche Erklärung

Hiermit erkläre ich, dass ich diese Diplomarbeit selbstständig verfasst habe, dass ich die verwendeten Quellen vollständig angegeben habe und dass ich Zitate die anderen Publikationen im Wortlaut oder dem Sinn nach entnommen sind, unter Angabe der Herkunft als Entlehnung kenntlich gemacht habe.

Wien, am

eigenhändige Unterschrift

1 Abstract

Acetate is a low-cost carbon source for biotechnological processes that can be obtained from ecological resources such as CO_2 or lignocellulosic wastewater. However, its high toxicity and energetically unfavourable metabolism require efficient process strategies, one of which is ATP-coupled production which can improve energy availability and enhance cell growth and/or production.

In this study, we developed the *E. coli* W IPA_ptb_buk (pbu) strain, which produces ATP-coupled isopropanol (IPA) from acetate using the novel IPA_ptb_buk pathway. This pathway employs the Ptb and Buk enzymes derived from *C. acetobutylicum*. The Ptb enzyme converts acetoacetyl-CoA to acetoacetylphosphate, which is then converted by the Buk enzyme to acetoacetate while generating one ATP molecule. According to the literature, the conversion of acetoacetyl-CoA to acetoacetate was typically accomplished in a single step using the AtoDA enzyme. Nonetheless, by employing the Ptb and Buk enzymes, we were able to couple the production of ATP and IPA molecules, resulting in a more energetically favourable process for IPA production in *E. coli*.

We cultivated the developed pbu strain in lab-scale bioreactors under N-starved conditions. The higher ATP availability in the pbu strain may have resulted in prioritizing biomass formation over IPA production, leading to a relatively high μ_{max} of 0.22 h^{-1} and onset of IPA production only under growth-arrested N-starved conditions. The IPA titers reached 2.2 $g{\cdot}L^{-1}$ after 43 hours of N-starvation. These titers were 1.5 times higher than the titers reported in the literature. However, they were at least twice lower than the titers achieved by the non-ATP-coupled AtoDA-containing (aDA) strain previously developed by our group. The aDA strain had a slower growth rate but was capable of producing IPA in varying quantities during the entire 120-hour process. Under growth-arrested conditions, both pbu and aDA strains exhibited similar specific acetate uptake and IPA production rates.

Overall, this work demonstrates the potential of the novel ATP-coupled IPA-producing pathway, IPA_ptb_buk, implemented in *E. coli* and encourages its application in future metabolic engineering strategies.

2 List of Abbreviations, Units and Variables

Enzymes

AckA	...	Acetate kinase
Acs	...	Acetyl-CoA synthetase
Adc	...	Acetoacetate decarboxylase
Adh	...	Alcohol dehydrogenase
AtoDA	...	Acetoacetyl-CoA transferase
Buk	...	Butyrate kinase
CtfAB	...	Acetoacetyl-CoA: acetate/butyrate CoA transferase
Pta	...	Phosphotransacetylase
Thl	...	Thiolase
Ptb	...	Phosphate butyryltransferase

Microorganisms

E. coli	...	*Escherichia coli*
C. acetobutylicum	...	*Clostridium acetobutylicum*
C. beijerinckii	...	*Clostridium beijerinckii*
T. brockii	...	*Thermoanaerobacter brockii*

Variables

$Y_{IPA/acetate}$	$[g \cdot g^{-1}]$	Isopropanol to acetate yield
$Y_{acetate/NH_4}$	$[g \cdot g^{-1}]$	Acetate to ammonium yield
μ	$[h^{-1}]$	Specific growth rate
$r_{acetate}$	$[g \cdot (L \cdot h)^{-1}]$	Volumetric rate of acetate consumption
r_{IPA}	$[g \cdot (L \cdot h)^{-1}]$	Volumetric rate of isopropanol production

$q_{acetate}$	$[g \cdot (g \cdot h)^{-1}]$	Specific rate of acetate consumption
q_{IPA}	$[g \cdot (g \cdot h)^{-1}]$	Specific rate of isopropanol production

Units

AU	...	Absorption units
nm	...	Nanometer
rpm	...	Stirrer speed unit, revolutions per minute
rcf	...	Relative centrifugal force
vvm	...	Volume of air per volume of solution per minute

Chemical formulas

CO	...	Carbon monoxide
CO_2	...	Carbon dioxide
CH_4	...	Methane
HAc	...	Acetic acid
HCL	...	Hydrochloric acid
H_3PO_4	...	Phosphoric acid
KH_2PO_4	...	Potassium dihydrogen phosphate
KOH	...	Potassium hydroxide
NaCl	...	Sodium chloride
NH_4^+	...	Ammonium ion

Other abbreviations

ATCC	...	American Type Culture Collection
BB1	...	Backbone 1
BB2	...	Backbone 2
BB3	...	Backbone 3
bp	...	Base pair
carb	...	Carbenicillin

CDS	...	Coding sequences
DCW	...	Dry cell weight
DNA	...	Deoxyribonucleic acid
DO	...	Dissolved oxygen
DSMZ	...	German Collection of Microorganisms and Cell Cultures
EPS	...	Extracellular polymeric substances
Golden MOCS	...	Golden Gate derived Multiple Organism Cloning System
HPLC	...	High-performance liquid chromatography
IPA	...	Isopropanol
kan	...	Kanamycin
K_m	...	Michaelis constant of the enzyme
MQ	...	Milli-Q® Direct Water Purification System
OD_{600}	...	Optical density
pKa	...	Acid dissociation constant
RI	...	Refractive index
SFE	...	Shake flasks experiment
TCA	...	Tricarboxylic acid cycle

Contents

3 Acknowledgements

I would like to express my gratitude to the entire Sustainable Bioprocess Solutions group, and particularly to their leader Univ.Ass. Dipl.-Ing.(FH) Dr. Stefan Pflügl, as well as to my supervisor Dipl.-Ing. R. Kutscha, for giving me the opportunity to carry out my master's thesis within their team.

During the project, I conducted various stages of microbial product development, including genetic modification of bacteria, shake flask cultivations, and bioreactor cultivations using different operating modes and strategies such as batch, fed-batch, and N-starvation. I especially enjoyed working in the areas of upstream process control and consequent data analysis and was able to enrich my knowledge in these topics.

I would also like to extend my heartfelt thanks to my friends and colleagues who supported me throughout this rollercoaster in various ways. They provided me with food, listened to me and cheered me up when I most needed it. Special thanks to Nata, Arda, Anton, Chris, Alina G, Wolfgang, Ivo, Remi, Fabi, Bettina, and many others. Dom, luv u.

4 Introduction

Caring for our planet is of paramount importance in the nowadays society. The natural environment is complex but fragile, and highly susceptible to human influence. According to [1], atmospheric CO_2 concentration has increased drastically during a relatively short period of time since the industrial revolution started, contributing to the "greenhouse effect" and climate change. In order to fight the negative effects of human actions, multiple methods and approaches for CO_2 fixation, storage and re-usage are currently being developed [2], [3], [4].

One promising solution for achieving long-term environmentally sustainable CO_2 capture involves the use of carbon-fixing microorganisms [3], particularly acetogenic bacteria that can consume CO_2 and produce acetate [5]. Although acetate is a valuable commercial product in itself, there is also interest in its direct conversion into other compounds.

This study focuses on the microbiological conversion of acetate to isopropanol, as a part of the SUJECO project (Figure 4.1).

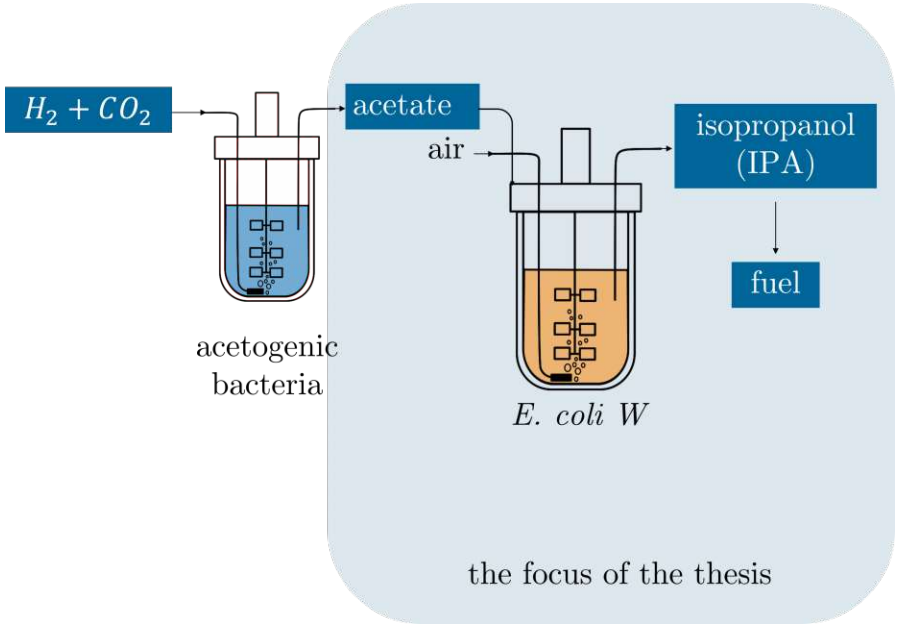

Figure 4.1: SUJECO project

4.1 *E. coli* as a production host

A variety of microorganisms can use acetate as a carbon source. The span goes from eukaryotes to bacteria [6]. The focus of this study lies on *Escherichia coli*, a fast-growing, well-studied microorganism widely used in bio-engineering. *E. coli* can grow on acetate [7], but it does not naturally produce isopropanol. Nevertheless, plasmid-mediated gene transfer makes it possible to introduce new metabolic pathways, expanding the range of the feasible products (as demonstrated in studies [8], [9], [10], [11], [12]).

The non-pathogenic *E. coli* W strain (ATCC 9637, DSM 1116) has been chosen because of its high resistance to acetate inhibition [13]. The growth rate of *E. coli* W goes up to 0.36 - 0.46 h^{-1} on 85 - 169 mM acetate [14], [13], in contrast to the common K12 *E. coli* strain growing with 0.10 - 0.28 h^{-1} rate on 10 - 60 mM acetate [15].

4.2 Acetate as a challenging carbon source

In this study, acetate was used as the sole carbon source for bacteria. Acetate is a negatively charged ion derived from acetic acid. Industrially the majority of acetate is produced in the form of acetic acid either petrochemically (85 %, methanol carbonylation) or biotechnologically (10 %, ethanol oxidation via acetic acid bacteria). Acetate is a relatively inexpensive chemical substance, costing between $ 300-450 per ton in 2020, [16] and $ 800 per ton in 2022, [17]). Moreover, acetate is present in large quantities in various alternative feedstocks such as waste streams or lignocellulosic biomass. It could also be produced via the conversion of such gases as CO, CH_4 or CO_2.

The abundance of cheap acetate sources makes it an important potential substrate in industrial biotechnology [18].

Despite its availability, acetate has some limitations, including its lower energy content when compared to glucose or glycerol [6] or inhibition of cell growth in various microorganisms [13]. In the absence of glucose, *E. coli* cells grown on pure acetate are unable to engage in energy-yielding glycolysis. Moreover, they tend to increase flux towards glyoxylate in the TCA cycle, further reducing the production of NADPH, NADH, and ATP molecules. This metabolic adaptation is likely aimed at minimizing the release of CO_2 [7]. Furthermore, it was shown that the growth rate of *E. coli* decreases as a monotonic function of the acetate concentration [19, 20, 21]. The addition of 5-6 $g{\cdot}L^{-1}$ acetate to the growth medium containing glucose as the main carbon source reduced the growth rate of the cells by half [19].

Consequently, the utilization of acetate as the single carbon source in bioprocesses results in decreased titers, lower growth rates, extended lag phases (more than 10 hours) and long process times in general, compared to sugar-based substrates [22]. Mentioned limitations hinder the widespread usage of acetate as a sole carbon source and require

customized process development using physiological data and the advantages of genetic engineering.

4.3 Isopropanol as a product of interest

This study focuses on the conversion of acetate to isopropanol (IPA). IPA is a valuable common chemical that is currently in high demand. Various applications of IPA include its usage as rubbing alcohol, solvent, a part of biofuel or as a pharmaceutical ingredient [23, 24]. The global COVID-19 pandemic (emphasizing the importance of disinfection), climate change and the energy crisis of 2022 (both forcing the development of biofuels) are actively contributing to the growing IPA demand.

In the chemical industry, there are two major routes for producing IPA: indirect (common in the USA) and direct (common in Europe and Japan) hydration of propylene [23]. Both routes rely on the availability of fossil fuels (propylene being mostly produced via petrochemical steam cracking and oil refineries [25]), therefore the renewable ways of IPA production are under consideration. Usage of agricultural or paper mill waste as a carbon source for the growth of IPA-producing microorganisms seems to be a promising environment-friendly approach [26].

However, generating IPA with *E. coli* poses challenges due to the toxicity of IPA for the cells and the simultaneous need to achieve economically sustainable production titers. For instance, the growth of *E. coli* MDS42 is significantly impacted by the presence of 21 $g{\cdot}L^{-1}$ IPA in the media, with no growth observed at 25.5 $g{\cdot}L^{-1}$ IPA [27]. Fortunately, isopropanol is a volatile chemical and the use of gas-stripping methods can prevent high concentrations of IPA in the reactor, ensuring proper cell growth [28].

For example, the application of gas stripping methods led to an extension of the production hours and resulted in an increase in the total IPA titers from 40 $g{\cdot}L^{-1}$ over 60 hours to 143 $g{\cdot}L^{-1}$ during an extended cultivation period of 240 hours. These results were achieved by IPTG-induced 25 mL cultures of *E. coli* grown on a complex medium with glucose as the main C-source [28, 29]. However, when employing a similar IPA-producing pathway with acetate as the main C-source, Yang et. al. reported lower IPA titer, with a value of 1.47 $g{\cdot}L^{-1}$ reached in 36 hours [8]. Therefore, there is a need to enhance the efficiency of IPA production in *E. coli* when utilizing acetate as the substrate.

It is worth mentioning that certain microorganisms possess the natural ability to produce IPA [30]. One well-known natural producer is *C. beijerinckii* DSM 6423 [31]. This strain is capable of anaerobic IPA production, along with other solvents such as n-butanol. The achieved IPA titers range from 2.2 to 4.1 $g{\cdot}L^{-1}$ during chemostat cultivation [32]. However, the lack of available genetic modification tools and limited understanding of metabolic regulations have hindered further process development [29].

Only recently, in 2018, the genome of *C. beijerinckii* DSM 6423 has been sequenced, and transcriptomics analyses have been reported [31, 33].

4.4 Metabolic pathways for acetate conversion into isopropanol in *E. coli*

4.4.1 Diffusion into the cell

The protonated form of acetate, acetic acid (HAc), is taken up in *E. coli* cell via passive diffusion through the membrane [34]. Once inside the cell, HAc breaks down into an acetate anion (Ac-) and a proton (H+), since HAc has a lower pKa (4.8, [35]), than intracellular pH (approximately 7.6, [36]). The acetate anion, commonly referred to as acetate, is further converted to acetyl-CoA via two pathways: reversibly via AckA and Pta enzymes or irreversibly by Acs enzyme [37, 38, 39, 40] (see figure 4.2). Mutants lacking the *acs*, *ackA*, and *pta* genes are unable to grow on acetate [37].

4.4.2 AckA/Pta vs Acs

The AckA enzyme has a relatively low affinity for acetate, with a K_m value of 7 mM [41], making it suitable for acetate uptake at higher concentrations in the medium ($\geq$ 1.5 g·L^{-1}) [37]. Moreover, AckA and Pta enzymes are responsible for acetate production during growth on an excess of glucose, a phenomenon known as overflow metabolism [42].

On the other hand, the Acs enzyme exhibits a higher affinity for acetate, with a K_m value of 0.2 mM [41], allowing for efficient acetate uptake at lower concentrations ($\leq$ 0.6 g·L^{-1}) [37]. It is worth mentioning that cells with the intact *acs* gene but deleted *ackA* and *pta* genes exhibit retarded growth at higher acetate concentrations ($\geq$ 1.5 g·L^{-1}), highlighting the importance of both the AckA/Pta and Acs acetate uptake pathways [37].

Additionally, the Acs pathway requires more energy for the conversion of acetate to acetyl-CoA compared to the two-step AckA/Pta pathway. In the Acs pathway, ATP is converted to AMP, while in the AckA/Pta pathway, ATP is converted to ADP (see figure 4.2, [43, 41]).

4.4.3 Importance of acetyl-CoA

Produced acetyl-CoA is a precursor for the production of isopropanol through natural and synthetic pathways. Furthermore, acetyl-CoA represents a key node in metabolism due to its intersection with many metabolic pathways and transformations. It is involved in both catabolism such as fatty acid oxidation and the TCA cycle and in biosynthetic pathways, such as the synthesis of fatty acids and cholesterol [7, 6, 16, 8].

Therefore, it should be noted, that the production of IPA interferes with the central metabolism of *E. coli*, as it requires the use of a crucial metabolite, acetyl-CoA.

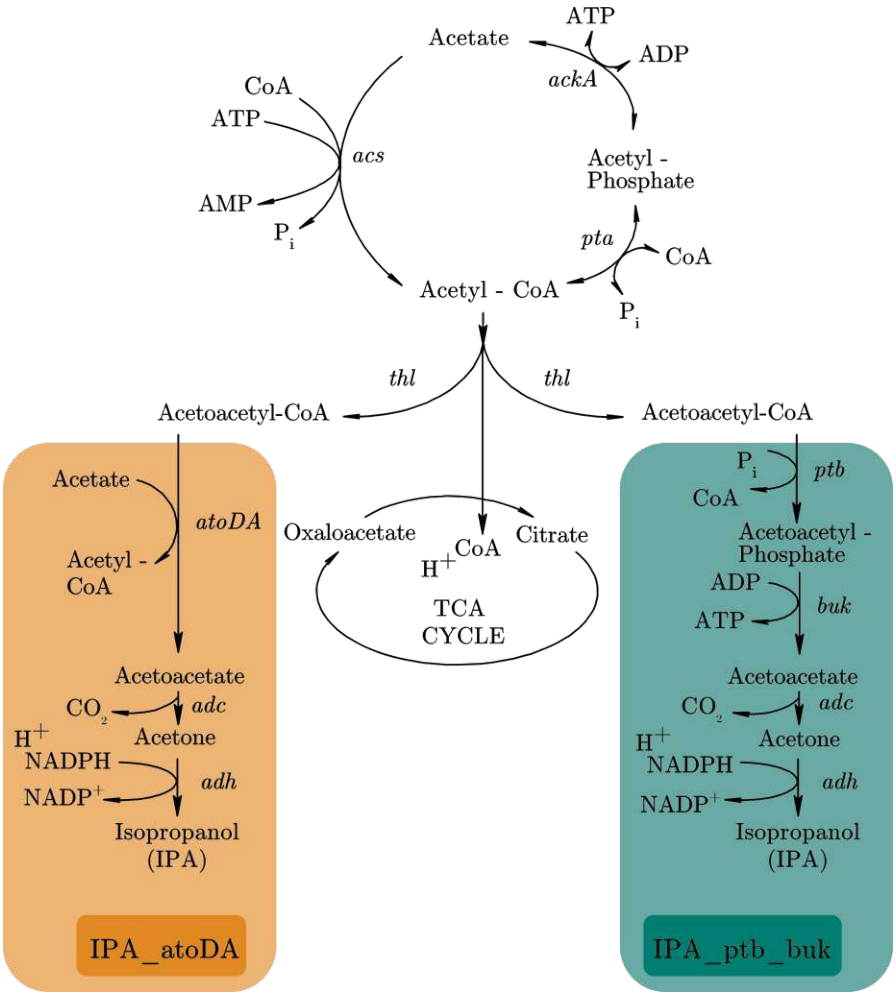

Figure 4.2: IPA_atoDA and IPA_ptb_puk pathways for IPA production in *E. coli* using acetate

4.4.4 IPA_atoDA: commonly utilized synthetic pathway for IPA production in *E. coli*

In figure 4.2 two pathways for the conversion of acetyl-CoA to IPA are shown. The IPA_atoDA pathway, highlighted in orange, is one of these pathways.

Following the IPA_atoDA pathway, the Thl enzyme combines two molecules of acetyl-CoA to form acetoacetyl-CoA. Then, acetoacetyl-CoA transferase (AtoDA) converts acetoacetyl-CoA and an additional acetate molecule to acetoacetate. The Adc enzyme

turns acetoacetate into acetone and releases one molecule of CO_2. At last, the Adh enzyme uses the NADPH cofactor to reduce acetone into isopropanol.

The IPA_atoDA pathway is commonly used in literature for IPA production in *E. coli* [29, 28, 44, 8]. As was mentioned in section 4.3 the maximal IPA titers achieved by this pathway on glucose were 143 $g{\cdot}L^{-1}$ in 60 hours of cultivation by the use of inducible promoters [28].

During the application of the IPA_atoDA pathway with inducible promoters for *E. coli* cultivation on acetate, Yang et al. reported in 2020 a yield range of 0.25 to 0.56 $mol{\cdot}mol^{-1}$ and a titer range of 1.11 to 1.47 $g{\cdot}L^{-1}$ achieved within 36 hours [8]. The maximal reported yield exceeded the theoretical value ($Y_{IPA/acetate\ theory} = 0.50\ mol{\cdot}mol^{-1}$). It is likely that this happened due to the use of a complex medium, which included additional carbon sources such as yeast extract.

The *thl* and *adc* genes used in the IPA_atoDA pathway originate from *C. acetobutylicum*, a species closely related to the well-known natural IPA producer *C. beijerinckii* [29]. Interestingly, the Acetoacetyl-CoA transferase from *E. coli* (AtoDA) has shown greater efficiency compared to the Acetoacetyl-CoA transferase from *C. acetobutylicum* (CtfAB), which is sometimes employed in other IPA producing pathways [45, 29]. Additionally, the *adh* gene obtained from *C. beijerinckii* has demonstrated improved acetone to IPA conversion compared to the *adh* gene from *T. brockii* [29].

4.4.5 IPA_ptb_buk: novel synthetic pathway for ATP-coupled IPA production in *E. coli*

In this study, we were interested in coupling IPA production with ATP production in *E. coli*. ATP is a crucial energy source for most living organisms. It is possible, that an increased ATP availability in *E. coli* cells grown on acetate could help counteract the toxicity and low energetic value of acetate. Also, the metabolic flux towards the ATP-producing production pathway could be increased. To achieve ATP-coupled IPA production, we utilized the Ptb and Buk enzymes.

Origin and function of Ptb and Buk enzymes

Originally *ptb* and *buk* genes come from *Clostridium acetobutylicum*. They form an operon (with *ptb* being transcribed at first) [46] and are involved in the butyrate-synthesis pathway as shown in figure 4.3. Ptb converts butyryl-CoA to butyryl-phosphate which is then turned into butyrate by Buk enzyme.

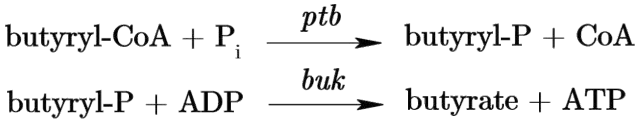

Figure 4.3: ptb_puk pathway in *C. acetobutylicum*. Butyrate formation

In 1989 Thompson and Chen [47] showed that Ptb enzyme of *Clostridium beijerinckii* has the capability to convert not only butyryl-CoA, but also acetyl-CoA or acetoacetyl-CoA substrates. According to their study, the maximum velocity to Michaelis constant ratio (V_{max}/K_m) for butyryl-CoA, acetoacetyl-CoA, and acetyl-CoA were 39000, 1180, and 170, respectively, indicating a less-efficient but possible conversion of non-native substrates.

In 2017, a patent [48] was published that revealed the potential of using the Ptb enzyme from various organisms, including *C. acetobutylicum*, for converting non-native substrates, such as acetoacetyl-CoA. The patent also describes the use of acetoacetyl-phosphate as a substrate for the Buk enzyme, originating from *C. acetobutylicum*. Therefore, both Ptb and Buk, derived from *C. acetobutylicum*, are able to make the conversion of acetoacetyl-CoA to acetoacetate.

To demonstrate the ability of the Ptb and Buk enzymes to convert acetoacetyl-CoA to acetoacetate, the authors introduced a plasmid containing *thl*, *ptb_buk*, and *adc* genes into *E. coli* BL21 (DE3). This pathway enabled the production of acetone, with a titer of 0.19 g·L^{-1} achieved in 1.5 mL cultures grown on glucose. The authors also suggest that the further conversion of acetone to isopropanol may be possible with the introduction of the Adh enzyme. However, there is no available information on this being tested in practice.

In this study, the *ptb_buk* operon is a component of the novel IPA_ptb_buk pathway and is employed for the utilization of a non-native substrate, acetoacetyl-CoA.

Steps of the IPA_ptb_buk pathway

The IPA_ptb_buk pathway, highlighted in green, is shown in figure 4.2. Similar to the IPA_atoDA pathway, the first step involves the Thl enzyme from *C. acetobutylicum*, which catalyzes the combination of two molecules of acetyl-CoA to form acetoacetyl-CoA. Then, phosphate butyryltransferase from *C. acetobutylicum* (Ptb) turns acetoacetyl-CoA into acetoacetyl-phosphate (additional inorganic phosphate required). Next, butyrate kinase from *C. acetobutylicum* (Buk) converts acetoacetyl-phosphate to acetoacetate. During this conversion, one ADP molecule is phosphorylated to ATP. Finally, acetoacetate is converted to acetone, and then to isopropanol, following the same steps as in the IPA_atoDA pathway.

4.4.6 Comparison of IPA_atoDA and IPA_ptb_buk metabolic pathways

The difference between IPA_atoDA and IPA_ptb_buk metabolic pathways lies in the conversion of acetoacetyl-CoA to acetoacetate. In the IPA_atoDA pathway, only one enzyme (AtoDA) is needed. The IPA_ptb_buk pathway utilises two enzymes, Ptb and Buk, increasing protein construction costs for the cell. Also, there is no additional uptake of an acetate molecule in the IPA_ptb_buk pathway. On the other hand, the Ptb enzyme produces an energy-rich ATP molecule via substrate-level phosphorylation.

As mentioned previously, two acetyl-CoA molecules are required for the production of acetoacetyl-CoA by the Thl enzyme. Assuming that acetate is taken up by the cell via the AckA/Pta pathway and that both required acetyl-CoA molecules are also obtained through the AckA/Pta pathway, the following can be calculated: the IPA_ptb_puk pathway requires less ATP (1 molecule instead of 2) for the production of 1 IPA molecule, compared to the IPA_atoDA pathway. Additionally, the acetate uptake for IPA production is less energetically demanding: only $1/2 \times$ ATP molecules are needed to take up one molecule of acetate (compared to $2/3 \times$ ATP molecules in the IPA_atoDA pathway, see table 4.1, a).

However, if we assume that one of the required acetyl-CoA molecules can be produced by the AtoDA enzyme using acetate taken from the medium without the need to use ATP, both pathways become similarly advantageous (see table 4.1, b).

In the scenario where acetate is taken up by the cell through the more energy-demanding Acs pathway, and considering that one of the acetyl-CoA molecules can be supplied by the AtoDA enzyme, the IPA_atoDA pathway becomes slightly more advantageous (requiring 1 ATP molecule for the production of one IPA molecule) compared to the IPA_ptb_buk pathway (requiring 1 ATP and 1 ADP molecules) (see Table 4.1, d).

Therefore, it can be concluded that the energy efficiency of IPA production through both the IPA_atoDA and IPA_ptb_buk pathways is directly influenced by the method of acetate uptake. It should be noted that to our knowledge, acetate uptake solely via the AtoDA enzyme has not been reported in *E. coli*, and the contribution of AckA/Pta and/or Acs enzymes is of the highest importance [37, 38, 39, 40]. Further experimental data are required to validate the effectiveness of the novel IPA_ptb_buk pathway for IPA production in *E. coli* on acetate.

Table 4.1: How many ATP and acetate molecules are needed for the production of 1 molecule of isopropanol? Comparison between IPA_atoDA and IPA_ptb_puk synthetic pathways. Reactions were calculated stoichiometrically without considering the full energy balance of a cell

		IPA_atoDA	**IPA_ptb_buk**
a)	acetate uptake by **AckA/Pta**, 2nd acetyl-CoA provided by AckA/Pta	3 × acetate 2 × ATP	2 × acetate 1 × ATP
b)	acetate uptake by **AckA/Pta**, 2nd acetyl-CoA provided by AtoDA	2 × acetate 1 × ATP	
c)	acetate uptake by **Acs**, 2nd acetyl-CoA provided by Acs	3 × acetate 2 × ATP	2 × acetate 1 × ATP & 1 × ADP
d)	acetate uptake by **Acs** 2nd acetyl-CoA provided by AtoDA	2 × acetate 1 × ATP	

4.5 Nitrogen starvation & limitation

The nitrogen starvation strategy is employed in bioprocess development to enhance product titers. By halting cell proliferation, nitrogen starvation conserves resources that would otherwise be utilized for biomass formation. This strategy is particularly advantageous when the target product is not directly linked to biomass formation, allowing the saved resources to be redirected towards product synthesis.

It should be distinguished between N-limitation and N-starvation strategies. The first one implies a low amount of N-source fed to the bioreactor, partially allowing the controlled growth of microorganisms. The second one refers to the complete unavailability of N-source and results in no further cell amplification. To implement either strategy correctly, it is important to use a defined medium [49].

However, both nitrogen limitation and starvation strategies are widely used for increasing the production of a broad range of products in various microorganisms. Protocols for producing the following chemicals could be found in literature: citric acid in *Aspergillus niger* fungi [50], lipids in *Yarrowia lipolytica* oleaginous yeast [51], itaconate in genetically modified *Corynebacterium glutamicum* gram-positive bacteria [52] and storage products like poly(hydroxybutyrate) in *Synechocystis* cyanobacteria [53]. For IPA generation both approaches were successfully applied: N-limitation in *Cupriavidus necator* (9.1 $g{\cdot}L^{-1}$, after 82 hours, [54]) and N-starvation in *E. coli* (achieving a maximum of 2.5 $g{\cdot}L^{-1}$, after 15 hours, [44]).

In the case of [44] (Okahashi et al., 2017), the IPA_atoDA pathway was implemented to convert glucose to IPA. Surprisingly, the authors observed that *E. coli* cells were unable to produce IPA during the exponential growth phase. Metabolic flux analysis revealed a deficiency in NADPH generation, which is necessary for the final reduction step of acetone to IPA. To overcome this issue, the authors cultivated the same strain under nitrogen-starved conditions, where NADPH consumption for biomass formation is eliminated. These conditions resulted in an increase in IPA production, with levels reaching 0.5 $g{\cdot}L^{-1}$ after 15 hours of the process [44].

Therefore, N-starvation appears to be a beneficial strategy for redirecting the resources of IPA_atoDA-containing *E. coli* cells towards IPA production.

4.6 Goals of this study

Problem Statement The aim of this study was to investigate the potential of microbial conversion of acetate to IPA. Acetate presents a challenge as a sole carbon source due to its toxicity and lower energy content compared to sugar-based substrates. To overcome these difficulties and improve IPA production yields, process intensification strategies focusing on genetic and metabolic engineering of the chosen production host, *E. coli* W, were considered.

Novelty of the Approach This study aimed to investigate the feasibility of energy-coupled production of isopropanol using the *ptb_buk* operon originating from *C. acetobutylicum*. The promiscuous nature of the *ptb_buk* operon enables the 2-step conversion of acetoacetyl-CoA to acetoacetate, making it possible to include the operon in the acetate to isopropanol conversion pathway - IPA_ptb_buk. When the *ptb_buk* operon produces acetoacetate, one extra ATP molecule is generated, improving energy availability in the cells and theoretically enhancing their growth and/or production. The pathway was not previously used for isopropanol production in *E. coli*.

Goals of the study The main goals of the thesis were (i) an assembly of the IPA_ptb_buk pathway and its introduction to *E. coli* W, (ii) characterisation of the derived *E. coli* W IPA_ptb_buk (**pbu**) strain and following (iii) comparison of the strain carrying IPA_ptb_buk

pathway with a previously developed strain with the IPA_atoDA pathway (the *E. coli* W IPA_atoDA strain (**aDA**), acetoacetyl-CoA to acetoacetate conversion via AtoDA enzyme).

A special emphasis was placed on comparing the growth rates, acetate uptake, and productivity of the pbu and aDA strains under the following conditions:

1) Preliminary comparison during shake flask fermentation.

2) Comparison during bioreactor fermentation under conditions promoting maximal cell growth (C-excess).

3) Comparison during bioreactor fermentation under similar specific growth rates (C-limitation conditions).

4) Comparison during bioreactor fermentation under nitrogen-starved conditions.

The main question addressed in this study was whether the implementation of the ATP-coupled IPA production strategy in the pbu strain could lead to improved cell viability and/or increased IPA titers.

5 Materials and Methods

5.1 Molecular biology

5.1.1 Bacterial strains

Three different strains derived from *Escherichia coli* W (ATCC 9637, DSM 1116, German Collection of Microorganisms and Cell Cultures GmbH, Germany) were used as production hosts during this study (Figure 5.1).

The ***E. coli* W IPA_ptb_buk (pbu)** strain contained a plasmid with a DNA construct of *p114_thl p114_ptb_buk p114_adc p105_adh*, representing the IPA_ptb_buk pathway. The pbu strain was developed during this work.

The ***E. coli* W IPA_atoDA (aDA)** strain contained a plasmid with a DNA construct of *p114_thl p114_atoDA p114_adc p105_adh*, representing the IPA_atoDA pathway. The aDA strain was developed previously in the Sustainable Bioprocess Solutions Group by R. Kutscha.

The ***E. coli* W IPA_no_atoDA (reference)** strain contained a plasmid with a DNA construct of *p114_thl p114_adc p105_adh*, representing the IPA_no_atoDA pathway. The reference strain was developed during this work.

Expression cassettes of the genes included constitutive promoters BBa_J23105 (p105) or BBa_J23114 (p114) from the J. Anderson library [55] and the TT_B1001 (TT) terminator [56] (see figure 5.1).

E. coli TOP10 (ThermoFisher Scientific, USA) and CopyCutter EPI400 (Lucigen Corporation, USA) were used as intermediate hosts for cloning steps and for plasmid propagation.

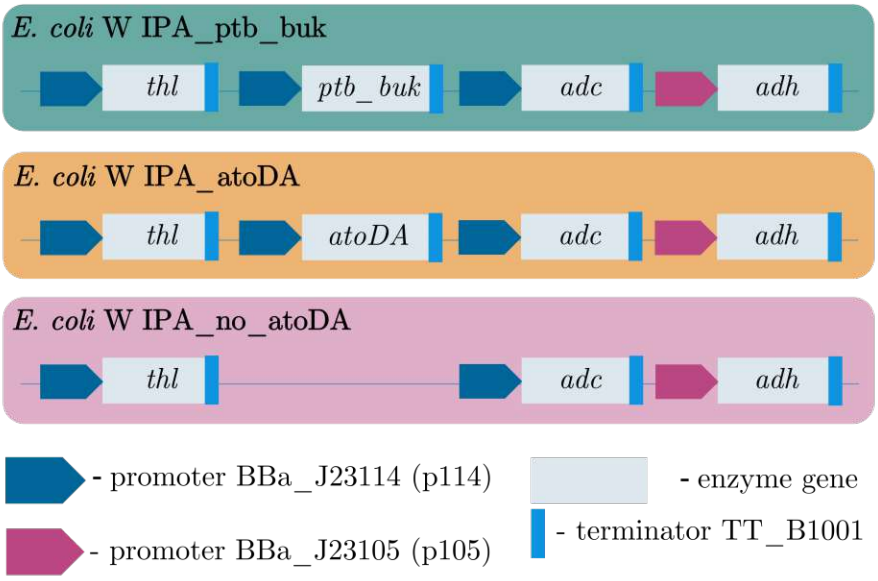

Figure 5.1: DNA constructs inserted in *E. coli* W IPA_ptb_buk, *E. coli* W IPA_atoDA and *E. coli* W IPA_no_atoDA strains

5.1.2 Strain development

The strains were developed via plasmid-mediated gene transfer.

Plasmid assembly via GoldenMOC System

The plasmids were assembled with the Golden Gate derived Multiple Organism Cloning System (GoldenMOCS) [57], which is based on Golden Gate Cloning [58]. The assembly procedures were performed as described in [57].

The construction of the plasmid containing the **IPA_ptb_buk** metabolic pathway involved three levels.

BB1 The first level involved the use of individual elements, such as promoter (p114), coding sequences (CDS (*ptb_buk*)), and terminator (TT). These elements were separately assembled to backbone 1 (BB1), forming BB1_p114, BB1_TT or BB1_ptb_buk plasmids with the help of BsaI endonuclease. BB1_ptb_buk was constructed during this study.

BB2 The second level involved combining a promoter (from BB1_p114), CDS (from BB1_ptb_buk), and terminator (from BB1_TT) together to form a functional expression cassette, which was incorporated into backbone 2 (BB2) with the help of BpiI endonuclease. BB2_ptb_buk plasmid was constructed during this study.

BB3 In the third level, multiple expression cassettes - BB2_thl, BB2_ptb_buk, BB2_adc and BB2_adh were combined together to form a DNA construct, which was incorporated into backbone 3 (BB3) with the help of BsaI endonuclease. BB3_IPA_ptb_buk plasmid was constructed during this study.

BB3_IPA_ptb_buk was ready to be transformed to and express the IPA_ptb_buk metabolic pathway in *E. coli*.

For the construction of the plasmid, containing the **IPA_no_atoDA** metabolic pathway, BB2_thl, BB2_adc, BB2_adh and BB3 recipient vectors were assembled.

The *ptb_buk* DNA sequence was purchased from TWIST Bioscience (USA). BB1_p114, BB1_TT, BB2_thl, BB2_adc, BB2_adh and recipient vectors BB1, BB2 and BB3 were already in possession of the Sustainable Bioprocess Solutions Group, TU Wien (Table 9.2, see Additional file) and were used during this study without previous assembly. The primers were purchased from Integrated DNA Technologies (USA). The genes originated from different organisms and the sequences had to be codon optimised (Table 5.1). The QIAGEN CLC Genomics Workbench (USA) program was used to visualise the plasmids and plan the restriction experiments.

Table 5.1: Enzyme gene origins

Gene	Donor organism
thl, adc, ptb, buk	*C. acetobutylicum*
atoDA	*E. coli*
adh	*C. beijerinckii*

Plasmid propagation and transformation

Freshly assembled BB1_ptb_buk, BB2_ptb_buk, BB3_IPA_ptb_buk and BB3_ IPA_no_atoDA plasmids were transformed to the chemically- or electro-competent intermediate hosts using the heat shock method or *E. coli* protocol from Gene Pulser Xcell Electroporation System (Bio-Rad, USA) respectively. The final construct was transformed into the electro-competent *E. coli* W (the production host).

The transformants were plated on Lysogeny Broth (LB) plates (per L: 10 g soy peptone, 10 g NaCl, 5 g yeast extract, 15 g agar) supplemented with 50 $mg{\cdot}L^{-1}$ kanamycin for BB1 and BB3 transformants or with 100 $mg{\cdot}L^{-1}$ carbenicillin for BB2 transformants. Grown colonies were picked and incubated overnight in 5 mL LB medium (LB-plates recipe without agar) with the respective antibiotic at 37 °C. 2-4 mL of the overnight

cultures of *E. coli* TOP10 or *E. coli* W were centrifuged and the pellet was used for plasmid extraction. The CopyCutter overnight cultures were used for the inoculation of the induced CopyCutter culture in 250 mL shake flasks (9.75 mL LB/kan medium, 750 μL overnight culture, 10 μL induction solution). The cells were incubated for 4.25 hours. 2-4 mL of the induced culture was centrifuged and the pellet was used for plasmid extraction. The HiYield Plasmid Mini Kit (SLG, Germany) was used for the plasmid extraction. The concentration of the extracted DNA was measured with the NanoDrop ND-1000 UV-Vis (ThermoFisher Scientific, USA).

Successful assembly and transformation were confirmed by restriction procedures with AseI (ThermoFisher Scientific, USA) for BB1 and BB2 or XmaJI (ThermoFisher Scientific, USA) for BB3. The restricted products together with the 1 kb GeneRuler (ThermoFisher Scientific, USA) were loaded on the 1 % agarose gel (supplemented with 0.01 % SYBR Safe DNA Gel Stain, ThermoFisher Scientific, USA) and run at 100 Volt for 30 min.

The final confirmation of the successful assembly was done with Sanger sequencing (Microsynth AG, Switzerland).

5.2 Cultivation procedures

The strains were stored at -80 °C in 25 % (w/v) glycerol. For the cultivation, the cells were streaked onto the LB-kan plates and grown overnight at 37 °C or over the weekend at room temperature. Individual colonies were picked and inoculated into a liquid medium (SFEs, bioreactor precultures). Biological replicates were obtained by picking distinct colonies.

5.2.1 Shake flask experiments (SFEs)

Preculture 50 mL of the LB-kan medium (50 mg·L^{-1} kanamycin) was transferred to 500 mL Erlenmeyer flasks and inoculated. The preculture was grown overnight at 37 °C, 200 rpm.

Washing of the cells After reaching an optical density (OD_{600}) of 2-3 AU, the cells were washed aseptically. The cells were transferred into 50 mL FALCON tubes and (i) centrifuged at room temperature and 5000 rcf for 5 minutes, (ii) the supernatants were removed, (iii) the cell pellets were resuspended in 20 mL of sterile NaCl 0.9 % (w/v) solution. Afterwards, the cells were again (iv) centrifuged at room temperature and 5000 rcf for 5 minutes and (v) resuspended in 4 mL NaCl 0.9 % (w/v) solution. The OD_{600} was then measured.

Main culture 20 mL of the DeLisa medium (5 g·L^{-1} acetate, 4 g·L^{-1} $(NH_4)_2HPO_4$, [59], Table 5.2) was transferred to 500 mL Erlenmeyer flasks and inoculated with the

cells after the washing procedure at an OD_{600} of approximately 0.5 AU. The main culture was grown at 25 °C or at 37 °C with continuous shaking at 200 rpm.

The residual volume at the end of each SFE was measured and compared to the expected residual volume (calculated as the starting volume subtracted from the sampling volume). The difference between these values represented the volume lost due to evaporation during the SFE. A linear volume correction was applied to account for this volume loss.

Sampling Samples were collected from the main culture at maximum 12-hour intervals, with a volume of 1 mL per sample. OD_{600} was measured for each sample prior to centrifugation at 4 °C, 21913 rcf for 10 min. Supernatants were collected and analyzed via high-performance liquid chromatography (HPLC) (see analytic section 5.3 for further details).

Table 5.2: DeLisa[59] Medium

Compound	**Concentration, per L**
KH_2PO_4	13.3 g
$(NH_4)_2HPO_4$	1.0 - 4.0 g
Citric acid	1.7 g
Trace elements:	
$MgSO_4 \times 7\ H_2O$	1.2 g
Fe(III) citrate	0.1 g
EDTA	8.4 mg
$Zn(CH_3COO)_2 \times 2\ H_2O$	13.0 mg
$CoCl_2 \times 6\ H_2O$	2.5 mg
$MnCl_2 \times 4\ H_2O$	15.0 mg
$CuCl_2 \times 4\ H_2O$	1.5 mg
H_3BO_4	3.0 mg
$Na_2MoO_4 \times 2\ H_2O$	2.5 mg
C-source: Acetate / Glucose	5.0 - 10.0 / 20.0 g
Kanamycin	50 mg

The pH was adjusted to 7.0 using 10 M NaOH. Trace elements and kanamycin were added after sterile filtration, while the carbon source was added after separate autoclaving. The amount of $(NH_4)_2HPO_4$, the only nitrogen source in the DeLisa medium, was varied between the SFEs and fermentations to achieve the desired biomass concentration.

5.2.2 Bioreactor Set-Up and cultivations

Bioreactor Set-Up

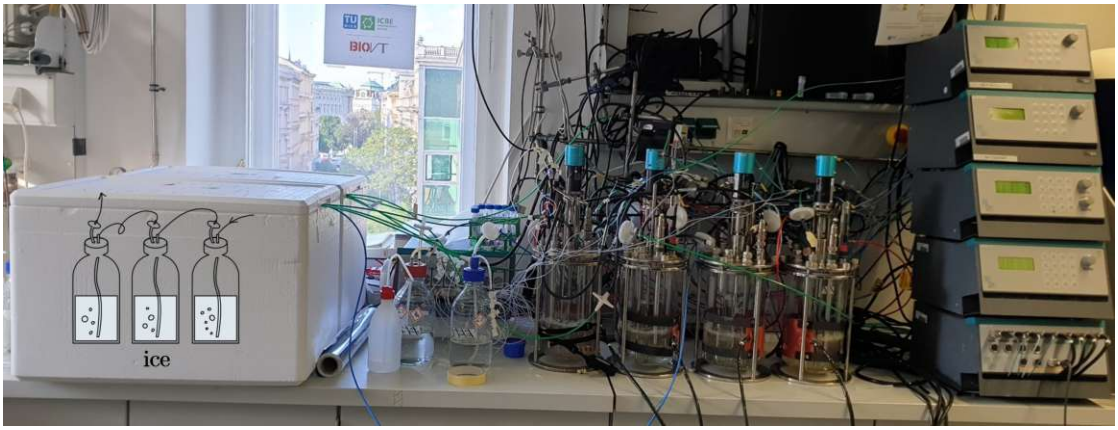

Figure 5.2: Set-Up for the microbial IPA production using the DASGIP parallel bioreactor system

All fermentations were performed in the DASGIP parallel bioreactor system (Eppendorf AG, Germany) equipped with 4 × 2.5 L vessels. Parallel processes were monitored with optical dissolved oxygen (DO) probes (VisiFerm DO 225 (ECS), Hamilton, Switzerland) and potentiometric pH-Sensors (EasyFerm Plus PHI K8 225, Hamilton, Switzerland). pH value was maintained at 7.0 by automatically controlled additions of H_3PO_4 (5 or 10 M) and KOH (5 M). Dissolved oxygen was held on above 30 % saturation via stirrer speed adaptations in the 400 - 1000 rpm range. The constant airflow through the reactor was set to 0.5 vvm (30 $L \cdot h^{-1}$). The off-gas was led through 3 × 1 L Schott bottles (washing flasks) filled with MQ, which were kept on ice for the collection of volatile products, isopropanol and acetone. Off-gas analysis was performed via the DASGIP GA (Eppendorf AG, Germany), CO_2 and O_2 percentages were measured. Acid, base and feed were added to bioreactors with the help of the DASGIP MP8 multi-pump module. The feed pump speed was adjusted manually if needed. Pulses were delivered through a septum on top of each reactor. All four bioreactors were held on separate balances during the process. All signals, values and set points were processed and recorded with the help of the DASGIP Control System (Eppendorf AG, Germany).

First preculture 50 mL of the LB-kan medium was transferred to 500 mL Erlenmeyer flasks and inoculated. The first preculture was grown for 8-10 hours at 37 °C, 230 rpm until the OD_{600} of the culture reached 1-2 AU.

Second preculture 200 mL of the DeLisa medium (20 $g \cdot L^{-1}$ glucose, [59], Table 5.2) in 2 L Ultra Yield shake flasks were inoculated with the cells from the first preculture

to achieve an initial OD_{600} of 0.05 AU. The second preculture was grown at 37 °C, 200 rpm.

Washing of the cells and inoculation of bioreactors In approximately 15 hours, after reaching an OD_{600} of 15-20 AU, the cells were washed aseptically. The cells were (i) centrifuged at room temperature and 4000 rcf for 5 minutes, (ii) the supernatant was removed, (iii) the cell pellet was resuspended in 50 mL of sterile NaCl 0.9 % (w/v) solution. Afterwards, the cells were again (iv) centrifuged at room temperature and 4000 rcf for 5 minutes and (v) resuspended in 15 mL NaCl 0.9 % (w/v) solution. OD_{600} was then measured and the bioreactors were inoculated to achieve an initial OD_{600} of 0.5 AU.

Cultivations in bioreactors

Fermentations were carried out using a pulsed fed-batch mode.

The starting volume was 1 L. The temperature was held at 25 °C or 37 °C. The DeLisa medium (5 $g{\cdot}L^{-1}$ acetate) was used for the bioreactor cultivations. The initial concentration of $(NH_4)_2HPO_4$ was 1.2 $g{\cdot}L^{-1}$ during the fermentations at 25 °C and 2 $g{\cdot}L^{-1}$ during the fermentations at 37 °C. The reactors were supplied with acetate either through feeding or pulsing. Pulses and feed medium were made similar to DeLisa medium, but containing only trace elements and carbon source, per L: 12.45 g $MgSO_4 \times 7\ H_2O$, 24.9 mg Fe(III) citrate, 8.1 mg EDTA, 10.0 mg $Zn(CH_3COO)_2 \times 2\ H_2O$, 2.5 mg $CoCl_2 \times 6\ H_2O$, 15.0 mg $MnCl_2 \times 4\ H_2O$, 1.5 mg $CuCl_2 \times 4\ H_2O$, 3.0 mg H_3BO_4, 2.5 mg $Na_2MoO_4 \times 2\ H_2O$, and 150 g acetate. A few drops of sterile polypropylene glycol were used intermittently during the process to prevent foam formation.

At the end of the fermentation, the rest volumes in the bioreactors and off-gas Schott bottles were measured. The linear volume correction was made for each bioreactor.

Sampling All reactors were sampled at intervals no longer than 8 hours. 4-5 mL of the culture broth were collected. OD_{600} was measured in duplicates per sample. One sample was distributed 3 times in 1 mL volume to reaction tubes. The tubes were centrifuged at 4 °C, 21913 rcf for 10 minutes and the supernatants were collected. The supernatants were analyzed with the CEDEX BioHT (Roche Diagnostics GmbH, Switzerland) and HPLC (see analytic section 5.3 for further details).

The Schott bottles connected with the off-gas of the reactors were sampled shortly before the bioreactor. The volume of the off-gas Schott bottle sample was 1 mL. These samples were analyzed with HPLC (see analytic section 5.3 for further details).

For the quick determination of nitrogen and acetate concentrations, 1 mL samples were taken from bioreactors at periodic intervals. After centrifuging at 4 °C, 21913 rcf for 1 minute the supernatants were measured with the CEDEX (see analytic section 5.3 for further details).

5.3 Analytics

Freshly taken samples were held on ice. The off-gas Schott bottle samples and the supernatants from culture broths were stored at -20 °C.

5.3.1 Biomass. Optical density (OD_{600})

Biomass concentration was measured by determining the optical density of the culture broth. The samples were diluted in order to stay between 0.05 and 0.8 AU (linear range of the spectrophotometer, ONDA V-10 PLUS, Labbox, Spain). Optical density was measured at 600 nm wavelength. Distilled water was used as a blank.

5.3.2 Biomass. Dry cell weight

For the dry cell weight (DCW) determination samples of 5 mL volume were taken in triplicates, once during the fermentation, close to the maximal reached density. OD_{600} was measured, samples were centrifuged in pre-weighed glass tubes (4 °C, 10 min, 5000 rcf), supernatants were removed, remaining pellets were washed with 0.9 % NaCl (w/v) solution and centrifuged again. Afterwards, the biomass was dried at 120 °C for at least 72 hours. Tube weight differences were noted and the DCW to OD_{600} ratio was calculated and applied for the evaluation of the whole fermentation. The coefficient slightly differs between each fermentation due to the different experiment parameters (e.g. 0.3706, 0.3475, 0.3667).

During shake flasks experiments (SFEs) presented in this study, the DCW was not directly determined. The coefficient used for their calculations is taken from the previously performed SFEs (data not shown) and is 0.3475.

5.3.3 Biomass composition

The biomass composition of the *E. coli* W IPA_atoDA strain is $C_1H_{1.691}N_{0.176}O_{0.152}$. For the carbon balance calculations of the *E. coli* W IPA_ptb_buk strain the same formula was used.

5.3.4 Acetate, IPA, acetone. HPLC

HPLC (high-performance liquid chromatography) analysis was performed using Aminex HPX-87H column (Bio-Rad, USA) on Vanquish Core Quaternary HPLC System (ThermoFisher Scientific, USA). Concentrations of the acetate and isopropanol were determined using a refractive index (RI) detector and concentrations of acetone using an

ultraviolet (UV) lamp detector with the 280 nm wavelength. The integration and evaluation of the peaks were done with the help of the Chromeleon 7.3.1 CDS (ThermoFisher Scientific, USA) program. The used instrument method lasted for 30 min, with 60 °C in the column compartment and 0.6 mL·min^{-1} isocratic flow of 4 mM H_2SO_4 solution.

The calibration curve of 6 standards with the following concentrations (10, 5, 2.5, 1, 0.5, 0.05 g·L^{-1}) was measured with the samples during each new run. The samples and standards were mixed with 40 mM H_2SO_4 (10 × running buffer) in a 9:1 ratio (450 µL to 50 µL), centrifuged (4 °C, 10 min, 21913 rcf) and pipetted into the glass inlets in HPLC vials, 200 µL each.

5.3.5 NH_4, acetate. CEDEX

CEDEX BioHT (Roche Diagnostics GmbH, Switzerland) was used for the quick determination of the NH_3 (Cedex Kit NH3B 914) and acetate (Cedex Kit AC2B 068) concentrations.

5.3.6 Data evaluation

Data evaluation was carried out with Excel 2016 (Microsoft Office, USA).

IPA and acetone titers

The IPA titers were calculated with formula 5.1. Acetone titers were calculated respectively.

$$c_{IPA} = \frac{m_{IPA\ in\ WF1} + m_{IPA\ in\ WF2} + m_{IPA\ in\ WF3} + m_{IPA\ in\ bioreactor}}{V_R} \left[\frac{g}{L}\right] \quad (5.1)$$

$m_{IPA\ in\ WF1/2/3}$	[g]	Mass of IPA in the 1st/2nd/3rd washing flasks
$m_{IPA\ in\ bioreactor}$	[g]	Mass of IPA in a bioreactor
V_R	[L]	Bioreactor volume

Carbon balance

The assumed carbon balance of the fermentation process is represented in equation 5.2.

$$C_{acetate} = C_{CO_2} + C_{biomass} + C_{IPA} + C_{acetone} \left[mol\right] \quad (5.2)$$

C_i	[mol]	Mol of carbon contained in the component i

6 Results

The results are organized as follows:

First, section 6.1 presents the results of the IPA production and the corresponding process design that was developed by the Sustainable Bioprocess Solutions group prior to this study (the *E. coli* W IPA_atoDA (**aDA**) strain, 25 °C).

Next, section 6.2 describes the development of the ATP-coupled IPA-producing *E. coli* W IPA_ptb_buk (**pbu**) strain.

Then, in section 6.3, the results of cultivating the pbu and aDA strains in shake flasks at 25 °C and 37 °C are presented. This section focuses on the preliminary characterisation of the pbu strain and provides a preliminary comparison between the pbu and aDA strains under the specified conditions.

Section 6.4 provides an overview of the conducted bioreactor runs of both pbu and aDA strains and of their customized process design at 37 °C. Subsequently, the following sections specifically focus on characterizing the pbu strain in bioreactors under conditions of C-excess (6.5 & 6.6), C-limitation (6.7 & 6.8) and N-starvation.

Finally, the comparison between the pbu and aDA strains is provided in 6.9.

6.1 Overview of the initial process design: Productivity and behaviour of the N-starved *E. coli* W IPA_atoDA strain at 25 °C

The *E. coli* W IPA_atoDA (**aDA**) strain was previously developed in the Sustainable Bioprocess Solutions group (TU Wien) for acetate to IPA conversion. The IPA_atoDA pathway, responsible for IPA production, was implemented in the aDA strain using constitutive promoters.

This section presents data from quadruplicate cultivations of the aDA strain conducted at 25 °C under carbon-excess and nitrogen-starved conditions. These cultivations were performed by the Sustainable Bioprocess Solutions group at TU Wien prior to this study. This data is presented to provide an initial overview of the process design for IPA production employed by the Sustainable Bioprocess Solutions group. The focus is

given to the impact of nitrogen starvation conditions on IPA production and the process limitations observed in the experimental set-up.

The process was divided into two phases. At first, in the growth phase, cells multiplied until NH_4 was completely depleted. Then, in the production phase, cells were N-starved, they could not proliferate but could produce. The acetate was provided in excess. Pulses of acetate were added to maintain the acetate concentration between 0.5-14 g·L^{-1}. Figure 6.1 shows the results of one of the four fermentation runs - 54_F1.

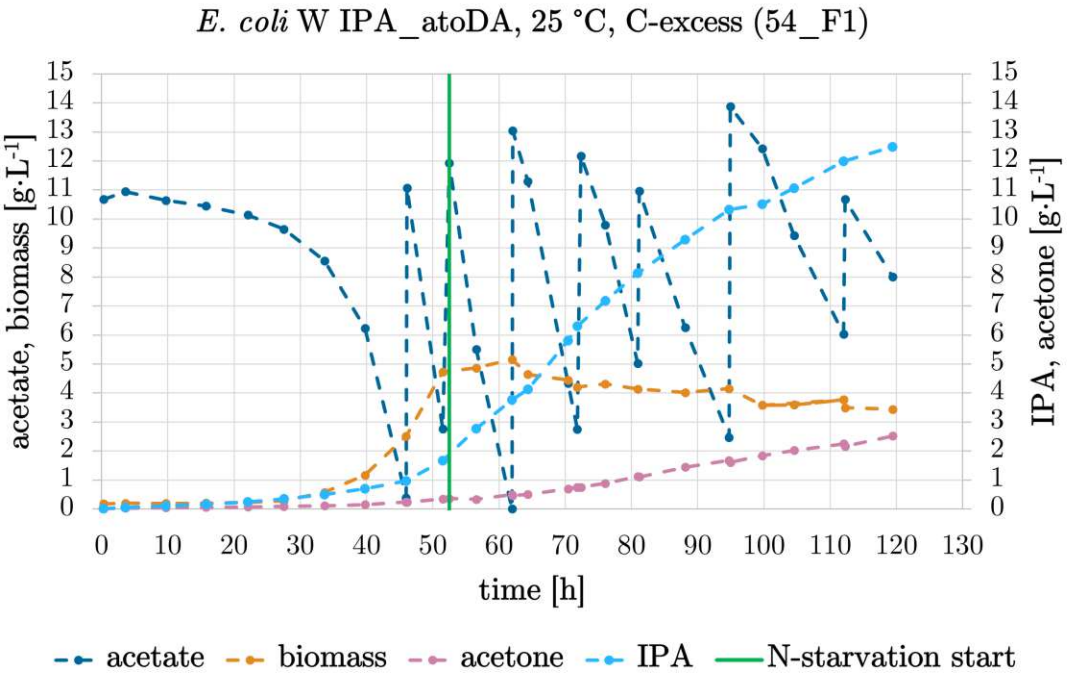

Figure 6.1: Fermentation results of *E. coli* W IPA_atoDA strain at 25 °C grown under carbon excess. 54_F1 run

IPA titers averaged 11.09 ± 1.48 g·L^{-1} in the four bioreactor runs after 120 hours of fermentation. (The titers were calculated as mentioned in section 5.3.6 and will be referred to as such hereon.) The production started already in the growth phase but increased after nitrogen depletion.

For example, the yield of carbon directed towards IPA (calculated as the ratio of C-mol of produced IPA to the C-mol of consumed acetate, expressed as a percentage) increased from 14 % during the growth phase to 37 % during nitrogen starvation, resulting in a total increase of 23 %. In contrast, the carbon yield towards biomass decreased by 24 % (see figure 6.2). The N-starvation strategy may have redirected most of the carbon previously used for biomass formation to IPA production.

It should be noted, that the N-starved conditions also increased the CO_2 excretion yield by 10 %. An increase in CO_2 formation was expected due to the fact that the IPA_atoDA pathway includes CO_2 producing step - acetoacetate to acetone conversion by the Adc enzyme. Thus, increased production during N-starved conditions would likely lead to a corresponding increase in CO_2 emissions. However, despite the increase in CO_2 emissions, the 24 % increase in IPA production seems to make N-starvation a useful strategy to direct carbon flux toward IPA formation.

Therefore, N-starvation was determined to be advantageous for IPA production and should be employed in subsequent fermentation processes.

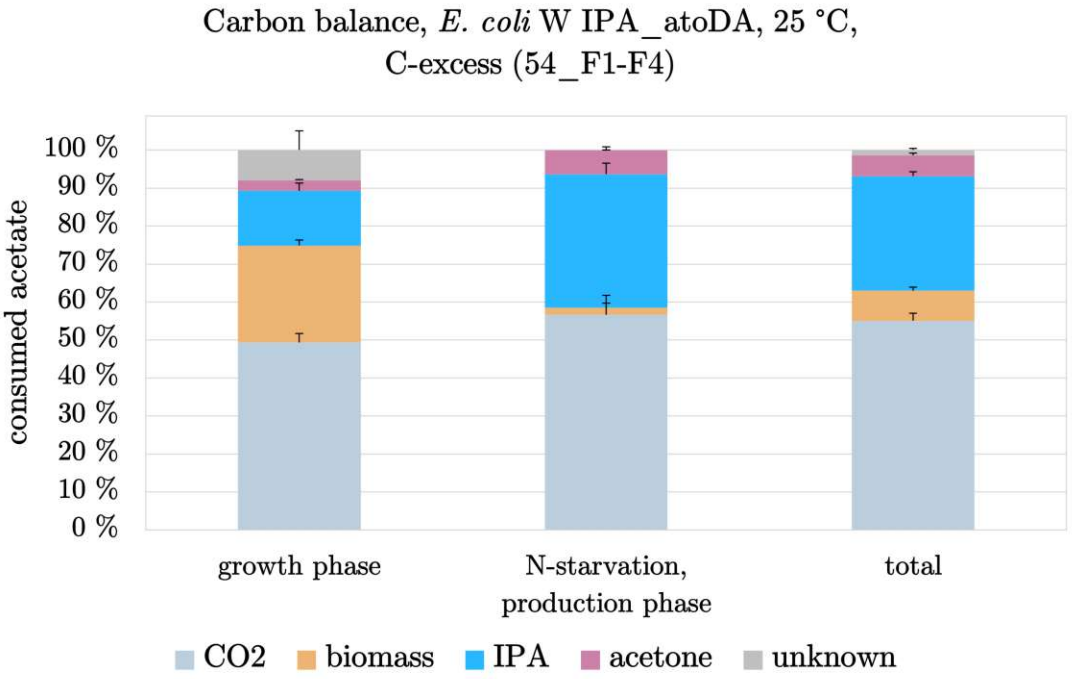

Figure 6.2: Carbon balance of *E. coli* W IPA_atoDA strain at 25 °C grown under carbon excess. Distribution of the consumed carbon mole of acetate to CO_2, biomass, IPA and acetone in percentage. Biological quadruplicates in 54_F1-F4 fermentation runs

The developed process had limitations, such as a 20-40 hour lag phase and variability between the biological quadruplicates (see figure 6.3). For example, 54_F1 and 54_F2 runs differed by 28.5 hours until nitrogen was depleted.

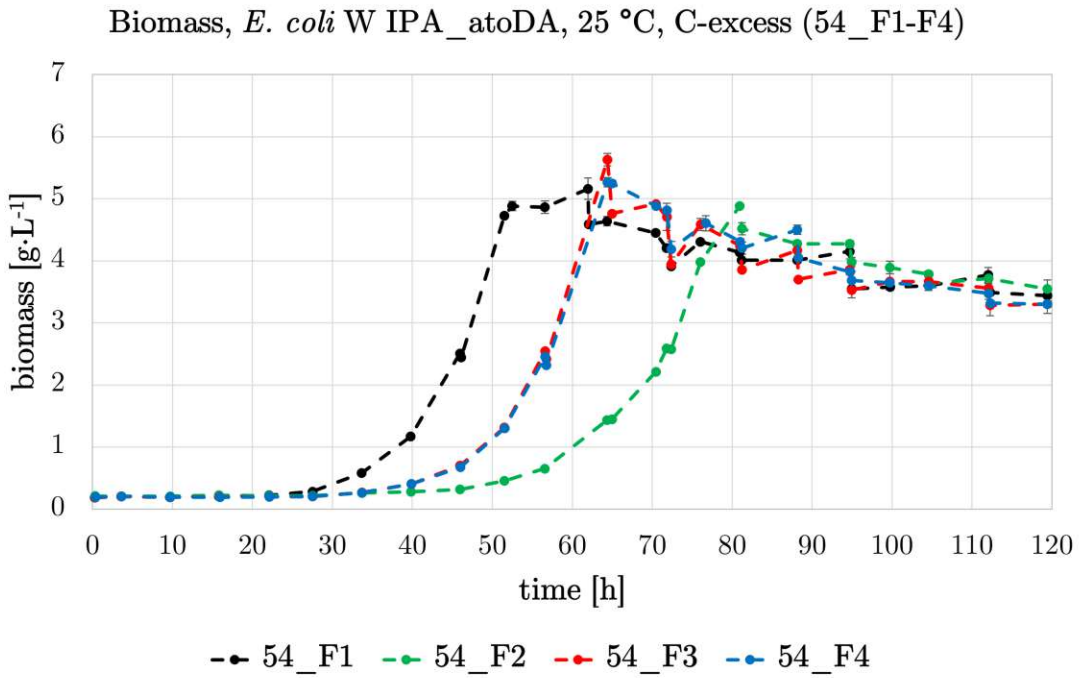

Figure 6.3: Biomass concentrations reached during the fermentation of *E. coli* W IPA_atoDA strain at 25 °C under carbon excess. Biological quadruplicates in 54_F1-F4 fermentation runs

To summarize, the aDA strain under carbon excess at 25 °C produced 11 g·L^{-1} IPA in 120 hours. However, the aDA cells exhibited long lag phases. As a result, there was high variability between the biological quadruplicates. N-starved conditions increased the productivity of the cells by possibly redirecting the carbon flux from biomass formation towards IPA production.

The lag phases in the growth of the aDA cells may have come from acetate being a challenging C-source (see 4.2). Development of another strain - *E. coli* W IPA_ptb_buk, which implements the ATP-coupled acetate to IPA conversion strategy, was of interest. This approach had the potential to improve the viability and/or productivity of the cells.

6.2 Strain development

We developed *E. coli* W IPA_ptb_buk (**pbu**) strain, containing IPA_ptb_buk pathway and *E. coli* W IPA_no_atoDA strain, containing IPA_no_atoDA pathway. The *E. coli* W IPA_no_atoDA strain, also referred to as the **reference** strain, was utilized as a negative control (see section 6.2.2 for more detailed information). The plasmids containing IPA_ptb_buk or IPA_no_atoDA pathways were assembled with GoldenMOC System, as described in detail in 5.1.2 section and [57] and transformed to *E. coli* W.

6.2.1 Development of the *E. coli* W IPA_ptb_buk strain

The BB1 GoldenGate assembly reaction [57] was used to integrate the *ptb_buk* sequence into the BB1 recipient vector. The reaction product (BB1_ptb_buk) was transformed into *E. coli* TOP10 (intermediate host used for plasmid propagation) via the heat shock method. The BB1_ptb_buk was then extracted and the accuracy of the assembly was confirmed by restriction enzyme analysis using agarose gel electrophoresis. 6 plasmids with the correct restriction pattern were sequenced. Mutations were identified in all of them. One of the plasmids contained a single-point mutation, converting the original ATT base sequence to ATC (*ptb* gene, c.462T>C). Despite this change, the codon was still coding for the isoleucine - the mutation was silent. Therefore, this BB1_ptb_buk plasmid was selected for subsequent assembly steps.

BB2_ptb_buk and BB3_IPA_ptb_buk were developed with a similar chain of steps. Finally, the accurately assembled BB3_IPA_ptb_buk construct was transformed into electro-competent *E. coli* W (production host) via electroporation. Plasmids from 4 colonies of *E. coli* W transformants were extracted and the accuracy of the assembly was confirmed by restriction enzyme analysis using agarose gel electrophoresis (see figure 6.4).

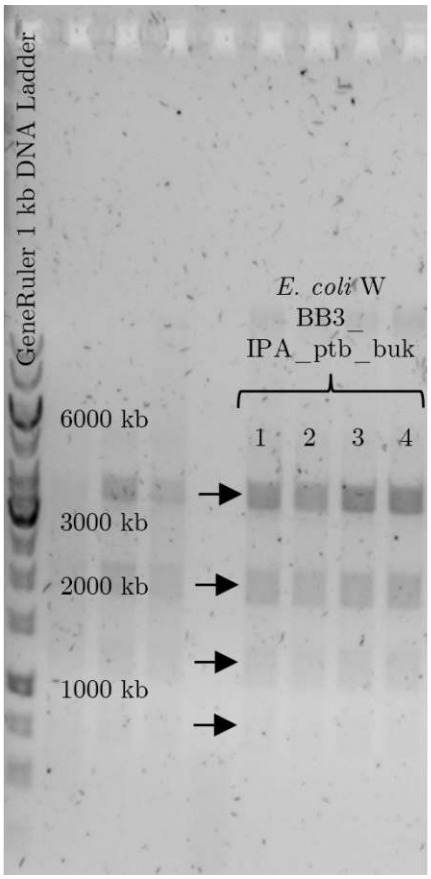

Figure 6.4: Agarose gel electrophoresis of BB3_IPA_ptb_buk plasmids extracted from *E. coli* W IPA_ptb_buk strain and restricted with XMAJI enzyme. A 1 kb DNA Ladder was used as a reference on the left side of the gel. Four samples were analyzed and all displayed the expected restriction pattern with bands at 844 bp, 1288 bp, 2102 bp and 3753 bp

Additionally, the (1) BB3_IPA_ptb_buk plasmid was sequenced. The silent mutation was maintained (*ptb* gene, c.462T>C).

The *E. coli* W cells from the colony with the sequenced BB3_IPA_ptb_buk plasmid were proliferated and stored at -80 °C. They were used in further experiments and are referred to as *E. coli* W IPA_ptb_buk (or pbu) strain.

6.2.2 Development of the reference strain

The BB3_IPA_no_atoDA plasmid was assembled with GoldenGate assembly reaction [57]. Accurately assembled BB3_IPA_no_atoDA was transformed into chemically competent *E. coli* W (production host) via the heat shock method. Plasmids from 7 colonies of *E. coli* W transformants were extracted and the accuracy of the assembly was confirmed in

5 of these colonies by restriction enzyme analysis using agarose gel electrophoresis - 844 bp, 1328 bp and 3753 bp bands were detected.

The *E. coli* W cells from the colony with the correct restriction pattern of the BB3_IPA_no_atoDA plasmid were proliferated and stored at -80 °C. They were used in further experiments and are referred to as *E. coli* W IPA_no_atoDA (or reference) strain.

Importance of the reference strain

The use of the reference strain is crucial since it was assumed that IPA production can occur even without additional copies of genes encoding enzymes for the acetoacetyl-CoA to acetoacetate conversion step on plasmids. The assumption was based on the natural occurrence of the AtoDA enzyme in *E. coli*. Therefore, the IPA titers of both strains should be compared to the titers reached by the reference strain (rather than to a baseline of zero), in order to evaluate the efficiency of the implemented pathway. If the reference strain would produce no IPA, it would indicate that any IPA produced by the pbu strain comes from the Ptb and Buk enzymes, thus confirming ATP-coupled IPA production.

6.3 Shake flasks: *E. coli* W IPA_ptb_buk at 25 °C and 37 °C

We cultured the pbu strain in shake flasks (SFs) to (i) characterize the pbu strain at two different cultivation temperatures for the first time; (ii) confirm the ATP-coupled IPA production by the pbu strain, through its comparison with the productivity of the reference strain; and (iii) conduct a preliminary comparison between the pbu strain and the aDA strain.

Shake flask experiments (SFEs) were carried out at 25 °C and at 37 °C. In each experiment, three strains - pbu, aDA and reference, were grown in triplicates.

6.3.1 Behaviour of the pbu strain

The pbu strain was able to produce IPA - the titer reached 0.19 ± 0.15 g·L^{-1} at 37 °C and even higher titers of 0.35 ± 0.02 g·L^{-1} at 25 °C, as shown in figure 6.5a. Notably, the higher titers at 25 °C were not accompanied by higher biomass levels, as seen in figure 6.5b. On the contrary, the specific growth rate of the pbu strain was higher at 37 °C not at 25 °C (0.046 ± 0.015 h^{-1} and 0.013 ± 0.001 h^{-1}, accordingly). Interestingly, the specific ($q_{acetate}$) and volumetric ($r_{acetate}$) acetate consumption rates are decoupled. For example, at 37 °C $r_{acetate}$ is higher, but $q_{acetate}$ is lower than at 25 °C.

These results suggest that the pbu strain tends to use the resources either for growth or for IPA production, for example, at 37 °C biomass production is preferred. This behaviour may indicate an uncoupling between growth and production in the pbu strain.

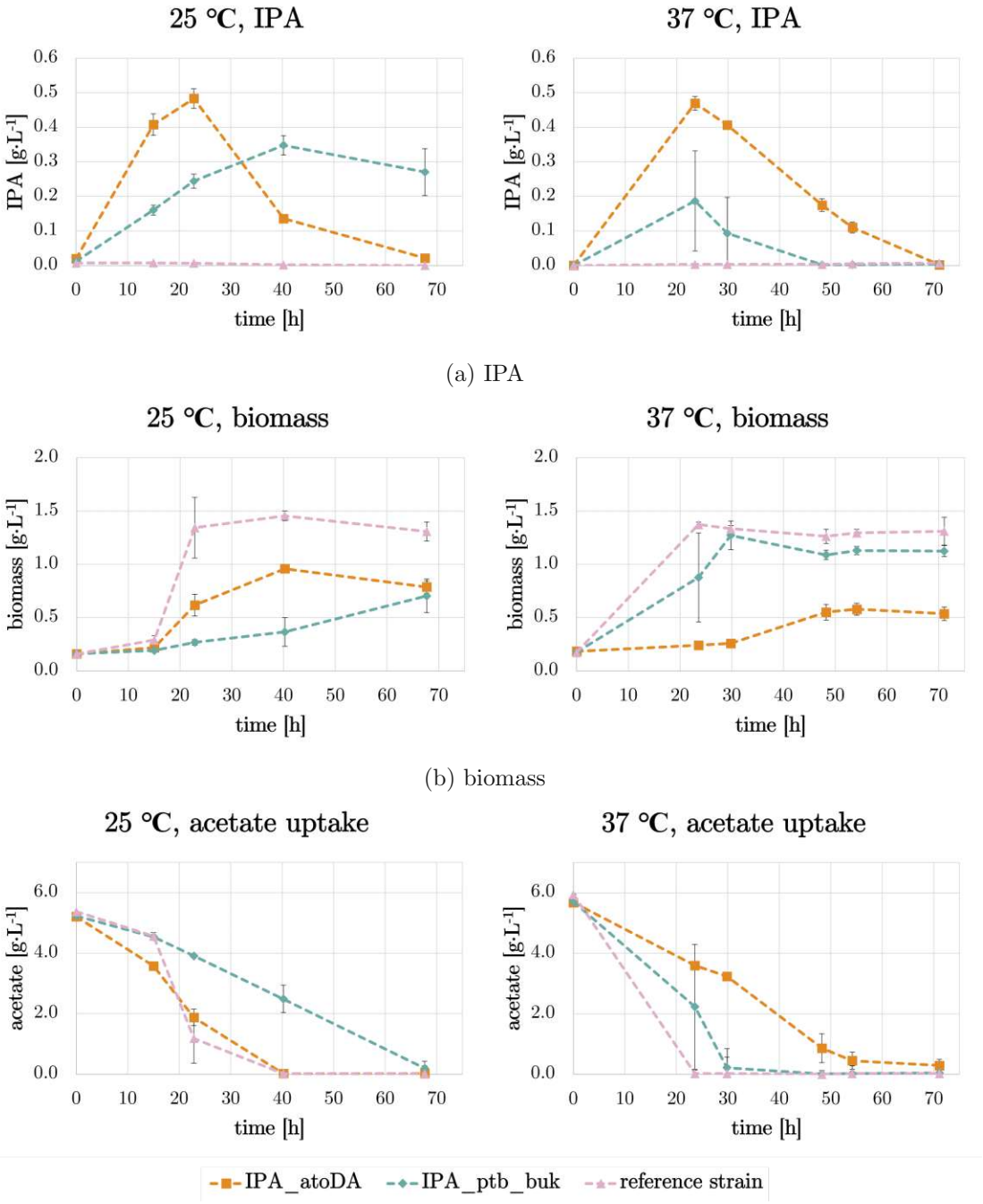

Figure 6.5: Isopropanol, biomass and acetate concentrations during the course of the SFEs at 25 °C and 37 °C. *E. coli* W IPA_ptb_buk, *E. coli* W IPA_atoDA and *E. coli* W IPA_no_atoDA (reference) strains

6.3.2 Confirmation of the ATP-coupled production of the pbu strain

The reference strain (*E. coli* W IPA_no_atoDA) did not produce significant amounts of IPA (see figure 6.5a). The HPLC analysis showed that the produced amounts of IPA were below the limit of quantification. Thus, it can be confirmed that the IPA produced by the pbu strain is mainly attributed to the activity of the Ptb and Buk enzymes, rather than an AtoDA enzyme that naturally occurs in *E. coli*. Consequently, whenever referring to the pbu strain, we can assume ATP-coupled IPA production.

6.3.3 Preliminary comparison between pbu and aDA

At both cultivation temperatures, the pbu strain reached lower titers than the aDA strain. In contrast to the pbu strain, the IPA titers of the aDA strain were not strongly dependent on the cultivation temperature, reaching 0.47 ± 0.02 g·L^{-1} at 37 °C and 0.48 ± 0.03 g·L^{-1} at 25 °C, as shown in figure 6.5a. However, the temperature did affect the specific growth rates of the aDA strain, with a lower μ at higher temperatures - a behaviour opposite to that of the pbu strain. Specifically, the μ of the aDA strain was 0.005 ± 0.002 h^{-1} at 37 °C and 0.044 ± 0.004 h^{-1} at 25 °C.

The aforementioned represents an intriguing finding: during the initial 23 hours of cultivation at 37 °C, the aDA strain achieved high IPA titers with minimal biomass growth. The $q_{acetate}$ was found to be the highest under these conditions and measured 0.555 ± 0.020 g·(g·h)$^{-1}$.

These results suggest that at 37 °C, the aDA cells prioritize directing the majority of the consumed acetate towards IPA production rather than biomass growth, which is opposite to the behaviour observed in the pbu strain at the same temperature.

6.3.4 Production of acetone, the precursor of IPA

The acetone titers of the pbu strain reached 0.13 ± 0.10 g·L^{-1} at 37 °C after 23 hours (see figure 6.6). Under identical experimental conditions, the aDA strain produced 0.33 ± 0.01 g·L^{-1} acetone.

Since acetone serves as a precursor for IPA in both the IPA_ptb_buk and IPA_atoDA pathways, all excreted acetone could have been converted to IPA. We calculated an acetone-to-IPA ratio for both the pbu and aDA strains at 37 °C and found it to be approximately 0.7. As a comparison, an acetone-to-IPA ratio of 1 would mean that the cells produce IPA and acetone in similar amounts. We consider a ratio of 0.7 to be quite high and assume difficulties during the acetone-to-IPA conversion step.

At 25 °C, both strains showed lower acetone to IPA ratios, with values of approximately 0.2 and 0.5 for pbu and aDA, respectively.

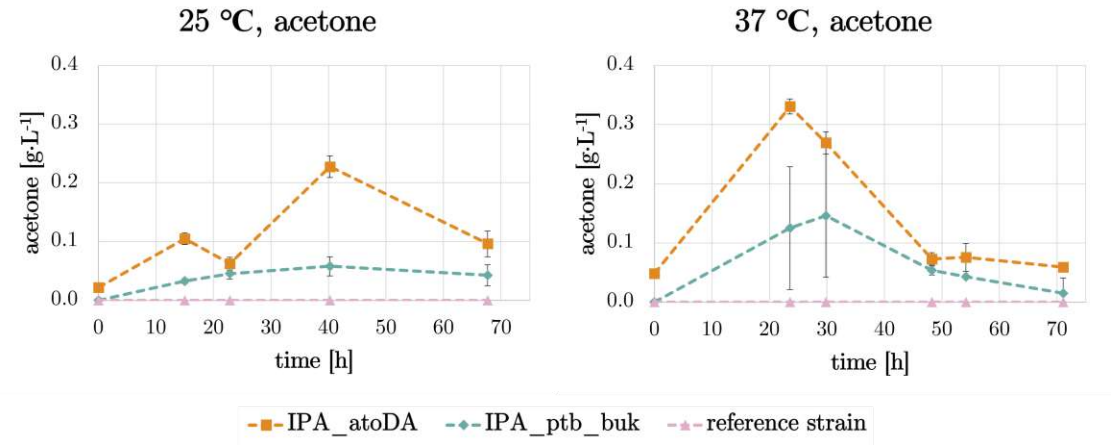

Figure 6.6: Acetone concentration during the shake flask experiments at 25 °C and 37 °C. *E. coli* W IPA_ptb_buk, *E. coli* W IPA_atoDA and *E. coli* W IPA_no_atoDA (reference) strains

Both acetone and IPA concentrations decreased at the end of the SFEs, which indicates a product loss due to evaporation, and the exact acetone-to-IPA ratios should be interpreted with care.

In general, factors such as product loss, insufficient oxygen supply and lack of pH control can influence the accuracy of the SFE results. Therefore, the exact numerical values from shake flask experiments should be interpreted cautiously and only the major behavioural trends are to be noted and considered (see table 9.1 in Additional file for a summary of the numerical values of the SFEs).

To summarize, the shake flasks results showed that pbu was able to produce IPA and the IPA production of the pbu strain can be seen as the ATP-coupled IPA production. The behaviour of the pbu strain strongly depended on the cultivation temperature and showed signs of uncoupled growth and production. At 37 °C, more biomass and less IPA were synthesized, whereas, at 25 °C it was more IPA and less biomass. Faster growth at 37 °C was accompanied by accelerated volumetric acetate uptake but, also, by a lower specific acetate uptake rate. In comparison with the aDA, the pbu strain reached lower IPA titers and lower specific acetate uptake rates at both temperatures. However, the growth and volumetric acetate uptake were quicker by the pbu strain at 37 °C.

The limitations of the SFEs may have affected the accuracy of the IPA production results of the pbu strain, indicating a need for more precise and controlled cultivation using bioreactors. Previous experiments involving the N-starved aDA strain at 25 °C (see section 6.1) have shown the efficacy of N-starvation in redirecting carbon from biomass to IPA production, resulting in higher productivity. Therefore, it was of interest to cultivate the pbu strain at 37 °C, rapidly multiplying cells during the growth phase, and

then redirecting all cell resources from the quick growth towards IPA production with the application of the N-starvation strategy. This approach was expected to increase IPA yields and titers of the pbu strain while reducing the processing time.

6.4 Bioreactors: an overview of the fermentation runs

Table 6.1 presents an overview of the fermentation runs conducted at 37 °C that will be presented and discussed in the course of this work in later sections. These runs were performed to characterize the pbu strain and evaluate its major behavioural traits in comparison to the aDA strain.

Similarly to the "overview of the process design" section (6.1), all fermentation runs were divided into growth and N-limited production phases. In the growth phase, two different conditions were tested: (i) fermentation under C-excess, where acetate was provided through pulses or/and non-limited feed, and (ii) fermentation under C-limitation, where acetate was provided in limited amounts exponentially through a feed pump. The C-excess runs aimed to achieve the desired biomass levels rapidly while simultaneously determining the maximum specific growth rates of both strains at 37 °C. In addition, these runs allowed the evaluation of the rates of IPA production and acetate uptake during non-limited growth. The C-limitation runs were performed to compare the acetate uptake and productivity of the strains under the same specific growth rate, which was maintained using a limiting feed strategy.

The subsequent sections, 6.5 & 6.6, discuss the main characteristics of the aDA strain and pbu strain under the C-excess conditions, respectively. Then, in sections 6.7 & 6.8, the results from the aDA strain and pbu strain under C-limitation are shown. Finally, section 6.9 provides a final comparison between the two strains. At the end of each section, a brief summary of the main findings presented in that section can be found.

Table 6.1: Fermentation runs at 37 °C presented and discussed in course of this thesis

Strain	Run	Conditions	Goal
E. coli W IPA_atoDA (**aDA**)	71_F3	C-excess, see 6.5	The runs were conducted in order to provide a comparison for the pbu strain cultivated under the same conditions, specifically under C-excess and under the same specific growth rate (C-limitat)
	71_F4	C-limit, see 6.7	
E. coli W IPA_ptb_buk (**pbu**)	69_F1	C-excess, see 6.6	The runs were conducted to evaluate the performance of the novel pbu strain in bioreactors under conditions of C-excess, under the set specific growth rate (C-limit), and under nitrogen-starvation
	69_F3		
	69_F2	C-limit, see 6.8	
	69_F4		

6.5 Bioreactors: *E. coli* W IPA_atoDA at 37 °C under carbon excess

As stated in the summary of the SFE section (6.3), our intention was to cultivate the pbu strain at 37 °C. The performance of both the aDA and pbu strains in shake flasks was significantly influenced by temperature. Therefore, it would be inaccurate to directly compare the results of the pbu strain at 37 °C with the previous findings of the aDA strain at 25 °C (presented in the "overview of the process design" section 6.1).

To enable a fair comparison between the two strains, we conducted fermentations of the aDA strain at 37 °C under N-starved conditions. Cultivation presented in this section was carried out under C-excess conditions during the growth phase. The acetate concentration was maintained within the range of 1.5-11 $g \cdot L^{-1}$ through the use of pulses and/or feed. The production phase started after nitrogen depletion.

The data presented in this section are derived from a single fermentation run (71_F3) to serve as a point of comparison for the pbu strain. Nonetheless, it is important to note that the crucial behavioural characteristics observed during the growth phase in 71_F3 were reproducible during the other runs, which were not included in this thesis.

6.5.1 Is the metabolic switch in the growth phase the moment of highest productivity in the aDA strain?

The aDA strain produced predominantly IPA, with the titers reaching 10.5 g·L^{-1} in 121 hours (see figure 6.7). The acetone titers reached 3.0 g·L^{-1}. The acetone to IPA ratio was, approximately, 0.3.

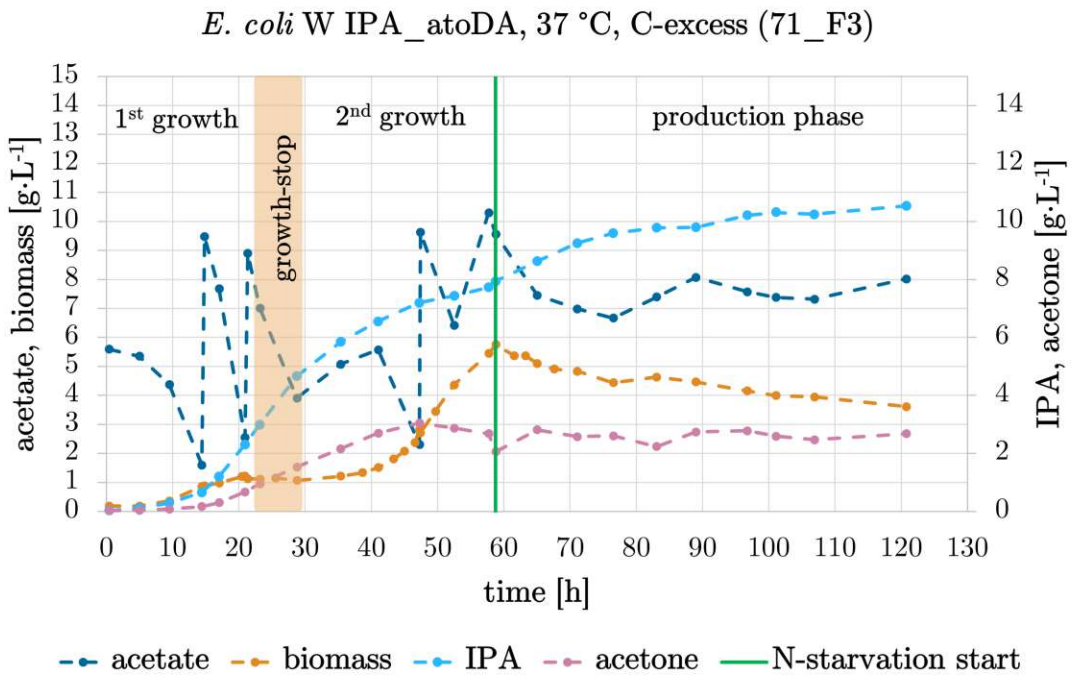

Figure 6.7: Fermentation results of *E. coli* W IPA_atoDA at 37 °C grown under carbon excess in 71_F3 fermentation run. The growth-stop period around 23-29 process hours is highlighted

Growth retardation during the growth phase increased IPA production

The aDA strain began IPA production during the growth phase, with the highest q_{IPA} value of 0.34 g·(g·h)$^{-1}$ observed around 23-29 hours of fermentation (see figure 6.8). This period is also characterized by the retardation of aDA cell growth and is referred to as the "growth-stop" period (6.7). During the growth-stop, specific acetate uptake also was high, with $q_{acetate}$ values of 1.2 g·(g·h)$^{-1}$. A similar period of quick IPA production, retarded growth and high $q_{acetate}$ was previously observed in SFEs at 37 °C (see section 6.3) The growth-stop period was not observed during the cultivations of the aDA strain at 25 °C (see section 6.1).

These results imply that during the growth-stop period (23-29 process hours), a significant portion of the consumed acetate was channelled towards IPA production instead

of biomass formation.

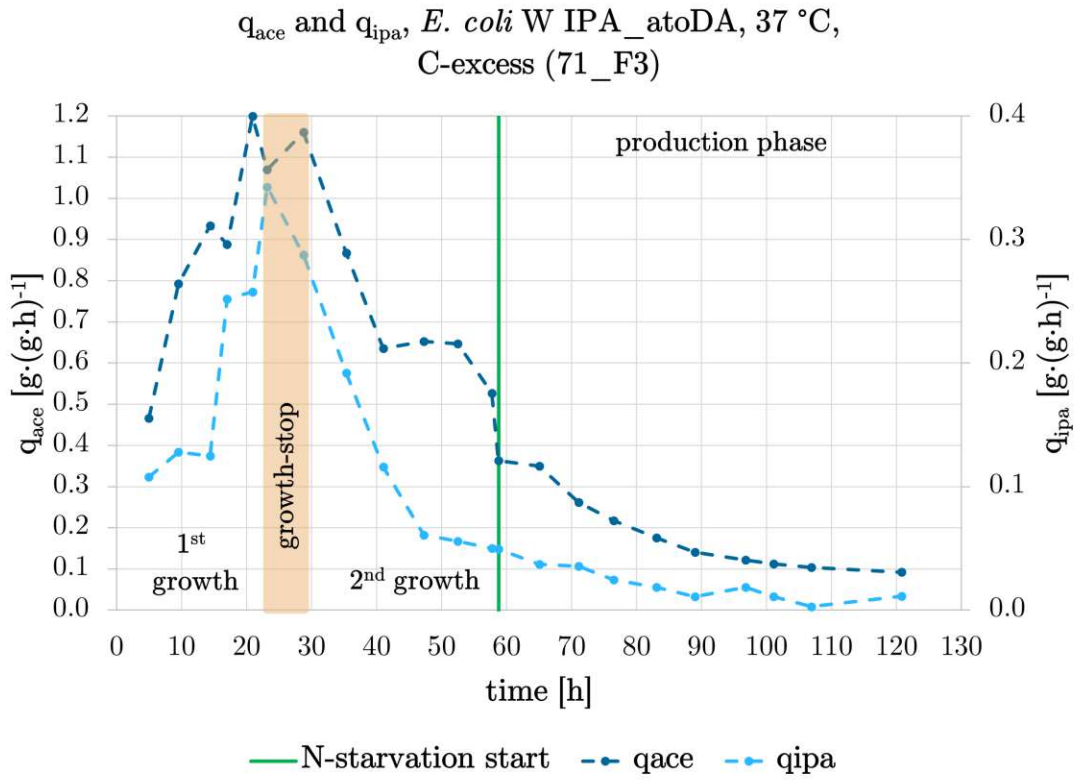

Figure 6.8: Specific rates of acetate consumption and IPA production during the fermentation of *E. coli* W IPA_atoDA at 37 °C under carbon excess. The growth-stop period around 23-29 process hours is highlighted

The "growth-stop" period: 53.5 % of consumed carbon directed towards IPA/acetone production

The carbon balance analysis confirms the direction of the consumed carbon towards IPA and acetone production. Figure 6.9 shows that during the growth-stop period, the aDA cells converted 53.5 % of all consumed carbon to products - 39 % to IPA and 14.5 % to acetone. The remaining carbon was excreted in the form of CO_2, with no carbon losses observed.

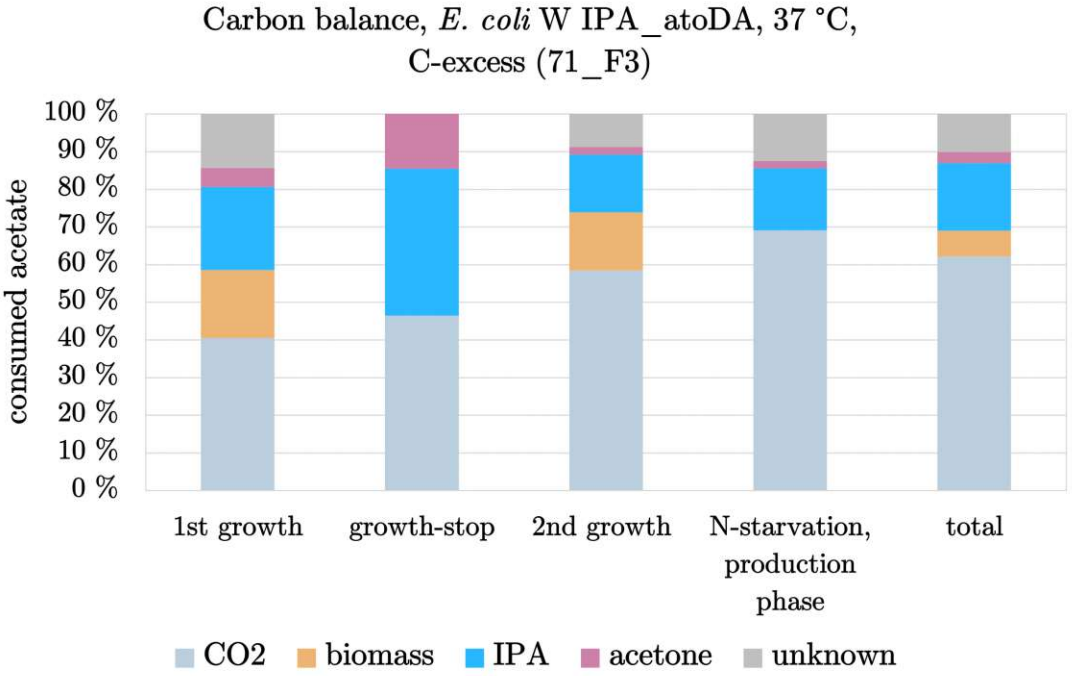

Figure 6.9: Carbon balance of *E. coli* W IPA_atoDA at 37 °C grown under carbon excess. Distribution of the consumed carbon mole from acetate to CO_2, biomass, IPA and acetone in percentage. The growth phase is divided into the 1st growth (0-14 hours), the growth-stop (23-29 hours) and the 2nd growth (41-59 hours) phases

Behavioral changes following the "growth-stop": Evidence of a metabolic switch?

The growth-stop period was also characterised by the retarded NH_4 consumption (data not shown). The NH_4 is important for biomass formation but is not needed for the IPA/acetone production. It is possible, that due to the stop of the growth of the aDA cells, less NH_4 was required and, therefore, less was consumed. Continued acetate, but retarded NH_4 consumptions during the growth-stop period resulted in the increased yield between the consumed acetate and consumed NH_4, further referred to as a C/N ratio.

The C/N ratio during the stop-growth period was five-fold higher than the C/N ratio of the 1st growth phase (see figure 9.1 in Additional file). Interestingly, the C/N ratio of the 2nd growth was 1.5-fold higher compared to the values of the 1st growth.

The changed C/N ratio was not the only difference between the 1st and 2nd growth phases. Also, lower growth rate, lower specific acetate uptake rate, decreased specific IPA production rate, lower NH_4 consumption rate and higher CO_2 emissions characterised the 2nd growth phase. The behavioural changes after the growth-stop period may indicate a

temperature-specific metabolic switch that is happening in the aDA cells at 37 °C during the stop-growth period.

The possible trigger of the metabolic switch could be the changes in biomass concentrations, causing the changed intercellular interactions between the cells. Another trigger could be the changes in the acetate concentration - the growth retardation happened at the end of the first acetate batch when the first acetate pulses were added. The acetate concentrations in a medium can influence the strain behaviour by inhibiting the growth and influencing the activity of the acetate uptake enzymes as was discussed in section 4.4.2. Lastly, the growth-stop behaviour may also be attributed to the necessary metabolic adaptation when transitioning from glucose as the main carbon source in the second preculture flasks to acetate as the main carbon source in the reactor cultivations. In the case of cultivations at 25 °C, this adaptation period between glucose and acetate may occur during the long lag phases (see results from section 6.1).

It is challenging to describe the probable metabolic switch in detail due to the lack of metabolic data. Additional metabolic research, which goes out of the scope of the master thesis, is crucial to fully understand the observed growth-stop behaviour of the aDA strain at 37 °C.

However, it is important to highlight that the stop-growth period was, in fact, the most efficient IPA production phase for the aDA cells at 37 °C.

To summarize, the aDA strain cultivated at 37 °C under C-excess conditions demonstrated IPA titers of 10.5 $g{\cdot}L^{-1}$ and acetone titers of 3.0 $g{\cdot}L^{-1}$. However, most of the IPA production by the aDA strain occurred during the growth-stop phase and may have been caused by a metabolic switch. Further evaluation of the pbu strain under similar conditions is necessary to provide additional insights.

6.6 Bioreactors: *E. coli* W IPA_ptb_buk at 37 °C under carbon excess. Comparison of the aDA and pbu strains under C-excess conditions

We conducted a cultivation of the pbu strain at 37 °C under N-starved conditions with two main objectives: (i) to gain a more comprehensive understanding of the productivity and behavior of the pbu strain, comparing it to the results obtained during the SFEs and the performance of the aDA strain, and (ii) to investigate the possibility of redirecting carbon flux from rapid biomass formation towards production through the implementation of the N-starvation strategy.

We conducted fermentation in biological duplicates and divided each process into two phases: growth - nitrogen batch and production - nitrogen starvation (figure 6.10).

Acetate was provided in excess via pulses and feed. The acetate concentration was kept in 0.5-12 $g \cdot L^{-1}$ range. The acetate was added as needed based on cell behaviour, resulting in varying acetate addition patterns between biological duplicates.

6.6.1 Negligible IPA production

The IPA titers of the pbu strain were found to be very low, with a maximum of 0.17 $\pm$ 0.02 $g \cdot L^{-1}$ reached after 75 hours. It is worth noting that both biological duplicates achieved similarly low IPA titers, indicating the robustness of the findings. Acetone production was predominant and reached 1.51 $\pm$ 0.07 $g \cdot L^{-1}$. In comparison, the aDA strain demonstrated IPA titers 62 times higher and acetone titers 2 times higher than those observed in the pbu strain (see section 6.5).

Additionally, one of the major differences in the productivity of pbu and aDA is the start of production. In the case of the aDA strain, the growth-stop phase prior to N-starvation represents a period of highly efficient production (see section 6.5). On the other hand, the pbu strain initiates production only after the start of N-starvation. These findings further support the hypothesis of the pbu strain exhibiting a decoupled growth and production behaviour, which was previously noted during the SFEs.

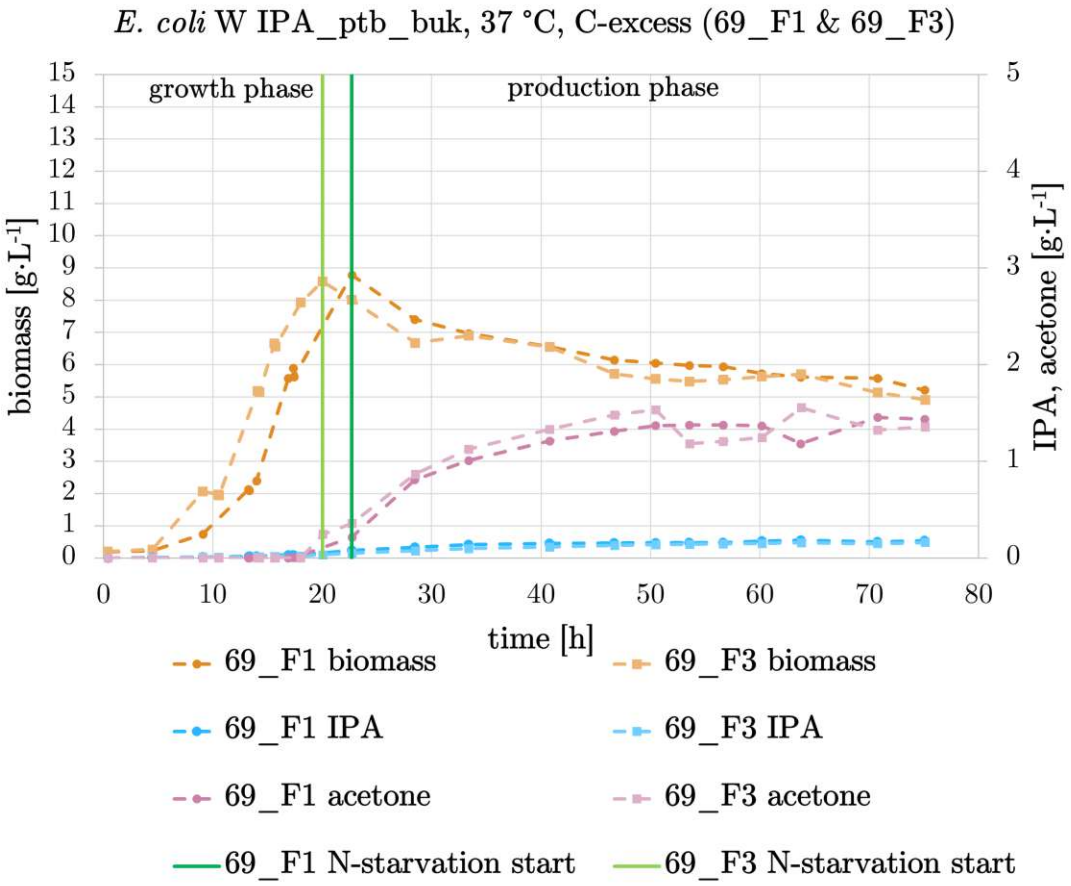

Figure 6.10: Fermentation results of *E. coli* W IPA_ptb_buk at 37 °C grown under carbon excess. Biological duplicates in 69_F1 and 69_F3 fermentation runs

6.6.2 Rapid growth

Similar to the behaviour observed during the SFEs at 37 °C, the pbu strain demonstrated a higher specific growth rate compared to the aDA strain. Specifically, the pbu cells exhibited rapid multiplication without a lag phase, with a μ of 0.25 $\pm$ 0.05 h^{-1}. In comparison, the specific growth rates of the aDA strain during the first and second growth phases were 1.7 and 3.3 times lower, respectively, than the specific growth rate of the pbu strain.

6.6.3 Specific acetate uptake rates

Figure 6.11 shows the specific acetate uptake rates of the pbu and aDA strain plotted against the time before the N-starvation. The line representing the acetate uptake of the aDA strain in the figure is longer compared to that of the pbu strain because the aDA strain required more time to consume all available nitrogen. As was mentioned in

section 6.5, this behaviour can be attributed to a possible metabolic switch that divided the growth phase into three distinct periods: the first growth, growth-stop, and second growth phases.

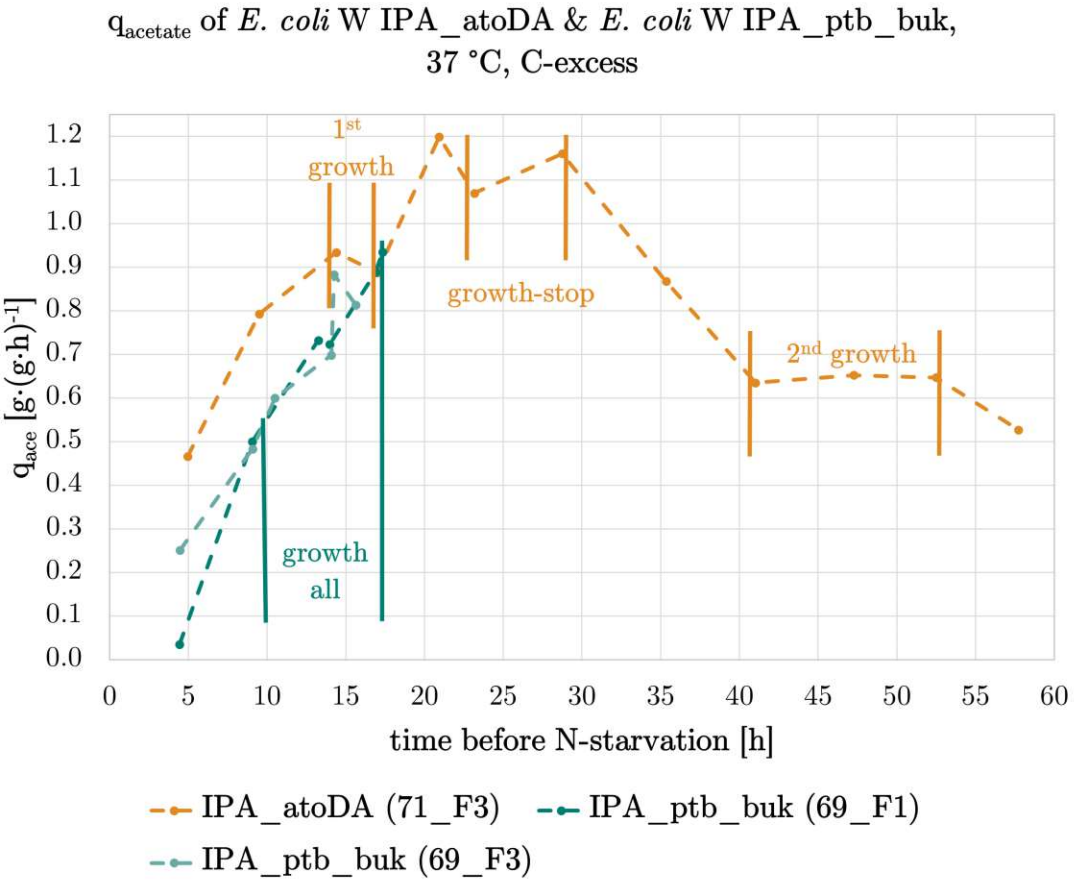

Figure 6.11: Comparison of specific acetate uptake rates between *E. coli* W IPA_ptb_buk and *E. coli* W IPA_atoDA strains before N-starvation start. 37 °C, carbon excess during the growth phase. The time periods, taken for the calculation of the rates presented in table 6.2 are highlighted. *E. coli* W IPA_atoDA: 1st growth (14-17 hours), the growth-stop (23-29 hours) and the 2nd growth (41-52 hours) phases; *E. coli* W IPA_ptb_buk: the "growth all" phase (10-18 hours)

To sum up, the specific acetate uptake rate of the pbu strain is (i) lower than the $q_{acetate}$ of the aDA strain in the 1st growth phase but is (ii) higher than the $q_{acetate}$ of the aDA strain in the 2nd growth phase. Additionally, as was mentioned in section 6.5, the highest specific acetate uptake rate was demonstrated by the aDA strain during the "stop-growth" period. The numerical summary can be found in table 6.2.

Table 6.2: $q_{acetate}$ during the growth phase under C-excess of *E. coli* W IPA_ptb_buk (**pbu**) and *E. coli* W IPA_atoDA (**aDA**) strains

Strain	Phase	Time [h]	$q_{acetate}$ [g·(g·h)$^{-1}$]	Data source
pbu	growth all	10 - 18	0.791 ± 0.002	69_F1 / 69_F3
	1st growth	14 - 17	0.911 ± 0.033	71_F3
aDA	growth-stop	23 - 29	1.115 ± 0.064	71_F3
	2nd growth	41 - 52	0.645 ± 0.009	71_F3

The higher specific acetate uptake rate of the aDA strain in the first growth phase can be attributed to the possible facilitation of acetate uptake through the involvement of the AtoDA enzyme from the IPA_atoDA pathway (see section 4.4.6). Subsequent metabolic alterations in the aDA strain may have led to changes in acetate uptake, resulting in lower $q_{acetate}$ values. However, since the precise mechanism underlying the potential metabolic switch remains unknown, it is challenging to develop further hypotheses at this time.

In addition, it is important to consider that specific acetate uptake rates are influenced by the specific growth rates of the strains. To make a more accurate comparison of acetate uptake capabilities between the two strains, it is necessary to compare them under conditions of the same specific growth rate.

6.6.4 High volumetric acetate uptake rates

Similar to the behaviour observed in the SFEs (6.3), the volumetric acetate consumption of the pbu strain exhibited a direct correlation with cell growth, reaching high values of 5.73 ± 0.52 g·(L·h)$^{-1}$. In comparison, the maximum $r_{acetate}$ values for the aDA strain were only half of this magnitude.

The high volumetric acetate uptake observed in the pbu strain prompted the initiation of additional acetate feed, along with acetate pulses, to maintain an excess of acetate concentration in the reactor.

6.6.5 Does N-starvation at 37 °C redirect the carbon rate from biomass formation to CO_2 emission?

Although the N-starved conditions positively influenced pbu productivity by initiating IPA and acetone production, the N-starvation also had its drawbacks. Carbon balance analysis revealed that after the start of N-starvation, the carbon yield to CO_2 increased

by 23 % from 44 % to 67 % (see figure 6.12). In comparison, the formation of biomass decreased by 30 %.

A similar impact from the N-starvation was also observed in the aDA strain, where the carbon yield to CO_2 after the start of N-starvation increased by 29 % compared to the first growth phase. The biomass yield decreased by 18 %. (see figures 6.12 or 6.9).

An increase in CO_2 emissions by approximately 10-15 % was expected based on the results from the "overview of the process design" section 6.1 and due to the fact that both the IPA_ptb_buk and IPA_atoDA pathways include a CO_2-producing step. Therefore, the observed increases of 23-29 % seem to be high. We assume that the carbon flux from biomass formation was mainly redirected towards CO_2 emission, not IPA/acetone production.

The impact of N-starvation may not be specific to a particular pathway but rather dependent on the cultivation temperature. This suggestion is supported by the contrasting results observed during cultivations of the aDA strain at 25 °C (see section 6.1) and at 37 °C (see section (6.5).

6.6.6 High carbon losses in the carbon balance analysis of the pbu strain

It is important to note that the carbon balance analysis used to calculate carbon distributions had its limitations. In the case of the pbu strain, a significant portion (27.1 ± 0.3 %) of the carbon moles consumed as acetate were not detected in either the off-gas, biomass, acetone or IPA (referred to as "lost carbon" in figure 6.12).

In comparison, the aDA strain fermented under similar conditions had a total carbon loss of only 10 %. (It is worth mentioning that the increased carbon losses observed in the aDA strain at 37 °C compared to its fermentation at 25 °C (where losses were only 2 %) may be attributed to higher product evaporation at the higher temperature.)

Possible reasons for the high carbon losses of the pbu strain include: (i) the excretion of unknown and non-analyzed metabolites, (ii) an unknown biomass composition of the pbu cells or (iii) the high volatility of the predominant product, acetone.

Non-analyzed excreted metabolites It is possible, that the pbu cells excreted some metabolites that were not included in the carbon balance equation (5.2). For example, it is known that *E. coli* is able to excrete extracellular polymeric substances (EPS) - high molecular weight polymers, playing a role in biofilm formation. EPS can be composed of polysaccharides [60] and/or proteins [61].

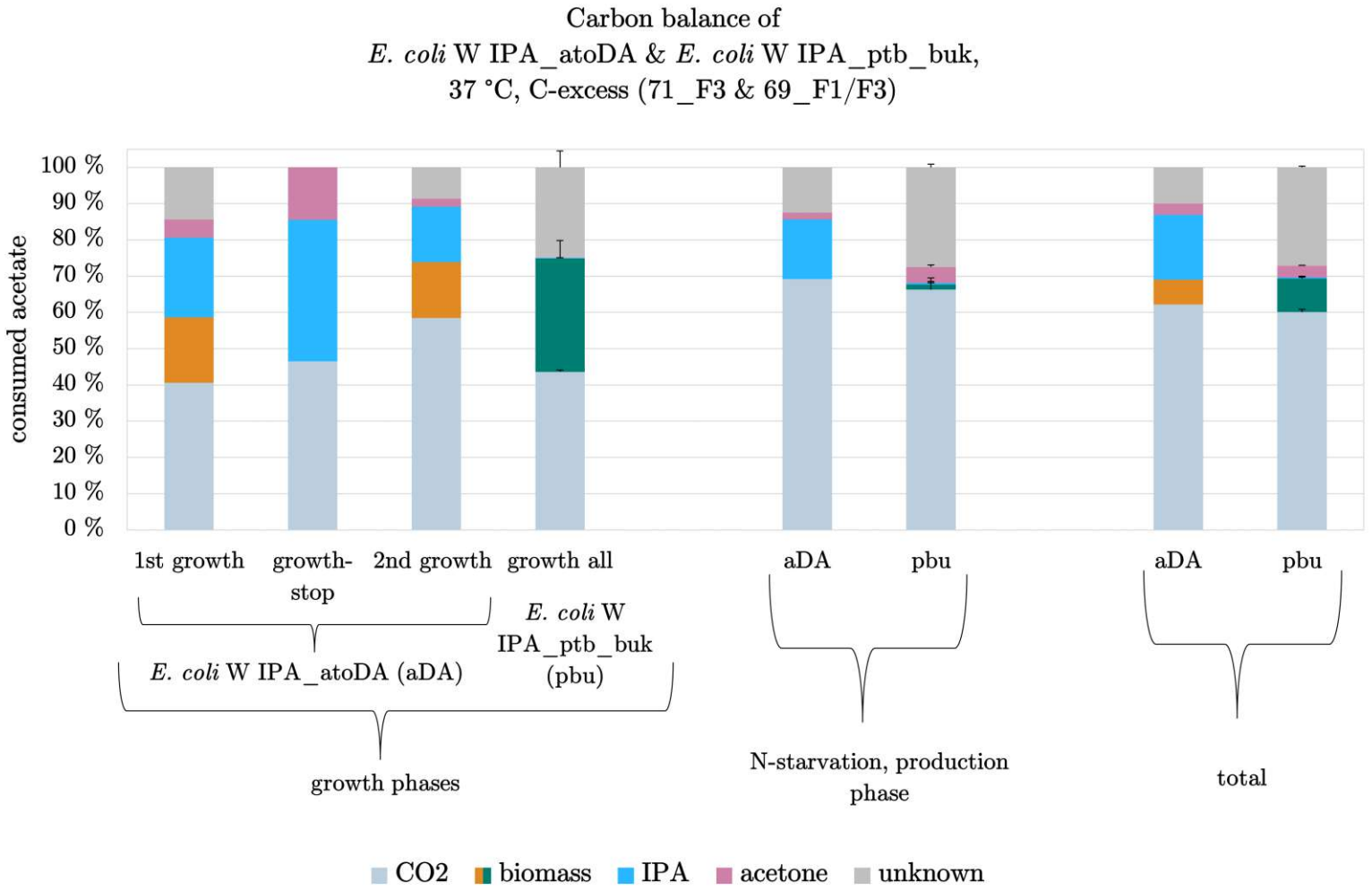

Figure 6.12: Comparison of carbon balances of *E. coli* W IPA_ptb_buk (pbu) and *E. coli* W IPA_atoDA (aDA) strains at 37 °C grown under carbon excess. Distribution of the consumed carbon mole from acetate to CO_2, biomass, IPA and acetone in percentage. The growth phase of the aDA strain is divided into the 1st growth (0-14 hours), the growth-stop (23-29 hours) and the 2nd growth (41-59 hours) phases

Unknown biomass composition The biomass composition of the pbu strain was not determined. We assumed the biomass composition is comparable between aDA and pbu strains and used the aDA values for the carbon balance calculations of the pbu strain. This influenced the calculations, especially because of the high biomass titers, reached by the pbu strain.

Acetone evaporation After 50 hours of process time, acetone concentrations in both reactors reached a plateau. This could be caused by the decreased productivity of the pbu cells or by inefficient acetone capture in bioreactors and washing flasks. Non-captured acetone was carried away with the gas flow in the off-gas tube, contributing to the observed carbon losses.

6.6.7 Was a mutation in the pbu strain responsible for the low IPA titers and rapid growth?

To sum up, the bioreactor experiments revealed that the pbu strain exhibited a behavioural pattern characterized by (i) rapid cell growth, (ii) quick volumetric acetate uptake, and (iii) relatively high acetone but very low IPA production when cultured under C-excess. This pattern is referred to as the pbu-C-excess behavioural pattern.

It is possible that the same pattern was also present during the SFEs. During the second sampling of the SFEs grown at 37 °C, a high standard deviation was observed between the triplicates of the pbu strain (see figure 6.5). One of the flasks exhibited the pbu-C-excess pattern, while the second one showed contrasting behaviour (slower growth and volumetric acetate uptake but higher IPA production together with low acetone production). The third flask's parameters were in between the parameters of the previously mentioned flasks.

Initially, it was challenging to explain the described variations between the SFs during the second sampling procedure and we had assumed that the shake flasks were most probably sampled during a phase of rapid exponential growth and that the product concentrations were influenced by evaporation issues. However, if taking into account the bioreactor results, we now hypothesize that the pbu-C-excess pattern may be attributed to the inability to conduct the acetone-to-IPA conversion step. By not producing IPA, resources may have been saved and used for cell growth, leading to faster multiplication of cells. The inability to convert acetone to IPA could be caused by either (i) a mutation in the *adh* gene sequence within the IPA_ptb_buk plasmid or (ii) metabolic regulation resulting in a lack of NADPH during N-starved conditions after growth on C-excess. The availability of NADPH molecules is crucial because the Adh enzyme requires NADPH for the acetone-to-IPA conversion step.

Indeed, it has been reported that IPA production during the exponential growth phase was hindered due to the lack of NADPH (Okahashi et al., [44]). However, it is important

to highlight that in their study, the authors used glucose as the carbon source, and they observed that IPA production became feasible after the onset of N-starvation conditions.

Therefore, it may be noted that a mutation could provide a more likely explanation for the observed low IPA titers in both shake flasks and bioreactors. A small number of mutated cells with a higher specific growth rate could outgrow the IPA-producing cells, leading to the preservation of the pbu-C-excess behavioural pattern in the population and homogenization of the behaviour in the SFs during the later experiment hours, as was observed. In turn, the low IPA titers observed in bioreactors could be explained by the presence of a few non-mutated IPA-producing pbu cells still present in the culture after the start of N-starvation. Over time, the IPA-producing cells would die off, and the titers would remain at the same level, as observed.

We cannot reliably determine from the collected data whether a mutation occurred or not, and we also cannot determine whether the observed pbu-C-excess pattern is characteristic of the original pbu strain or a mutated version. Therefore, we will approach the results from this section with caution and refrain from characterizing the behavior of the pbu strain based solely on this section.

To summarize, under N-starved, C-excess conditions at 37 °C, the pbu strain exhibited lower IPA and acetone titers compared to the aDA strain, despite having a higher specific growth rate. The production of acetone and IPA in the pbu strain started only after the initiation of N-starvation, whereas in the aDA strain, production was feasible throughout the entire process. Additionally, IPA titers of the pbu strain were negligible, indicating an inability to convert acetone to IPA. This could potentially be attributed to a mutation that may have occurred within the IPA_ptb_buk plasmid during the growth phase. Due to the lack of IPA production and the possibility of a mutation, it is cautioned against solely characterizing the behaviour of the pbu strain based on this section.

It is worth noting that at 37 °C, both the aDA and pbu strains exhibited a trend under N-starved conditions where the carbon flux, previously allocated to biomass formation, was redirected towards CO_2 emissions instead of acetone/IPA production. This behaviour highlights a limitation of implementing the N-starvation strategy at 37 °C.

6.7 Bioreactors: *E. coli* W IPA_atoDA at 37 °C under carbon limitation

Alongside the C-excess aDA run (see section 6.5), we cultivated the aDA strain at 37 °C under C-limited conditions during the growth phase. The N-starvation was again applied during the production phase. After the start of N-starvation, the acetate was provided in excess, and its concentration was maintained around 6-11 $g{\cdot}L^{-1}$.

The C-limiting acetate feed during the growth phase was enabling a constant specific growth rate (μ) of approximately 0.08 h^{-1}. We intended to grow both aDA and pbu at the same μ, allowing for a more reliable comparison of specific rates ($q_{acetate}$, q_{IPA}) during the growth phase. This section presents the key behavioural traits of the aDA strain, while the major traits of the pbu strain and the subsequent comparison are presented in the following sections.

The data presented in this section are derived from a single fermentation run (71_F4, see figure 6.13). However, it is important to note that the crucial behavioural characteristics observed during the growth phase in 71_F4 were observed during the other runs, which were not included in this thesis.

6.7.1 Metabolic switch observed during C-limited conditions

We assume that the aDA-strain-specific metabolic switch observed in section 6.5 may have occurred again, this time under C-limited conditions. Although the first growth phase, the growth-stop period and the second growth phase are less distinguishable due to applied feeding rates, growth retardation around 23-29 process hours was observed (see figure 6.13).

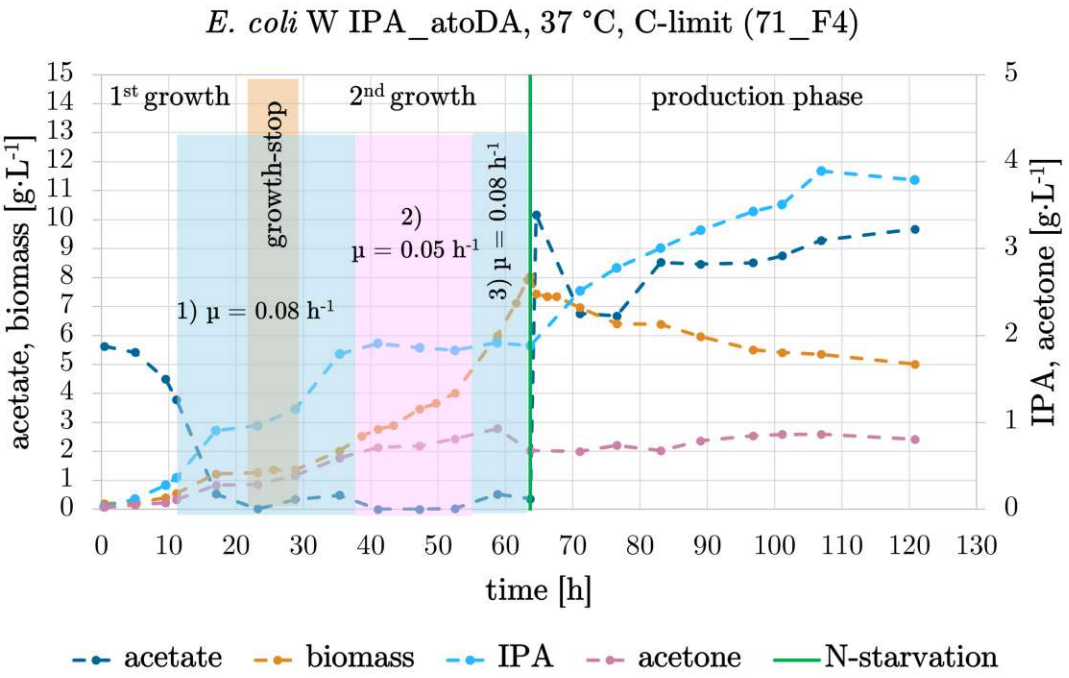

Figure 6.13: Fermentation results of *E. coli* W IPA_atoDA at 37 °C grown under carbon limitation in 71_F4 fermentation run. Feed: 1) 11.5-38 h; 2) 38-55 h; 3) 55-63.7 h. The growth-stop period around 23-29 process hours is highlighted

6.7.2 Was the desired μ higher as the μ_{max} of the aDA strain during the 2nd growth phase at 37 °C?

We experienced difficulties in reaching the C-limiting conditions during the growth of the aDA strain. We hypothesize that, it happened because the desired specific growth rate (0.077 h^{-1}) was slightly higher than the maximal specific growth rate of the aDA strain during the 2nd growth phase (0.076 ± 0.026 h^{-1}, calculated from the section 6.5 data). In order to better understand our hypothesis one can take a look at the pattern between the applied feeding control and reached acetate concentrations.

1) $\mu \approx$ 0.08 h^{-1}, highlighted blue in figure 6.13, 11.5-38 hours After 11.5 process hours, the feed rate calculated for the specific growth rate of 0.077 h^{-1} was initiated. However, the applied limitation was insufficient, and we measured the accumulated acetate around 28-35 process hours, during the 2nd growth phase of the aDA strain.

2) $\mu \approx$ 0.05 h^{-1}, highlighted pink in figure 6.13, 38-55 hours To address the issue of accumulated acetate, we decreased the feeding rate starting at 38 process hours. This led to a drop in acetate concentrations to zero, achieving C-limiting conditions. The specific growth rate between 38 and 55 hours was 0.053 ± 0.013 h^{-1}.

3) $\mu \approx$ 0.08 h^{-1}, highlighted blue in figure 6.13, 55-63.7 hours While conducting the experiment, we assumed that acetate accumulation between 28-35 process hours occurred due to the retarded cell growth during the "stop-growth" period. We, also, aimed to compare the aDA and pbu strains at similar specific growth rates. Therefore, we increased the feed rate back to its previous value after 55 hours and maintained it until 63.7 process hours, when N-starvation began. To our surprise, the acetate concentration started to slightly increase again during the 55-63.7 hour period. During this period no growth retardation was observed. On the contrary, the μ was calculated as 0.074 ± 0.002 h^{-1}.

Therefore, it is likely that the assumption regarding the retarded cell growth was incorrect, and the actual reason for the acetate accumulation was that the desired μ was higher as the μ_{max} of the aDA in the 2nd growth phase.

6.7.3 C-limited conditions decreased the productivity of the aDA strain during the growth phase

The IPA titer of the C-limited aDA strain showed a decrease of 63 % compared with the titer reached by the aDA strain grown under C-excess. In turn, the acetone titers decreased by 70 % under C-limited conditions.

This may have happened due to the reduced IPA and acetone production during the growth phase under C-limited conditions. We hypothesize that the production of IPA

or acetone is only possible when the acetate concentration in the cultivation medium is higher than zero.

Indeed, increased specific IPA production rate and overall IPA production during the growth phase of the C-limited aDA strain are correlated with periods when acetate was accumulated (specifically, at 28-35 and 58-63.7 process hours), as shown in figures 6.14 and 6.13. Also, no IPA or acetone production was observed when the acetate concentration in the medium was zero, suggesting a dependence on acetate availability. One possible explanation for this behaviour is the properties of the AtoDA enzyme, which will be discussed in section 7.3.

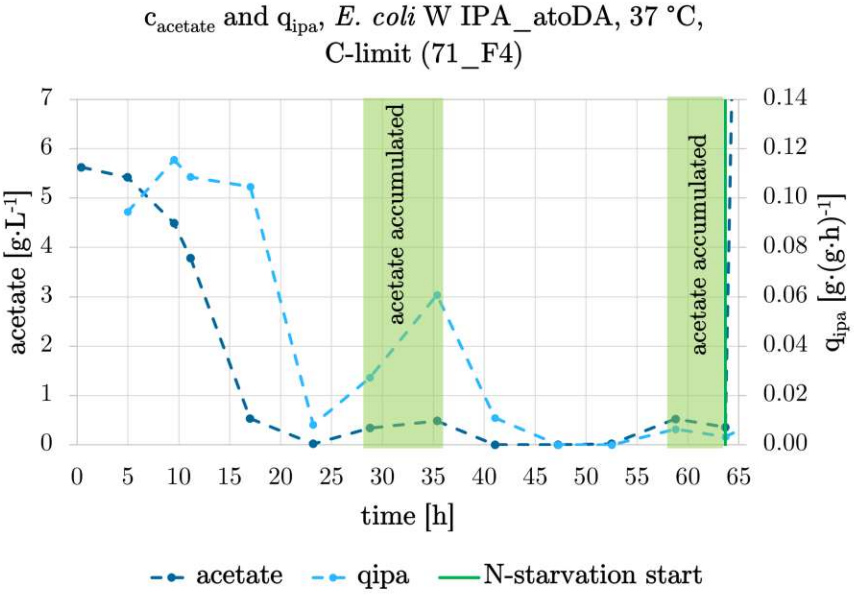

Figure 6.14: Specific IPA production rate plotted against the acetate concentrations during the growth phase of *E. coli* W IPA_atoDA at 37 °C under carbon limitation. 71_F4 run. The acetate accumulation periods during the growth phase around 28-35 and 58-63.7 process hours are highlighted

To summarize, it was not possible to maintain a constant specific growth rate of 0.077 h^{-1} in the aDA strain under C-limited conditions. However, between 55 and 63.7 process hours, the reached μ was very similar to the desired value, measuring 0.074 $\pm$ 0.002 h^{-1}. This period may be suitable for comparing the specific rates of the pbu and aDA strains grown at similar specific growth rates. The differences between the first and second growth phases (caused by the possibly occurring metabolic switch) should be noted during the strain comparison. Additionally, data imply, that the aDA strain is unable to produce IPA when there is no acetate in the culturing medium.

6.8 Bioreactors: *E. coli* W IPA_ptb_buk at 37 °C under carbon limitation

Alongside the C-excess pbu runs (see section 6.6), we cultivated two biological duplicates of the pbu strain under the same conditions as the aDA strain in 6.7 section, including C-limitation during the growth phase, N-starvation and a temperature of 37 °C. By employing a C-limited feed, we intended to set the same specific growth rate of approximately 0.08 h^{-1} in order to conduct a comparison between the pbu and aDA strains at similar specific growth rates.

The feed was started after 9.3 process hours. After the start of N-starvation, the feed was stopped and the acetate concentration was maintained around 7-11 $g{\cdot}L^{-1}$ with acetate pulses (see figure 6.15).

6.8.1 The C-limited pbu strain produced IPA

The IPA and acetone production in the pbu strain started in the production phase. The titers reached 2.15 ± 0.067 $g{\cdot}L^{-1}$ and 1.50 ± 0.27 $g{\cdot}L^{-1}$ in 75 hours, accordingly. In comparison, the aDA strain achieved IPA titers that were 1.8 times higher than those of the pbu strain, while the acetone titers of the aDA strain were half as low during the 120-hour process (see section 6.7).

Notably, the acetone and IPA concentrations produced by the pbu strain grown under C-limitation were similar, with the acetone to IPA ratio of 0.7 (the acetone to IPA ratio of the aDA strain was 0.2). This may indicate a less efficient conversion of acetone to IPA in the pbu strain compared to the aDA strain (see section 7.2).

The acetone-to-IPA conversion became possible in N-starved pbu cells only after the growth phase under C-limited conditions. This suggests that slower growth rates may have reduced a mutation risk of the *adh* gene or increased the availability of NADPH during the production phase.

It is also possible that the observed metabolic behaviour of no-production-after-C-excess-growth-but-production-after-C-limit-growth is related to changes in acetate uptake. As mentioned in section 4.4.2, the Acs enzyme tends to catalyze acetate uptake when its concentration in the medium is low, as was the case during the C-limited growth of the pbu strain. However, at higher acetate concentrations during the C-excess growth, acetate uptake is preferably carried out via the less energy-demanding AckA/Pta pathway. It should be noted that it is counterintuitive that under C-limited conditions, the more energy-demanding Acs pathway would result in increased IPA production. However, without additional metabolic data, it is not possible to determine if there were changes in the acetate uptake pathway betweeen the C-excess/C-limited

conditions. Consequently, it is challenging to formulate further hypotheses based solely on the assumption of altered acetate uptake.

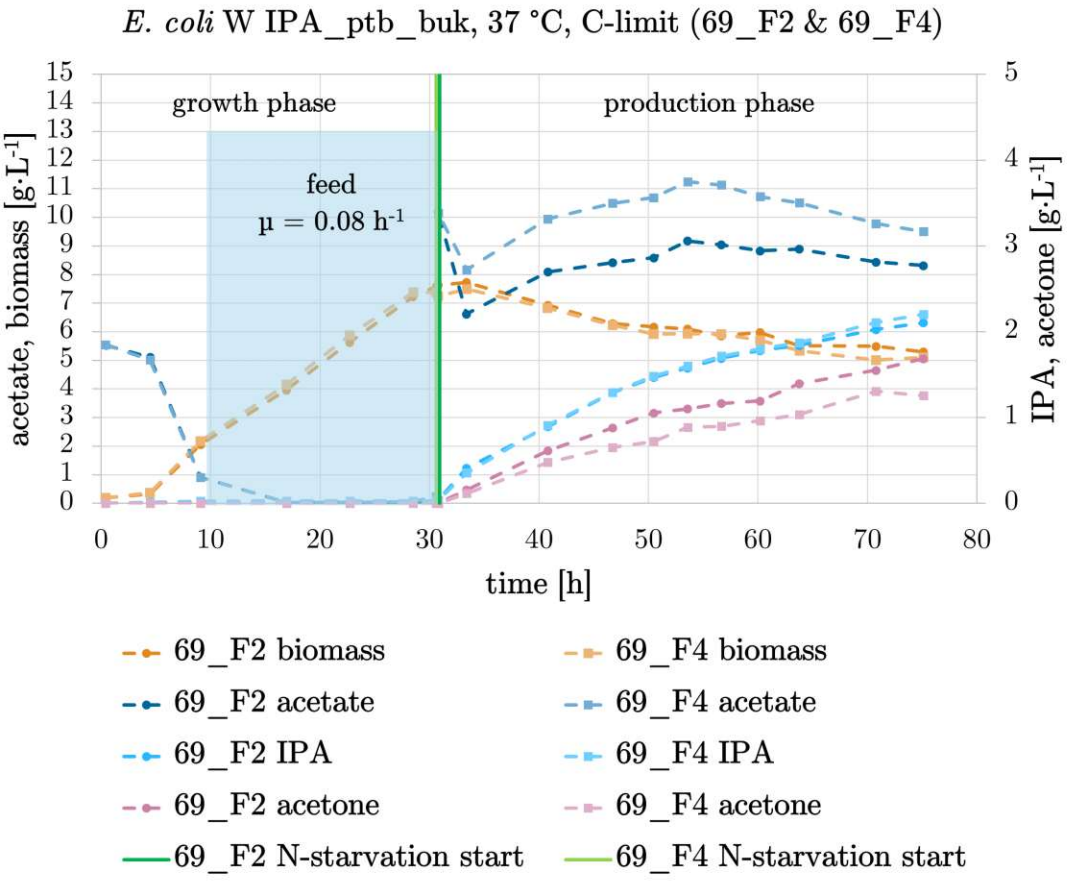

Figure 6.15: Fermentation results of *E. coli* W IPA_ptb_buk at 37 °C grown under carbon limitation. Biological duplicates in F2 and F4 bioreactors. Feed: 9.3-30.6 process hours

6.8.2 Control of the specific growth rate (μ) was achieved

It was possible to control the specific growth rate of the pbu strain with the C-limiting feed. The μ in the feed period stayed at 0.077 ± 0.009 h^{-1}. The corresponding value of the specific acetate uptake rate was 0.32 ± 0.03 $g \cdot (g \cdot h)^{-1}$ (see figure 6.16). Controlling the growth phase resulted in high reproducibility between the biological duplicates.

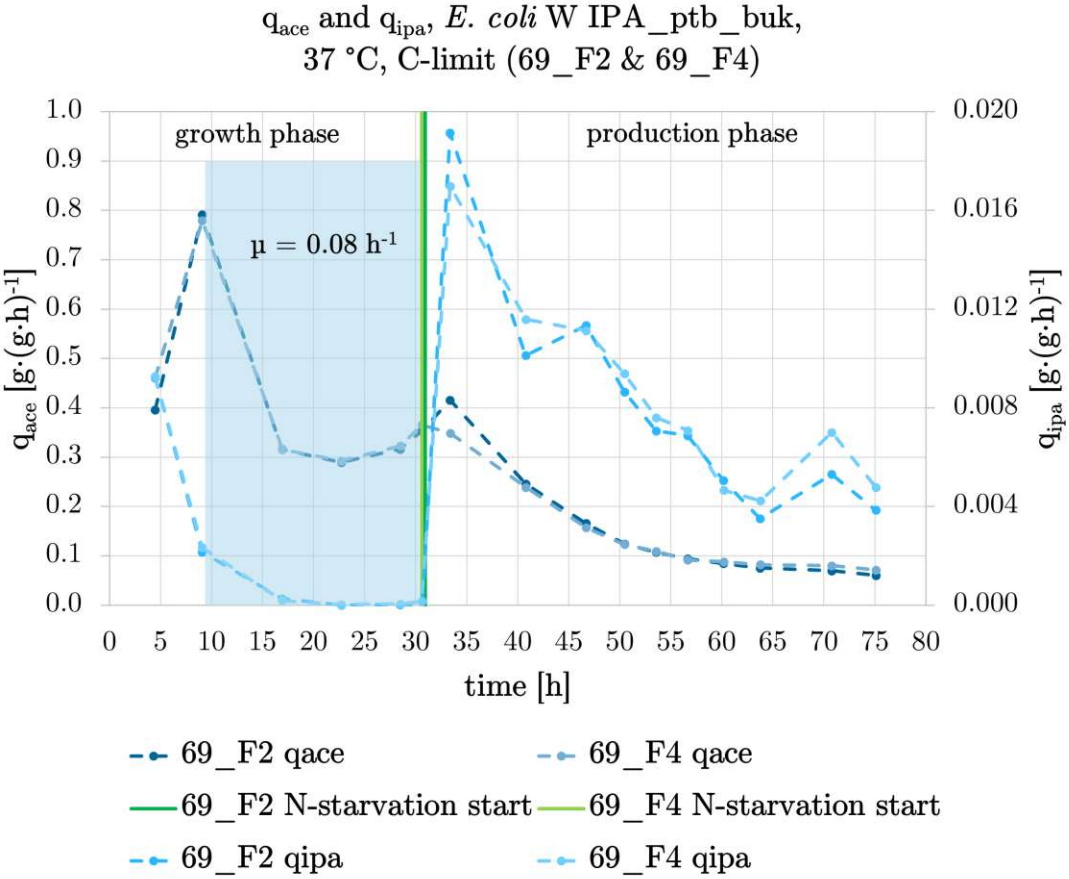

Figure 6.16: Specific rates of acetate consumption and IPA production during the fermentation of *E. coli* W IPA_ptb_buk at 37 °C under carbon limitation. Feed: 9.3-30.6 process hours

6.8.3 Insights from the carbon balance analysis - reduced C-losses

The carbon loss in the C-limited pbu strain was approximately 15 %, which is comparable to the carbon loss observed in the C-limited aDA strain (see figure 9.2 in Additional file). Notably, the carbon loss in the C-limited pbu strain was 50 % lower compared to the C-excess experiment (see section 6.6). This improvement could be attributed to the different metabolism allowing the acetone-to-IPA conversion step.

Furthermore, it is worth noting that the impact of N-starvation on carbon flux was similar to what was observed in the C-excess section (see 6.6). (Under N-starved conditions, both the aDA and pbu strains showed a shift in carbon flux away from biomass formation and towards CO_2 emissions instead of acetone/IPA production.)

To summarize, the pbu strain was successfully grown under C-limiting conditions with a constant specific growth rate of 0.077 ± 0.009 h^{-1}. This slower growth rate may have reduced the risk of mutations or increased the availability of NADPH and the pbu strain produced approximately 2 $g{\cdot}L^{-1}$ of IPA. The results of the IPA-producing pbu strain from this section can be used for the comparison between the pbu and aDa strains.

6.9 Final comparison of the *E. coli* W IPA_ptb_buk and *E. coli* W IPA_atoDA strains: C-limited and N-starvation conditions

6.9.1 Higher maximum specific growth rate of the pbu strain compared to the aDA strain

One of the first noticeable differences in behaviour between the pbu and aDA strains under both C-excess and C-limited conditions appears to be the quicker uninterrupted growth of the pbu strain.

However, as discussed in sections 6.6 and 6.5, the rapid growth of the pbu strain under C-excess conditions ($\mu \approx 0.25$ h^{-1}) may have been caused by its inability to convert acetone to IPA. This factor makes the C-excess data less reliable for comparison.

Therefore, to calculate the μ_{max} of the IPA-producing pbu strain, we used data from the C-limited runs during the time period prior to the start of the feed. The obtained value of 0.222 ± 0.102 h^{-1} gives an approximate estimation (see table 6.3). It should be noted, that the calculation has a high standard deviation due to the limited sampling during the first cultivation hours and the lower μ calculated for the first 4 hours of growth, likely caused by the cells adjusting to the bioreactor conditions. (The first 5 hours of cultivation were excluded from the calculation of the aDA strain's μ because of the mentioned reason.)

Due to the high standard deviation, the statement that the pbu strain grows faster than the aDA strain in the 1st growth phase (before the metabolic switch) is less robust. However, it is evident that the specific growth rate of the pbu strain is higher than the μ of the aDA strain in the 2nd growth phase. This is consistent with the challenges encountered when trying to C-limit the aDA strain at a μ of 0.077 h^{-1} (see 6.7).

Table 6.3: μ_{max} of *E. coli* W IPA_ptb_buk (**pbu**) and *E. coli* W IPA_atoDA (**aDA**) strains

Strain	**Phase**	**Time [h]**	$\boldsymbol{\mu}_{max}$ **[h^{-1}]**	**Data source**
pbu	growth	0.5 - 9.1	0.222 ± 0.102	69_F2 / 69_F4
aDA	1st growth	5.0 - 14.4	0.151 ± 0.021	71_F3
aDA	2nd growth	35.4 - 58.8	0.076 ± 0.026	71_F3

6.9.2 Similar q_{IPA} values between the pbu and aDA strains during the N-starvation phase

The main difference in productivity between the pbu and aDA strains, as discussed in previous sections, is the timing of IPA production. While the aDA strain begins producing IPA during the growth phase, the pbu strain starts producing IPA later during the production phase. Therefore it is only possible to compare the specific IPA production rates of the strains after the start of N-starvation. For this comparison, the C-limited runs are used, as the IPA titers observed during the cultivation of the pbu strain under C-excess conditions were negligible.

Figure 6.17 shows similar q_{IPA} values of both pbu and aDA after the start of the N-starvation. This similarity suggests that the two-fold higher titers achieved by the C-limited aDA strain compared to the C-limited pbu strain were due to the aDA strain's ability to start IPA production earlier.

The increase in IPA production observed in both strains after the start of the N-starvation (71_F4, 69_F2 and 69_F4 runs) can be attributed to the rise in q_{IPA} values immediately after the onset of N-starvation.

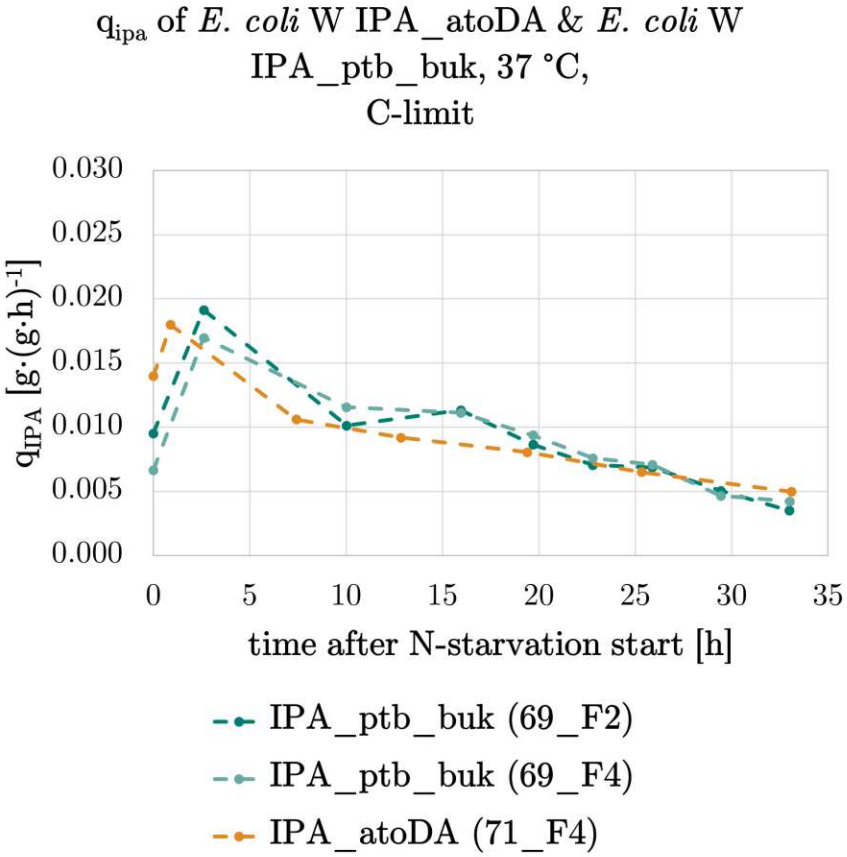

Figure 6.17: Comparison of specific IPA production rates between *E. coli* W IPA_ptb_buk and *E. coli* W IPA_atoDA strains after N-starvation start. 37 °C, carbon limitation during the growth phase

It should be noted that the productivities of both strains, as well as their acetate uptake rates (see section 6.9.3), decrease over time of N-starvation, most likely due to a gradual reduction in the number of active and alive cells caused by stressful starvation conditions. However, it appears that the rates of the aDA strain are more stable over time, with a slower decrease compared to the pbu strain. The possible reasons for this observation are discussed in more detail in section 6.9.3.

The approximate q_{IPA} values for both strains during the first 33 hours of the production phase are presented in table 6.4. The high standard deviation values are caused by the mentioned decrease in productivity over time.

Table 6.4: q_{IPA} in the production phase of *E. coli* W IPA_ptb_buk (**pbu**) and *E. coli* W IPA_atoDA (**aDA**) strains

Strain	Phase	Time after N-starvation start [h]	q_{IPA} [g·(g·h)$^{-1}$]	Data source
pbu	production	0.2 - 33.5	0.009 ± 0.004	69_F2 / 69_F4
aDA	production	0 - 33.1	0.010 ± 0.004	71_F4

6.9.3 Similar $q_{acetate}$ values between the pbu and aDA strains during the N-starvation phase

To analyze whether the pbu strain has a different ability to take up acetate compared to the aDA strain, we compared their $q_{acetate}$ values during two periods of similar specific growth rates. The first period was when both strains were C-limited and achieved similar μ values of ≈ 0.07 h^{-1}. The second period was during N-starvation when the cells were no longer able to grow. In both periods the acetate uptake rates are similar in both strains. The calculations for the C-limited period are presented in table 6.5.

It should be noted that the data from the aDA cells used for comparison were obtained during their second metabolic phase, following the aDA-specific metabolic switch. The acetate uptake rate during the first metabolic phase (first 14 hours of the 120-hour cultivation) of the aDA strain may differ from that of the pbu strain, as demonstrated in section 6.6.

Table 6.5: $q_{acetate}$ during the growth phase with the similar μ of *E. coli* W IPA_ptb_buk (**pbu**) and *E. coli* W IPA_atoDA (**aDA**) strains

Strain	Phase	Time [h]	$q_{acetate}$ [g·(g·h)$^{-1}$]	Data source
pbu	$\mu = 0.069 \pm 0.014$ [h^{-1}]	9.1 - 28.5	0.309 ± 0.014	69_F2 / 69_F4
aDA	$\mu = 0.074 \pm 0.002$ [h^{-1}]	52.5 - 63.7	0.317 ± 0.056	71_F4

The changes in the $q_{acetate}$ values during the course of the N-starvation and consequent calculations are presented in figure 6.18 and table 6.6.

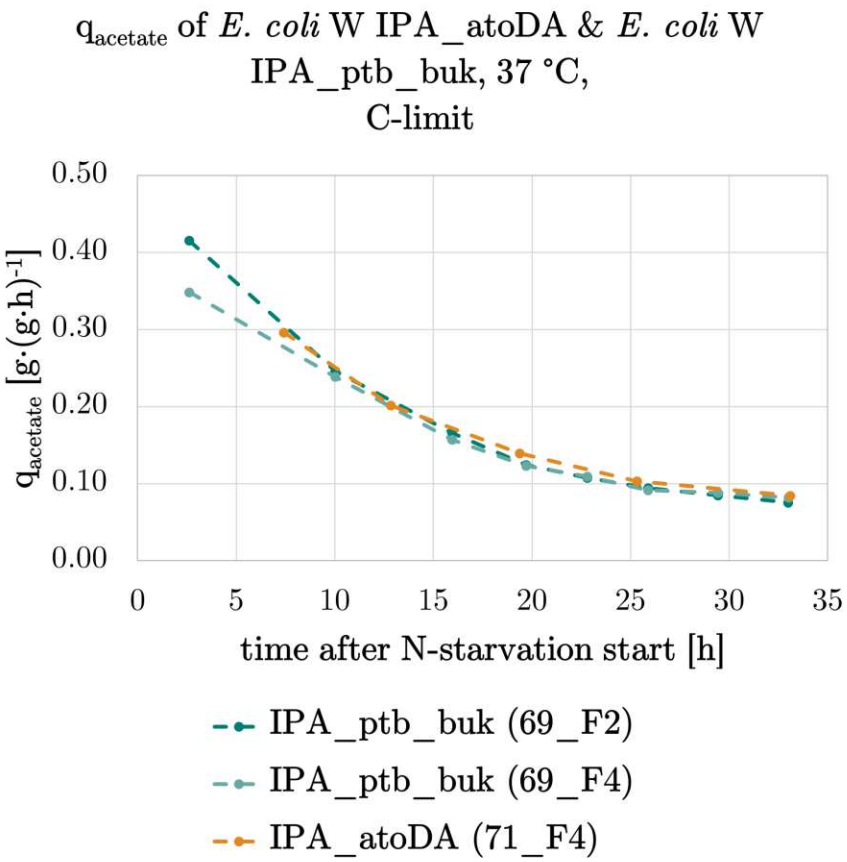

Figure 6.18: Comparison of specific acetate consumption rates between *E. coli* W IPA_ptb_buk and *E. coli* W IPA_atoDA strains after N-starvation start. 37 °C, carbon limitation during the growth phase

Table 6.6: $q_{acetate}$ during the production phase of the *E. coli* W IPA_ptb_buk (**pbu**) and *E. coli* W IPA_atoDA (**aDA**) strains grown under carbon limitation

Strain	**Phase**	**Time after N-starvation start [h]**	**$q_{acetate}$ [g·(g·h)$^{-1}$]**	**Data source**
pbu	production	0.2 - 33.5	0.160 ± 0.102	69_F2 / 69_F4
aDA	production	0 - 33.1	0.165 ± 0.086	71_F4

Similar acetate uptake rates and IPA production rates observed in both strains, especially after the onset of N-starvation, could be attributed to the comparable energy costs

associated with acetate uptake and IPA production in both pathways. This comparison was presented in section 4.4.6, specifically variant b) in table 4.1. (During N-starvation, where acetate is provided in excess, it is likely taken up via the less energy-demanding AckA/Pta pathway.) Overall, it is evident that the implementation of the IPA_ptb_buk pathways in the pbu strain did not lead to facilitated acetate consumption or increased IPA production.

The acetate uptake rates of both strains decreased in the course of the N-starvation period, but the decrease in $q_{acetate}$ was slightly slower for the aDA strain compared to the pbu strain. The more stable acetate uptake rates of the aDA strain could be a possible reason for the more stable IPA production rates observed for this strain. The acetate uptake in the aDA strain may be stabilized by the work of the AtoDA enzyme (see section 7.3).

To summarize, the higher μ observed in the pbu strain compared to the aDA strain is unlikely due to the significantly different specific acetate uptake rate but rather due to the different carbon distribution in the cells. In comparison with the aDA cells, the pbu cells seem to direct the taken-up carbon towards biomass formation, reducing or even stopping the carbon flux towards IPA production. Possible reasons for the prioritized biomass formation in the pbu cells are further discussed in section 7.1. Under growth-arrested conditions (N-starvation), both strains exhibit similar specific IPA production rates.

7 Discussion and Outlook

We developed the *E. coli* W IPA_ptb_buk (pbu) strain, containing the IPA_ptb_buk pathway characterised by an ATP-coupled isopropanol synthesis strategy.

Our hypothesis was that an additional ATP molecule, generated through the IPA production pathway, could potentially serve two purposes: (i) improve the viability of the *E. coli* cells that were cultured solely on acetate, a toxic and energetically-limited carbon source; and (ii) increase the yield of IPA production by promoting metabolic flux towards the energy-rich production pathway.

The results of cultivating the pbu strain, compared to the non-energy coupled *E. coli* W IPA_atoDA (aDA) strain suggest that the application of the ATP-coupled strategy may have increased the viability of pbu cells. However, this strategy also reduced the reached IPA titers.

The potential increase in viability of the pbu cells is associated with their accelerated growth discussed in section 7.1. The less efficient production of the pbu strain may be referred to several factors or a combination of these factors, including the possible NADPH deficiency of the pbu strain (7.2), properties of the enzymes used in the engineered pathways (7.3, 4.4.6) or tried fermentation conditions (7.4).

7.1 Did the ATP-coupled strategy influence the growth of the pbu cells?

The differences in the behaviours between the pbu and aDA strains started during the growth phase. Here, the pbu cell, in contrast to the aDA cells, showed faster growth but was unable to produce either acetone or IPA (see figures 6.10, 6.15). Two hypotheses may explain the described strain behaviour.

The first hypothesis suggests that during the growth phase of the pbu cells, the metabolic flux could not pass through the IPA_ptb_buk pathway, and the entire pathway was inactive, leading to no production. If this hypothesis is true, no additional ATP molecule was produced, and the quick growth of the pbu strain is not a result of the ATP-coupled strategy.

The quick growth could be explained by the fact that the pbu strain did not spend resources on the execution of the IPA_ptb_buk pathway, making more resources available for biomass synthesis. This theory is supported by the behaviour of the reference strain in SFEs, where the pathway was also most probably inactive, and the reference cells exhibited quick growth. A possible explanation for the lower flux towards the IPA_ptb_buk pathway compared to the IPA_atoDA pathway in the aDA strain is discussed in section 7.3.

The second hypothesis suggests that during the growth phase of the pbu cells, the metabolic flux passed through the IPA_ptb_buk pathway only until acetoacetate, leading to the production of an additional ATP molecule but no acetone or IPA production.

If this hypothesis is true, the additional ATP molecule could have caused the increased cell growth, similarly as was observed in [62] or [63]. Furthermore, the lack of acetone and IPA production may have saved resources that could be used for biomass synthesis, as in the first hypothesis. Nevertheless, the question of what inhibited the further conversion of acetoacetate to acetone remains open and requires further investigation.

Both hypotheses are not mutually exclusive and can be happening in alternation. To summarize, without additional metabolomic data, it is challenging to determine whether the ATP-coupled strategy influenced the growth and acetate uptake of the pbu strain.

7.2 Can ATP-coupled production influence the availability of the NADPH molecules?

The differences in the behaviours between the pbu and aDA strains continued during the production phase. Here, the pbu cells, in contrast to the aDA cells, were characterised by the higher acetone to IPA ratio (see sections 6.8 and 6.7)

We hypothesize that the application of the ATP-coupled strategy may have resulted in the lower availability of the NADPH molecules, leading to a less efficient reduction of acetone to IPA and ultimately resulting in lower production titers.

Our assumption is based on the fact that acetone is a precursor of IPA. For the acetone to isopropanol conversion in both IPA_ptb_buk and IPA_atoDA pathways, the Adh enzyme requires reducing power in the form of a NADPH molecule (see figure 4.2). Limitations in the availability of NADPH can lead to the less efficient acetone to IPA conversion step [8].

In *E. coli* grown on acetate, NADPH can be mainly produced via transhydrogenase systems and TCA cycle [8], [64]. As was mentioned previously, while *E. coli* grows on acetate the flux towards glyoxylate in the TCA cycle is increased [7], reducing the

NADPH production by isocitrate dehydrogenase. That fact as well as findings from [8], [65], [66] highlight the importance of transhydrogenases for the NADPH production in *E. coli* grown on acetate.

One of *E. coli* transhydrogenases, PntAB converts $NADP^+$ and NADH to NADPH and NAD^+ [67]. The needed $NADP^+$, in turn, is produced by the ATP-dependent NadK (NAD kinase) [68].

While theoretically, the higher ATP availability of the pbu strain could have stimulated the work of NadK and increased the overall NADPH availability, our experimental results did not support this assumption. This may be due to the fact that it is PntAB, not NadK, that has a greater impact on NADPH levels. After all, $NADP^+$, produced by NadK, can also be utilized in other metabolic reactions.

The higher importance of PntAB compared to NadK in NADPH production was also demonstrated by Yang et al. in [8]. Specifically, the authors introduced plasmids encoding PntAB or NadK into the *E. coli* strain engineered for IPA production. The resulting strains exhibited a decrease in acetone accumulation by 77.9 % or 35.7 %, respectively. Therefore, these data suggest that PntAB has a more significant impact on supplying NADPH for the IPA pathway than NadK. Moreover, higher PntAB levels led to increased IPA yields. On the other hand, the application of this strategy decreased acetate consumption and resulted in lower IPA titers.

The authors believe that the reason behind this is the increased NADH consumption by PntAB. That reduces the amounts of NADH, available for the respiratory chain for ATP production. Therefore less ATP could be produced and less ATP was used for acetate consumption [8].

In this work, we could have observed an opposite behaviour - higher ATP production resulting in less NADH for NADPH production. Therefore, we assume that the additional production of the ATP molecule, during the production phase of the pbu strain could have resulted in lower NADPH levels, making the acetone to IPA conversion step less efficient.

To summarize, it can be said, that the interplay between ATP, NADH, and NADPH in regulating metabolism is highly complex, and it remains a challenge to distinguish their individual roles [69] and fully explain the possible NADPH deficiency of the pbu strain.

The introduction of an additional plasmid containing *pntAB* gene to the pbu strain, or further analysis and implementation of other ways to increase NADPH availability, could potentially improve the acetone to IPA conversion step in the pbu strain and increase its IPA yields.

7.3 Can the properties of the Ptb and AtoDA enzymes influence the efficiency of ATP-coupled production?

We hypothesize that the efficiency of the ATP-coupled strategy in this study may be influenced by the properties of the chosen Pbu and Buk enzymes. Differences in the properties of Pbu/Buk and AtoDA enzymes may explain the lower productivity of the pbu strain in comparison to the aDA strain.

As was mentioned in section 4.4.6, the IPA_ptb_buk and IPA_atoDA pathways differ in the acetoacetyl-CoA to acetoacetate conversion step. In IPA_ptb_buk the step is done by Ptb and Buk enzymes and in IPA_atoDA by AtoDA enzyme (see figure 4.2).

7.3.1 Activation of the acetoacetyl-CoA to acetoacetate conversion

For effective acetoacetyl-CoA to acetoacetate conversion, the AtoDA-CoA complex should be activated with an acetate molecule [70], [71]. Therefore, the velocity of the AtoDA reaction is dependent on acetate concentration [71]. Additionally, in the absence of acetate, acetoacetyl-CoA may partially inhibit the AtoDA enzyme [71].

We assume, that activation of the acetoacetyl-CoA to acetoacetate conversion with acetate may have increased the metabolic flux towards the IPA_atoDA pathway, resulting in the possibility of simultaneous growth and IPA production in the aDA strain. (The aDA strain, in contrast to pbu, did produce low levels of IPA simultaneously to the growth at both 25 °C and 37 °C (as shown in figures 6.1, 6.7, and 6.13).)

The requirement of acetate for a successful conversion by AtoDA could explain the behaviour of the aDA strain in section 6.7. Zero concentrations of acetate in the medium during C-limiting feed could have resulted in the inactivity of AtoDA and thus no IPA production. The production became possible when acetate began to accumulate and initiated the work of the AtoDA enzyme.

7.3.2 Affinity to acetoacetyl-CoA

Another fact to consider is the affinity of Ptb and AtoDA to the substrate. Thomson and Chen [47] demonstrated that Ptb from *C. beijerinckii* is less efficient with non-native substrates, such as acetoacetyl-CoA, with a K_m value of 1.10 mM. In contrast, acetoacetyl-CoA is a native substrate for the AtoDA enzyme with a K_m value of 0.035 mM [70].

However, it is important to note that the exact values should be interpreted carefully, as they were obtained under slightly different pH and temperature conditions. Additionally, in this study, the Ptb enzyme sequence was obtained from *C. acetobutylicum*, not from *C. beijerinckii*. To our knowledge, there are no published kinetic studies from Ptb from *C. acetobutylicum* converting acetoacetyl-CoA as a substrate. Taking into account

the evolutionary relationship between the aforementioned Clostridium strains, one can suggest the similarities between the properties of the Ptb enzyme ([47], [72]).

Therefore, we believe that AtoDA probably has a higher affinity towards acetoacetyl-CoA compared with Ptb, and thus requires less substrate to start the efficient conversion. This could be also advantageous for the flux towards the IPA_atoDA pathway compared to IPA_ptb_buk.

To summarize, the usage of the Ptb and Buk enzymes made the ATP-coupled production of IPA possible in the *E. coli* W IPA_ptb_buk strain. However, activation and affinity of these enzymes may have contributed to the low efficiency of the pbu strain compared with the aDA strain and to the overall low efficiency of the ATP-coupled strategy.

Further metabolic analysis, such as through computational modelling of the metabolic network [73], could help identify other potential ways to couple ATP synthesis with IPA production in *E. coli*, potentially leading to more efficient production strategies.

However, it should be remembered that the production of IPA via the IPA_atoDA pathway depends on the acetate concentration in the culture medium. Therefore, the established IPA_ptb_buk pathway may be particularly advantageous when the culture medium for IPA production does not contain acetate.

7.4 Can the cultivation temperature increase the efficiency of ATP-coupled production?

Last but not least, we hypothesize, that the productivity of the pbu strain and, therefore, the efficiency of the ATP-coupled strategy could be increased by the adaptation of the process parameters. Especially promising could be a change towards lower production temperatures.

The optimal temperature for *E. coli* culturing is 37 °C [74], [75]. Lower temperatures such as 25 °C have been shown to reduce the growth [75] and metabolism [74] of *E. coli*. However, lower temperatures also reduce the evaporation of volatile products such as IPA and may result in higher plasmid stability [76].

Lower process temperatures have been previously used for IPA production [8, 44]. For instance, Yang et al. maintained a growth temperature of 37 °C and lowered it to 25 °C during the production phase [8]. Cultivations at 30 °C were conducted in another study [44].

Our findings during this work suggest that IPA production at 37 °C could have been too demanding for the metabolism of the pbu strain, particularly when grown under C-excess conditions.

Firstly, the pbu strain at 25 °C in SFEs (see section 6.3) grew slower and produced higher amounts of IPA, compared to its behaviour at 37 °C. Also, the acetone to IPA ratio was lower at 25 °C. Secondly, the pbu strain at 37 °C in bioreactors may have obtained plasmid mutations while grown under C-excess conditions (see section 6.6) and higher plasmid stability at 25 °C may become especially beneficial in this context. Thirdly, it appears that growing the cells at 37 °C may lead to increased CO_2 emissions during the N-starvation phase, which could have a negative impact on the amount of carbon available for the production process. This assumption is based on the data from the aDA strain fermented at 25 °C (see section 6.1) and 37 °C (see section 6.5).

To summarize, optimizing process conditions could further increase the productivity of the pbu strain. Lowering the fermentation temperature to 25 °C may result in higher yields of IPA and lower risks of plasmid mutations in the pbu strain. Due to the limited time available, it was not possible to ferment pbu at 25 °C as a part of the master's thesis.

7.5 Importance of the ATP-coupled production for other metabolic engineering strategies

Although the study showed low efficiency in the ATP-coupled IPA production on acetate, the ability to couple IPA and ATP production using Ptb and Buk enzymes can be a valuable first step towards developing a more efficient metabolic strategy for high titer IPA production.

For example, in [77], the authors combined an ATP-coupled production with knockouts or repressions of other pathways of ATP synthesis, and with an ATP-wasting strategy. A combination of these methods resulted in a 45 % increase in the 2,3-butanediol yield.

The knock-outs or repressions of other ATP synthesis pathways led to the production pathway becoming the only route for balanced ATP synthesis. That had possibly increased the flux towards the production pathway.

In turn, the ATP-wasting strategy increased both the consumption and production of ATP in the cells and may have led to higher metabolic flux towards ATP synthesis and increased substrate uptake. The ATP wasting strategy is a growing trend in the literature - [78], [79], [80], [81], [77], [82], [83], that states a counterintuitive idea, that not the ATP increase, but the ATP deficiency in the cells could result in their higher productivity (in the ATP-coupled production).

It should be noted, that the ATP-wasting strategy was mostly exhibited while *E. coli* was grown on glucose [78], [77], [81], [82]. The yield of ATP from glucose (26 moles) is higher than acetate (7 moles) [84]. Therefore, while *E. coli* is grown on acetate, the available ATP pool is not high and would require a well-thought ATP balancing strategy.

To summarize, ATP-coupled production can be complemented with additional metabolic engineering strategies. Therefore, the utilization of Ptb/Buk enzymes for the coupled production of ATP and IPA, as proposed in this study, represents a promising initial step towards implementing other metabolic approaches for enhancing IPA production.

We discussed several crucial factors that influenced the implementation of the ATP-coupled production strategy in this study. Further research, taking into account the discussed strengths and limitations is needed to increase the efficiency of the ATP-coupled strategy for IPA production in *E. coli* on acetate.

8 Conclusion

The study aimed to develop an ATP-coupled isopropanol synthesis strategy using *E. coli* W as the microbial host and acetate as the carbon source. We successfully developed the *E. coli* W IPA_ptb_buk (pbu) strain, which carries a novel ATP-coupled IPA-producing metabolic pathway (IPA_ptb_buk) and undergoes an ATP-coupled IPA production.

The pbu strain was grown at 37 °C in bioreactors under acetate-excess and acetate-limited conditions. The IPA production was stimulated with N-starvation. Under the stated experimental conditions, the pbu was characterised by:
(i) strictly uncoupled growth and IPA production, with production becoming possible only under growth-arrested conditions (N-starvation)
(ii) maximal specific growth rate (μ_{max}) of 0.222 ± 0.105 h^{-1}, absence of lag phase, good reproducibility
(iii) maximal IPA titer of 2.15 ± 0.07 $g{\cdot}L^{-1}$ produced after 43 hours of N-starvation, after the C-limited growth phase
(iv) specific IPA production rate (q_{IPA}) of 9 ± 4 $mg{\cdot}(g{\cdot}h)^{-1}$ during the first 33 hours of N-starvation, after the C-limited growth phase
(v) an inability to carry out the acetone-to-IPA conversion step when grown under C-excess conditions at 37 °C.

In comparison with the aDA strain, the pbu strain was characterised by:
(i) higher μ_{max}, likely due to prioritized biomass production, which may be attributed to either the theoretically increased ATP pool in the pbu strain or differences in properties of the Ptb and AtoDA enzymes between the two strains
(ii) similar $q_{acetate}$ during N-starvation, after the C-limited growth phase
(iii) similar q_{IPA} during N-starvation, after the C-limited growth phase
(iv) lower IPA titers at the end of fermentation processes due to uncoupled growth and production of the pbu strain
(v) less efficient acetone to IPA conversion
(vi) possibly faster decline in productivity during N-starvation, after the C-limited growth phase.

In conclusion, the ATP-coupled IPA synthesis strategy implemented in the pbu strain may have improved cell viability and accelerated cell growth. However, it did not result in higher specific or volumetric IPA production rates under the tested experimental conditions. This study highlights the strengths and limitations of the novel IPA_ptb_buk pathway for future applications. Further research is needed to enhance the efficiency of the ATP-coupled strategy.

9 Additional file

9.1 Figures: Comparison

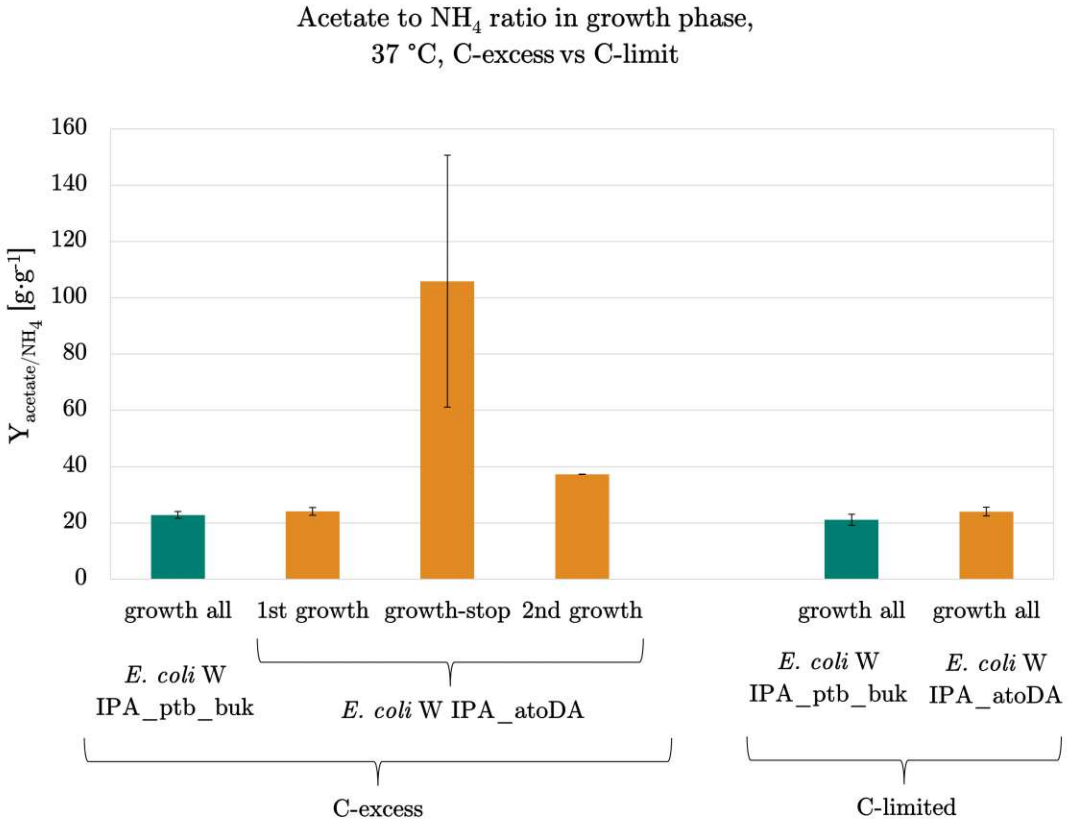

Figure 9.1: Acetate to NH_4 yield of *E. coli* W IPA_ptb_buk and *E. coli* W IPA_atoDA during the growth phase at 37 °C. C-excess and C-limited runs. The growth phase of *E.coli* W IPA_atoDA grown under C-excess is divided into the 1st growth (0-14 hours), the growth-stop (23-29 hours) and the 2nd growth (41-59 hours) phases

Note: Due to the low production, the growth phase of *E.coli* W IPA_atoDA grown under C-limited conditions is not divided to different phases.

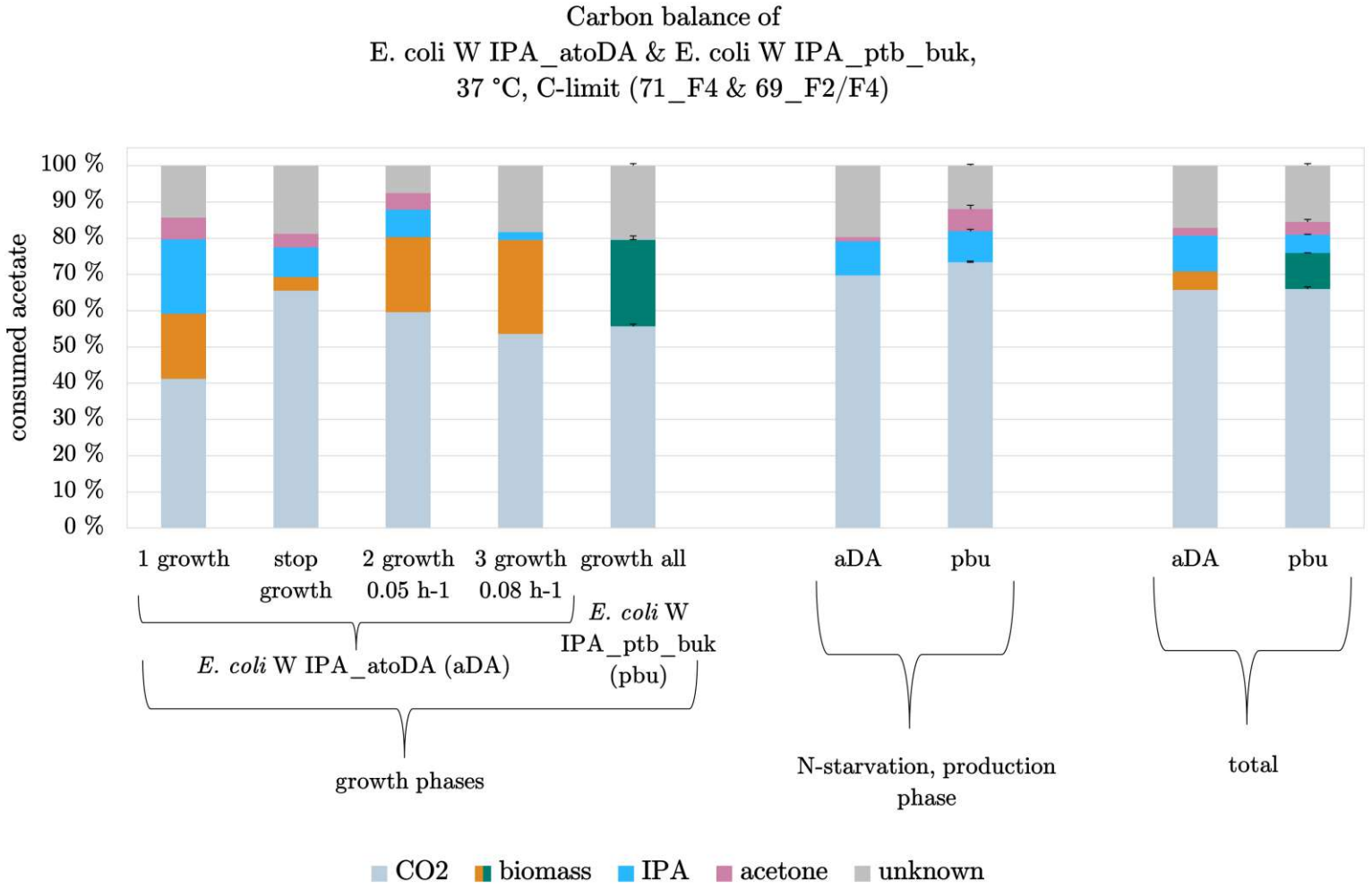

Figure 9.2: Comparison of carbon balances of *E. coli* W IPA_ptb_buk (pbu) and *E. coli* W IPA_atoDA (aDA) strains at 37 °C grown under carbon limitation. Distribution of the consumed carbon mole from acetate to CO_2, biomass, IPA and acetone in percentage. The growth phase of the aDA strain is divided into the 1st growth (5-17 hours), the growth-stop (23-29 hours), the 2nd growth ($\mu \approx 0.05$ h^{-1}, 35-52.5 hours) and the 3nd growth ($\mu \approx 0.08$ h^{-1}, 58.8-63.7 hours) phases

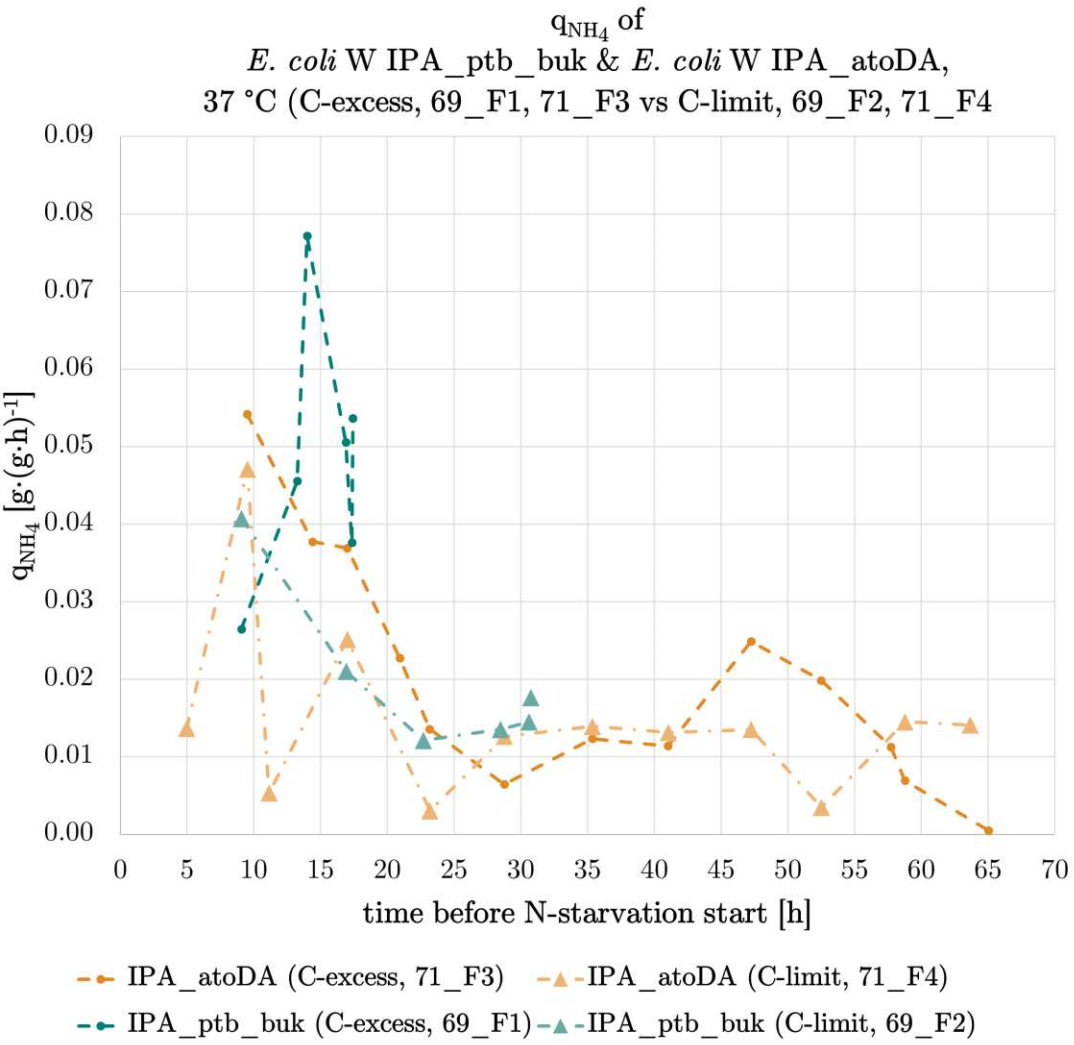

Figure 9.3: Comparison of specific NH_4 uptake rates between *E. coli* W IPA_ptb_buk and *E. coli* W IPA_atoDA strains before N-starvation start. 37 °C

Note: Figure 9.3 illustrates the similarities in specific NH_4 uptake between the pbu and aDA strains prior to the initiation of N-starvation. To avoid excessive overlap, the duplicate runs 69_F3 and 69_F4 are not included in the figure. These duplicates exhibit a similar trend to the 69_F1 and 69_F2 runs, respectively.

Specific acetate consumption and specific IPA production rates. C-limit. Before N-starvation

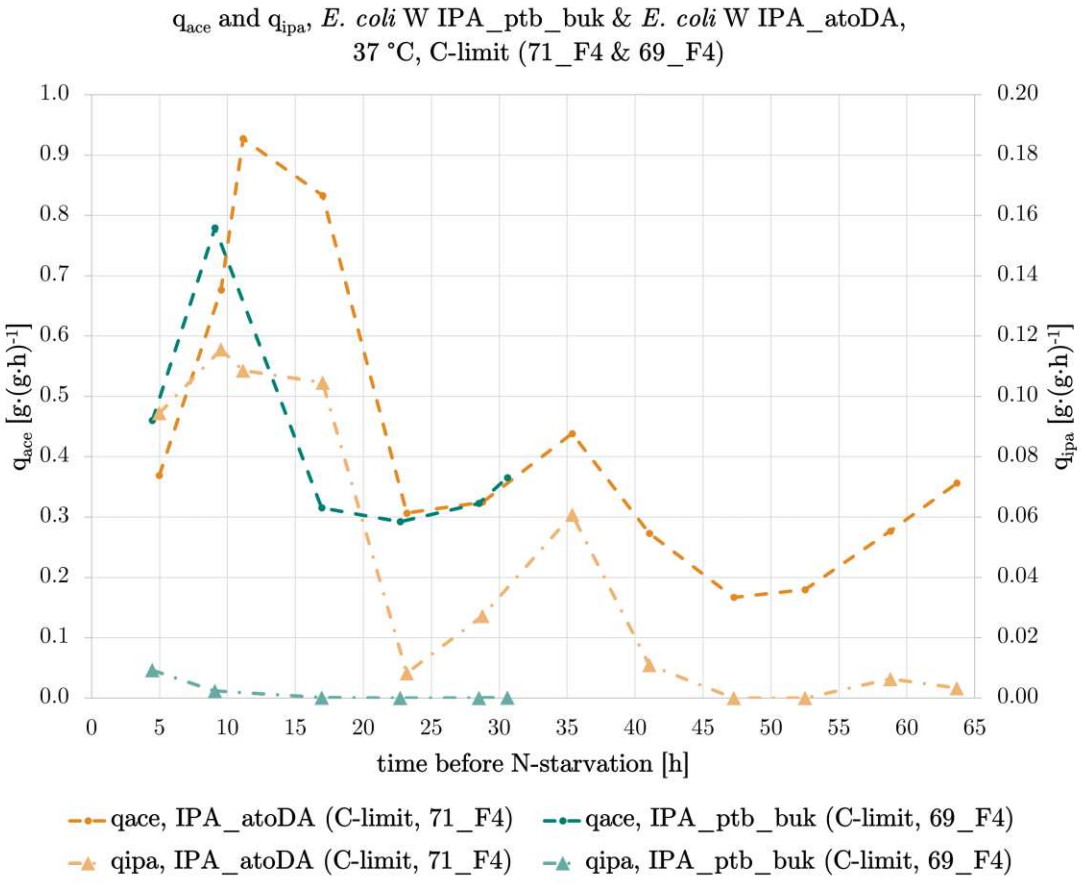

Figure 9.4: Specific rates of acetate consumption and IPA production during the cultivation of *E. coli* W IPA_ptb_buk and *E. coli* W IPA_atoDA before N-starvation. 37 °C. Carbon limitation

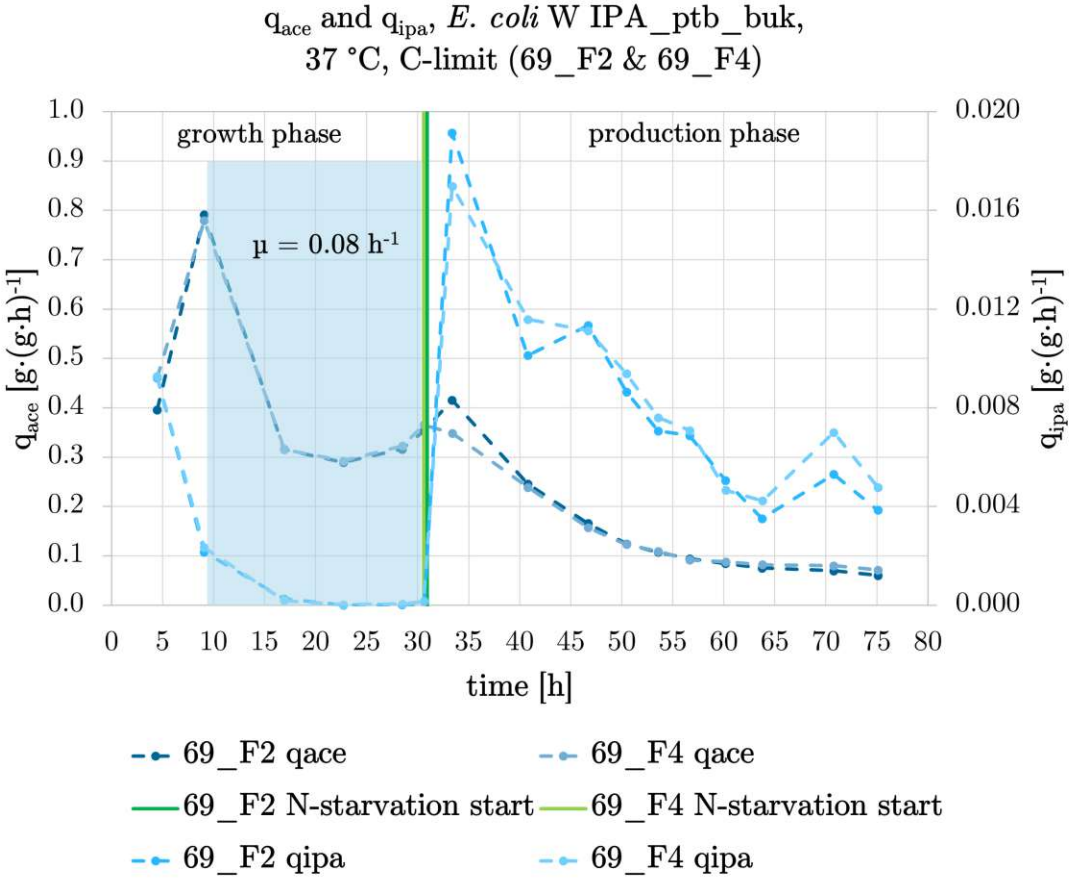

Figure 9.5: Specific rates of acetate consumption and IPA production during the fermentation of *E. coli* W IPA_ptb_buk at 37 °C under carbon limitation. Feed: 9.3-30.6 process hours

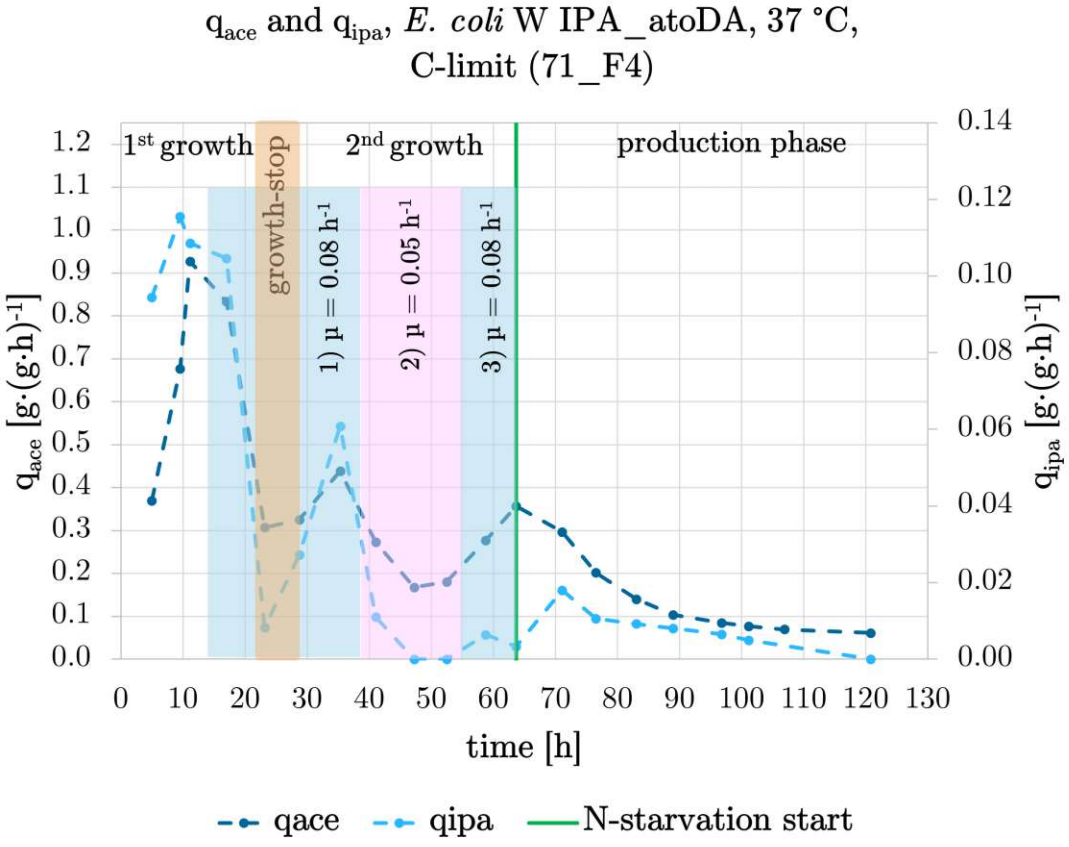

Figure 9.6: Specific rates of acetate consumption and IPA production during the fermentation of *E. coli* W IPA_atoDA at 37 °C under carbon limitation

9.2 Tables

Table 9.1: SFEs results at 25 °C and 37 °C. *E. coli* W IPA_ptb_buk and *E. coli* W IPA_atoDA strains. Yields, titers and rates were calculated during approximately 23 hours-long main culture growth.

		IPA_atoDA		**IPA_ptb_buk**	
		25 °C	**37 °C**	**25 °C**	**37 °C**
$\mathbf{c_{IPA}}$	$[\mathbf{g{\cdot}L^{-1}}]$	0.483 ± 0.029	0.469 ± 0.019	0.244 ± 0.020	0.187 ± 0.145
$\mathbf{Y_{IPA/acetate}}$	$[\mathbf{g{\cdot}g^{-1}}]$	0.110 ± 0.002	0.156 ± 0.002	0.110 ± 0.008	0.059 ± 0.051
$\boldsymbol{\mu}$	$[\mathbf{h^{-1}}]$	0.044 ± 0.004	0.005 ± 0.002	0.013 ± 0.001	0.046 ± 0.015
$\mathbf{r_{acetate}}$	$[\mathbf{g{\cdot}(L{\cdot}h)^{-1}}]$	0.170 ± 0.012	0.118 ± 0.004	0.088 ± 0.002	0.173 ± 0.082
$\mathbf{q_{acetate}}$	$[\mathbf{g{\cdot}(g{\cdot}h)^{-1}}]$	0.440 ± 0.029	0.555 ± 0.020	0.427 ± 0.004	0.325 ± 0.041
$\mathbf{q_{IPA}}$	$[\mathbf{g{\cdot}(g{\cdot}h)^{-1}}]$	0.048 ± 0.004	0.086 ± 0.004	0.047 ± 0.004	0.018 ± 0.017

Table 9.2: Used plasmids

Plasmid name	Source
BB1_BBa_J23114	R. Kutscha
BB1_BBa_J23105	R. Kutscha
BB1_BBa_TT_B1001	R. Kutscha
BB1_ptb_buk	This work
BB2_p114_thl	R. Kutscha
BB2_p114_adc	R. Kutscha
BB2_p105_adh	R. Kutscha
BB2_p114_ptb_buk	This work
BB3_ptb_buk	This work
recipient vector BB1 (kan)	R. Kutscha
recipient vector BB2 (carb)	R. Kutscha
recipient vector BB3 (kan)	R. Kutscha

Table 9.3: Used strains

Strain	Source
E. coli W *p114_thl* ***p114_atoDA*** *p114_adc p105_adh* (**aDA**)	R. Kutscha
E. coli TOP10 *p114_thl* ***...*** *p114_adc p105_adh*	This work
E. coli W *p114_thl* ***...*** *p114_adc p105_adh* (**reference**)	This work
CopyCutter EPI400 *p114_thl* ***p114_ptb_buk*** *p114_adc p105_adh*	This work
E. coli TOP10 *p114_thl* ***p114_ptb_buk*** *p114_adc p105_adh*	This work
E. coli W *p114_thl* ***p114_ptb_buk*** *p114_adc p105_adh* (**pbu**)	This work

Note: Italicized text in this table denotes relevant gene constructs introduced through plasmid-mediated gene transfer.

References

[1] R.K Core Writing Team Pachauri and A. et. al. Reisinger. "Climate Change 2007: Synthesis Report. Contribution of Working Groups I, II and III to the Fourth Assessment Report of the Intergovernmental Panel on Climate Change". In: *IPCC* (2007).

[2] Klaus S. Lackner. "Climate Change: A guide to CO2 sequestration." In: *Science* 300 (2003), pp. 1677–1678.

[3] Amit Kumar et al. "Enhanced CO2 Fixation and Biofuel Production via Microalgae: Recent Developments and Future Directions". In: *Trends in biotechnology* 28 (July 2010), pp. 371–80.

[4] Kenji Sorimachi. "Innovative method for CO2 fixation and storage". In: *Scientific Reports* 12 (Feb. 2022), p. 1694.

[5] Olivier Lemaire, Marion Jespersen, and Tristan Wagner. "CO2-Fixation Strategies in Energy Extremophiles: What Can We Learn From Acetogens?" In: *Frontiers in Microbiology* 11 (Apr. 2020).

[6] Regina Kutscha and Stefan Pflügl. "Microbial Upgrading of Acetate into Value-Added Products - Examining Microbial Diversity, Bioenergetic Constraints and Metabolic Engineering Approaches". In: *International Journal of Molecular Sciences* 21 (Nov. 2020), p. 8777.

[7] Oh MK et al. "Global expression profiling of acetate-grown *Escherichia coli*". In: *J Biol Chem.* (Apr. 2002).

[8] Hao Yang et al. "Efficient isopropanol biosynthesis by engineered *Escherichia coli* using biologically produced acetate from syngas fermentation". In: *Bioresource technology* 296 (Oct. 2019).

[9] Hao Yang et al. "Metabolic engineering of *Escherichia coli* carrying the hybrid acetone-biosynthesis pathway for efficient acetone biosynthesis from acetate". In: *Microbial Cell Factories* 18 (Jan. 2019).

[10] Xin Xu et al. "Microbial production of mevalonate by recombinant *Escherichia coli* using acetic acid as a carbon source". In: *Bioengineered* 9 (June 2017), pp. 1–8.

[11] Jing Chen et al. "Metabolic engineering of *Escherichia coli* for the synthesis of polyhydroxyalkanoates using acetate as a main carbon source". In: *Microbial Cell Factories* 17 (July 2018).

[12] Hao Niu et al. "Production of succinate by recombinant *Escherichia coli* using acetate as the sole carbon source". In: *3 Biotech* 8 (Oct. 2018).

[13] Myunghyun Noh et al. “Production of itaconic acid from acetate by engineering acid-tolerant *Escherichia coli* W”. In: *Biotechnology and Bioengineering* 115 (Dec. 2017).

[14] Eashwar Rajaraman et al. “Transcriptional analysis and adaptive evolution of *Escherichia coli* strains growing on acetate”. In: *Applied Microbiology and Biotechnology* 100 (Sept. 2016).

[15] Sara Castaño-Cerezo et al. “Regulation of acetate metabolism in *Escherichia coli* BL21 by protein N^{ϵ}-lysine acetylation”. In: *Applied microbiology and biotechnology* 99 (Dec. 2014).

[16] Guiping Gong et al. “Metabolic engineering using acetate as a promising building block for the production of bio-based chemicals”. In: *Engineering Microbiology* 2.4 (2022), p. 100036.

[17] Acetic acid 99 % China. “https://www.echemi.com/produce/pr2203103046-acetic-acid-99-supplier-in-china.html”. In: *www.echemi.com* (2022).

[18] Dirk Kiefer et al. “From Acetate to Bio-Based Products: Underexploited Potential for Industrial Biotechnology”. In: *Trends in Biotechnology* 39 (Oct. 2020).

[19] G Luli and William Strohl. “Comparison of growth, acetate production, and acetate inhibition of *Escherichia coli* strains in batch and fed-batch fermentations”. In: *Applied and environmental microbiology* 56 (May 1990), pp. 1004–11.

[20] Stéphane Pinhal et al. “Acetate Metabolism and the Inhibition of Bacterial Growth by Acetate”. In: *Journal of Bacteriology* 201 (Apr. 2019).

[21] Huiqing Chong et al. “Improving Acetate Tolerance of *Escherichia coli* by Rewiring Its Global Regulator cAMP Receptor Protein (CRP)”. In: *PloS one* 8 (Oct. 2013), e57628.

[22] Anna-Lena Heins et al. “The effect of acetate on population heterogeneity in different cellular characteristics of *Escherichia coli* in aerobic batch cultures”. In: *Biotechnology Progress* 35 (Feb. 2019), e2796.

[23] Warissara Panjapakkul and Mahmoud M. El-Halwagi. “Technoeconomic Analysis of Alternative Pathways of Isopropanol Production”. In: *ACS Sustainable Chemistry & Engineering* 6.8 (2018), pp. 10260–10272. eprint: `https://doi.org/10.1021/acssuschemeng.8b01606`.

[24] Liya Liang et al. “Synthetic Biology and Metabolic Engineering Employing Escherichia coli for C2–C6 Bioalcohol Production”. In: *Frontiers in Bioengineering and Biotechnology* 8 (2020).

[25] Amir Farshi. “Propylene Production Methods And FCC Process Rules In Propylene Demands”. In: Oct. 2008.

[26] Juan Ramos et al. “Addressing the energy crisis: using microbes to make biofuels”. In: *Microbial Biotechnology* 15 (Mar. 2022).

[27] Takaaki Horinouchi et al. “Improvement of isopropanol tolerance of *Escherichia coli* using adaptive laboratory evolution and omics technologies”. In: *Journal of Biotechnology* 255 (June 2017).

[28] Kentaro Inokuma et al. “Improvement of isopropanol production by metabolically engineered Escherichia coli using gas stripping”. In: *Journal of Bioscience and Bioengineering* 110.6 (2010), pp. 696–701.

[29] T Hanai, S Atsumi, and J.C. Liao. “Engineered Synthetic Pathway for Isopropanol Production in Escherichia coli”. In: *Applied and environmental microbiology* 73 (Jan. 2008), pp. 7814–8.

[30] Jiann-Shin Chen and Stephen F. Hiu. “Acetone-butanol-isopropanol production byClostridiumbeijerinckii (synonym,Clostridiumbutylicum)”. In: *Biotechnology Letters* 8 (1986), pp. 371–376.

[31] Hadrien Gérando et al. “Genome and transcriptome of the natural isopropanol producer Clostridium beijerinckii DSM6423”. In: *BMC genomics* 19 (Apr. 2018), p. 242.

[32] Shrikant Survase et al. “Continuous production of isopropanol and butanol using Clostridium beijerinckii DSM 6423”. In: *Applied microbiology and biotechnology* 91 (May 2011), pp. 1305–13.

[33] Petra Patakova et al. “Transcriptomic studies of solventogenic clostridia, Clostridium acetobutylicum and Clostridium beijerinckii”. In: *Biotechnology Advances* 58 (2022), p. 107889.

[34] John Grime et al. “Quantitative visualization of passive transport across bilayer lipid membranes”. In: *Proceedings of the National Academy of Sciences of the United States of America* 105 (Oct. 2008), pp. 14277–82.

[35] Herbert S. Harned and Russell W. Ehlers. “THE DISSOCIATION CONSTANT OF ACETIC ACID FROM 0 TO 35° CENTIGRADE1”. In: *Journal of the American Chemical Society* 54.4 (1932), pp. 1350–1357. eprint: `https://doi.org/10.1021/ja01343a013`.

[36] Jessica C. Wilks and Joan L. Slonczewski. “pH of the Cytoplasm and Periplasm of *Escherichia coli*: Rapid Measurement by Green Fluorescent Protein Fluorimetry”. In: *Journal of Bacteriology* 189.15 (2007), pp. 5601–5607. eprint: `https://journals.asm.org/doi/pdf/10.1128/JB.00615-07`.

[37] Sukanya Kumari et al. “Cloning, Characterization, and Functional Expression ofacs, the Gene Which Encodes Acetyl Coenzyme A Synthetase inEscherichia coli”. In: *Journal of bacteriology* 177 (May 1995), pp. 2878–86.

[38] Sara Castaño-Cerezo et al. “An insight into the role of phosphotransacetylase (PTA) and the acetate/acetyl-CoA node in Escherichia coli”. In: *Microbial cell factories* 8 (Oct. 2009), p. 54.

[39] Brice Enjalbert et al. “Acetate fluxes in *Escherichia coli* are determined by the thermodynamic control of the Pta-AckA pathway”. In: *Scientific Reports* 7 (Feb. 2017), p. 42135.

[40] James Orr et al. “Extracellular acidic pH inhibits acetate consumption by decreasing gene transcription of the TCA cycle and the glyoxylate shunt”. In: *Journal of Bacteriology* 201 (Oct. 2018).

[41] T. D. K. Brown, M. C. Jones-Mortimer, and H. L. Kornberg. “The Enzymic Interconversion of Acetate and Acetyl-coenzyme A in Escherichia coli”. In: *Microbiology* 102.2 (1977), pp. 327–336.

[42] Alan J. Wolfe. “The Acetate Switch”. In: *Microbiology and Molecular Biology Reviews* 69.1 (2005), pp. 12–50. eprint: `https://journals.asm.org/doi/pdf/10.1128/mmbr.69.1.12-50.2005`.

[43] D K Fox and S Roseman. “Isolation and characterization of homogeneous acetate kinase from Salmonella typhimurium and Escherichia coli.” In: *Journal of Biological Chemistry* 261.29 (1986), pp. 13487–13497.

[44] Nobuyuki Okahashi et al. “Metabolic engineering of isopropyl alcohol-producing *Escherichia coli* strains with 13 C-metabolic flux analysis”. In: *Biotechnology and Bioengineering* 114 (July 2017).

[45] T. Jojima, M. Inui, and H. Yukawa. “Production of isopropanol by metabolically engineered Escherichia coli”. In: *Applied microbiology and biotechnology* 77(6) (Jan. 2008), pp. 1219–1224.

[46] Karl A. Walter et al. “Sequence and arrangement of two genes of the butyrate-synthesis pathway of Clostridium acetobutylicum ATCC 824”. In: *Gene* 134.1 (1993), pp. 107–111.

[47] DK Thompson and JS Chen. “Purification and properties of an acetoacetyl coenzyme A-reacting phosphotransbutyrylase from Clostridium beijerinckii (”Clostridium butylicum”) NRRL B593”. In: *Appl Environ Microbiol.* 56(3) (Mar. 1990), pp. 607–613.

[48] Michael Koepke et al. “Genetically engineered bacterium comprising energy-generating fermentation pathway”. US9738875B2. Aug. 2017.

[49] Hemshikha Rajpurohit and Mark A. Eiteman. “Nutrient-Limited Operational Strategies for the Microbial Production of Biochemicals”. In: *Microorganisms* 10.11 (Nov. 2022), p. 2226.

[50] B. Kristiansen and R. Charley. “36 - CONTINUOUS PROCESS FOR PRODUCTION OF CITRIC ACID”. In: *Scientific and Engineering Principles*. Ed. by MURRAY MOO-YOUNG, CAMPBELL W. ROBINSON, and CLAUDE VEZINA. Pergamon, 1981, pp. 221–227.

[51] Eduard Kerkhoven et al. “Regulation of amino-acid metabolism controls flux to lipid accumulation in Yarrowia lipolytica”. In: *npj Systems Biology and Applications* 2 (Mar. 2016), p. 16005.

[52] Andreas Otten, Melanie Brocker, and Michael Bott. "Metabolic engineering of Corynebacterium glutamicum for the production of itaconate". In: *Metabolic Engineering* 30 (2015), pp. 156–165.

[53] Akhilesh Kumar Singh and Nirupama Mallick. "Advances in cyanobacterial polyhydroxyalkanoates production". In: *FEMS Microbiology Letters* 364.20 (Sept. 2017). fnx189. eprint: https://academic.oup.com/femsle/article-pdf/364/20/fnx189/23930199/fnx189.pdf.

[54] Jillian Marc et al. "Over expression of GroESL in Cupriavidus necator for heterotrophic and autotrophic isopropanol production". In: *Metabolic Engineering* 42 (2017), pp. 74–84.

[55] Prof. J. Christopher Anderson. *Anderson constitutive promoter collection for* E. coli. 2006. URL: http://parts.igem.org/Promoters/Catalog/Anderson (visited on 02/07/2023).

[56] Haiyao Huang. *Bidirectional artificial terminator BBa_B1001*. 2006. URL: http://parts.igem.org/wiki/index.php?title=Part:BBa_B1001 (visited on 02/07/2023).

[57] Parveen Sarkari et al. "An efficient tool for metabolic pathway construction and gene integration for Aspergillus niger." In: *Bioresour Technol.* 245 (Dec. 2017), pp. 1327–1333.

[58] Marillonnet S. Engler C Kandzia R. "A One Pot, One Step, Precision Cloning Method with High Throughput Capability". In: *PLoS One* (Nov. 2008).

[59] Rao G. et. al. DeLisa MP Li J. "Monitoring GFP-operon fusion protein expression during high cell density cultivation of *Escherichia coli* using an on-line optical sensor". In: *Biotechnol Bioeng.* 65 (Oct. 1999), pp. 54–64.

[60] Caitlin Sande and Chris Whitfield. "Capsules and Extracellular Polysaccharides in Escherichia coli and Salmonella". In: *EcoSal Plus* 9.2 (2021), eESP-0033–2020. eprint: https://journals.asm.org/doi/pdf/10.1128/ecosalplus.ESP-0033-2020.

[61] Peng-Fei Xia et al. "Extracellular polymeric substances protect Escherichia coli from organic solvents". In: *RSC Adv.* 6 (June 2016).

[62] Amarjeet Singh et al. "Manipulating redox and ATP balancing for improved production of succinate in E. coli". In: *Metabolic Engineering* 13.1 (2011), pp. 76–81.

[63] Hye-Jung Kim et al. "An engineered *Escherichia coli* having a high intracellular level of ATP and enhanced recombinant protein production". In: *Applied microbiology and biotechnology* 94 (Dec. 2011), pp. 1079–86.

[64] Sebastiaan Spaans et al. "NADPH-generating systems in bacteria and archaea". In: *Frontiers in microbiology* 6 (Aug. 2015), p. 742.

[65] Uwe Sauer et al. “The Soluble and Membrane-bound Transhydrogenases UdhA and PntAB Have Divergent Functions in NADPH Metabolism of”. In: *The Journal of biological chemistry* 279 (Mar. 2004), pp. 6613–9.

[66] Wei Li et al. “Effect of NADPH availability on free fatty acid production in E. coli”. In: *Biotechnology and Bioengineering* 115 (Oct. 2017).

[67] Tomas Johansson et al. “X-ray Structure of Domain I of the Proton-pumping Membrane Protein Transhydrogenase from *Escherichia coli*”. In: *Journal of Molecular Biology* 352.2 (2005), pp. 299–312.

[68] Shigeyuki Kawai et al. “Molecular characterization of *Escherichia coli* NAD kinase”. In: *European journal of biochemistry / FEBS* 268 (Aug. 2001), pp. 4359–65.

[69] Anders Holm et al. “Metabolic and Transcriptional Response to Cofactor Perturbations in *Escherichia coli*”. In: *The Journal of biological chemistry* 285 (Mar. 2010), pp. 17498–506.

[70] Stephen J. Sramek and Frank E. Frerman. “*Escherichia coli* coenzyme A-transferase: Kinetics, catalytic pathway and structure”. In: *Archives of Biochemistry and Biophysics* 171.1 (1975), pp. 27–35.

[71] Stanley J. Sramek and Frank E. Frerman. “Purification and properties of *Escherichia coli* coenzyme A-transferase.” In: *Archives of biochemistry and biophysics* 171 1 (1975), pp. 14–26.

[72] Dennis P. Wiesenborn, Frederick B. Rudolph, and Eleftherios Terry Papoutsakis. “Phosphotransbutyrylase from Clostridium acetobutylicum ATCC 824 and its role in acidogenesis”. In: *Applied and Environmental Microbiology* 55 (1989), pp. 317–322.

[73] Tobias Alter and Birgitta Ebert. “Determination of growth-coupling strategies and their underlying principles”. In: *BMC Bioinformatics* 20 (Aug. 2019).

[74] Mugdha Gadgil, Vivek Kapur, and Wei-Shou Hu. “Transcriptional Response of *Escherichia coli* to Temperature Shift”. In: *Biotechnology progress* 21 (May 2005), pp. 689–99.

[75] Rashed Noor et al. “Influence of Temperature on *Escherichia coli* Growth in Different Culture Media”. In: *Journal of Pure and Applied Microbiology* 7 (June 2013).

[76] Yankai Zhang, Li Taiming, and Jingjing Liu. “Low temperature and glucose enhanced T7 RNA polymerase-based plasmid stability for increasing expression of glucagon-like peptide-2 in *Escherichia coli*”. In: *Protein Expression and Purification* 29.1 (2003), pp. 132–139.

[77] Simon Boecker et al. “Increasing ATP turnover boosts productivity of 2,3-butanediol synthesis in *Escherichia coli*”. In: *Microbial Cell Factories* 20 (Mar. 2021).

[78] Thomas Causey et al. “Inaugural Article: Engineering the metabolism of *Escherichia coli* W3110 for the conversion of sugar to redox-neutral and oxidized products: Homoacetate production”. In: *Proceedings of the National Academy of Sciences of the United States of America* 100 (Mar. 2003), pp. 825–32.

[79] Y P Chao et al. “Control of gluconeogenic growth by pps and pck in *Escherichia coli*”. In: *Journal of Bacteriology* 175.21 (1993), pp. 6939–6944. eprint: `https://journals.asm.org/doi/pdf/10.1128/jb.175.21.6939-6944.1993`.

[80] Brian J. Koebmann et al. “The Glycolytic Flux in *Escherichia coli* Is Controlled by the Demand for ATP”. In: *Journal of Bacteriology* 184.14 (2002), pp. 3909–3916. eprint: `https://journals.asm.org/doi/pdf/10.1128/JB.184.14.3909-3916.2002`.

[81] Simon Boecker et al. “Broadening the Scope of Enforced ATP Wasting as a Tool for Metabolic Engineering in *Escherichia coli*”. In: *Biotechnology Journal* 14 (Mar. 2019), p. 1800438.

[82] Oliver Hädicke, Katja Bettenbrock, and Steffen Klamt. “Enforced ATP futile cycling increases specific productivity and yield of anaerobic lactate production in *Escherichia coli*: ATP Wasting to Improve Yield and Productivity”. In: *Biotechnology and Bioengineering* 112 (Apr. 2015).

[83] Oliver Hädicke and Steffen Klamt. “Manipulation of the ATP pool as a tool for metabolic engineering”. In: *Biochemical Society Transactions* 43.6 (Nov. 2015), pp. 1140–1145. eprint: `https://portlandpress.com/biochemsoctrans/article-pdf/43/6/1140/723652/bst0431140.pdf`.

[84] Christoph Kaleta et al. “Metabolic costs of amino acid and protein production in *Escherichia coli*”. In: *Biotechnology journal* 8 (Sept. 2013).

List of Figures

List of Tables